

High-Temperature Geochemistry

(8 Lectures and Practical sessions)

and

Igneous Petrology

(8 Lectures and Practical sessions)

By Prof. V.R. Troll
Uppsala University



UPPSALA
UNIVERSITET



Prof. Valentin R. Troll
Chair in Petrology

Department of Earth Sciences
Uppsala University, Sweden

Villavägen 16,
752 36 Uppsala, Sweden
Phone: +46-18-471-2570
Valentin.Troll@geo.uu.se
www.geo.uu.se/mpt
www.vrtroll.com

Course Outline – Geochemistry

Geochemistry:

The term Geochemistry was first used by the Swiss chemist Schönbein in 1838 and combines geology and chemistry. In geochemistry we use the tools of chemistry to solve geological problems; that is, we use chemistry to understand the Earth and how it works. Geochemistry contains various different sub-disciplines: e.g. atmospheric geochemistry, isotope geochemistry, marine chemistry, trace element geochemistry, soil chemistry, etc.

Aim of the course: To explore the use of chemical tools in Geology

Lecture 1: Formation and composition of the Solar system, evidence from meteorites (types and their compositions), and the chondrite model.

Lecture 2: Formation of the Earth, the Earth's structure, chemical composition of the Earth, and the Goldschmidt classification of element affinities.

Lecture 3: Secondary element distribution, major elements in magmatic processes, ionic substitution, Goldschmidt's radius ratio rule, trace elements in magmatic processes and distribution coefficients.

Lecture 4: The use of distribution coefficients in melting and crystallisation models, Batch melting, Rayleigh melting, Rayleigh crystal fractionation, and further applications of trace elements in high-T Geochemistry

Lecture 5: Radiogenic isotopes I, Sr-Nd system, Distribution of isotopic reservoirs in the Earth and the use of isotopic traces.

Lecture 6: Radiogenic isotopes II: U-Th-Pb system, helium isotopes, osmium isotopes.

Lecture 7: Stable isotopes: oxygen isotopes, hydrogen isotopes, sulphur isotopes, and their use in high-T geochemistry.

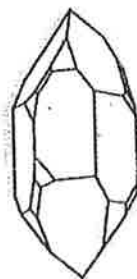
Lecture 8: Geochemistry of igneous ore bodies, layered ultrabasic intrusions, pegmatites, kimberlites, porphyry copper deposits, and low-T hydrothermal deposits.

HOMEWORK

The courses 'Geochemistry' and 'Igneous Petrology' are to a large degree inter-linked. You will get six homework sheets throughout this term, each of which deals with common topics from the two courses. The homework should be included in your Igneous Petrology lab-book (e.g. start from the back) and will form part of your lab-book assessment!

Textbooks:

- Mason B. *Principles of Geochemistry*, Wiley & Sons
- Henderson P. *Inorganic Geochemistry*, Pergamon Press
- Brownlow A. *Geochemistry*, Prentice Hall
- Rollinson H. *Using geochemical data*, Longman Publishers
- Li Y.-H. *A compendium of Geochemistry*, Princeton Univ. Press



PERIODIC TABLE OF THE ELEMENTS

1	2	3	4	5	6	7	8	9	10	11	12	13	14	15	16	17	18
1 H Hydrogen 1.0079	2 He Helium 4.0026	3 Li Lithium 6.941	4 Be Beryllium 9.0122	5 B Boron 10.81	6 C Carbon 12.011	7 N Nitrogen 14.007	8 O Oxygen 15.999	9 F Fluorine 18.998	10 Ne Neon 20.179	11 Na Sodium 22.990	12 Mg Magnesium 24.305	13 Al Aluminum 26.982	14 Si Silicon 28.086	15 P Phosphorus 30.974	16 S Sulfur 32.06	17 Cl Chlorine 35.453	18 Ar Argon 39.948
19 K Potassium 39.098	20 Ca Calcium 40.08	21 Sc Scandium 44.956	22 Ti Titanium 47.88	23 V Vanadium 50.942	24 Cr Chromium 51.996	25 Mn Manganese 54.938	26 Fe Iron 55.847	27 Co Cobalt 58.933	28 Ni Nickel 58.69	29 Cu Copper 63.546	30 Zn Zinc 65.39	31 Ga Gallium 69.72	32 Ge Germanium 72.59	33 As Arsenic 74.922	34 Se Selenium 78.96	35 Br Bromine 79.904	36 Kr Krypton 83.80
37 Rb Rubidium 85.468	38 Sr Strontium 87.62	39 Y Yttrium 88.906	40 Zr Zirconium 91.224	41 Nb Niobium 92.906	42 Mo Molybdenum 95.94	43 Tc Technetium (98)	44 Ru Ruthenium 101.07	45 Rh Rhodium 102.91	46 Pd Palladium 106.42	47 Ag Silver 107.87	48 Cd Cadmium 112.41	49 In Indium 114.82	50 Sn Tin 118.71	51 Sb Antimony 121.75	52 Te Tellurium 127.60	53 I Iodine 126.91	54 Xe Xenon 131.29
55 Cs Cesium 132.91	56 Ba Barium 137.33	57-71 Lanthanides	72 Hf Hafnium 178.49	73 Ta Tantalum 180.95	74 W Tungsten 183.85	75 Re Rhenium 186.21	76 Os Osmium 190.2	77 Ir Iridium 192.22	78 Pt Platinum 195.08	79 Au Gold 196.97	80 Hg Mercury 200.59	81 Tl Thallium 204.38	82 Pb Lead 207.2	83 Bi Bismuth 208.98	84 Po Polonium (209)	85 At Astatine (210)	86 Rn Radon (222)
87 Fr Francium (223)	88 Ra Radium (226.03)	89-103 Actinides	104 Rh Rhenium (261)	105 Unp Unilpentium (262)	106 Unh Unihexium (263)	107 Uns Unseptium (262)	108 Uno Unoctium (266)	109 Une Unennium (266)									

Lanthanides	57 La Lanthanum 138.91	58 Ce Cerium 140.12	59 Pr Praseodymium 140.91	60 Nd Neodymium 144.24	61 Pm Promethium (145)	62 Sm Samarium 150.36	63 Eu Europium 151.96	64 Gd Gadolinium 157.25	65 Tb Terbium 158.93	66 Dy Dysprosium 162.50	67 Ho Holmium 164.93	68 Er Erbium 167.26	69 Tm Thulium 168.93	70 Yb Ytterbium 173.04	71 Lu Lutetium 174.97
Actinides	89 Ac Actinium 227.03	90 Th Thorium 232.04	91 Pa Protactinium 231.04	92 U Uranium 238.03	93 Np Neptunium 237.05	94 Pu Plutonium (244)	95 Am Americium (243)	96 Cm Curium (247)	97 Bk Berkelium (247)	98 Cf Californium (251)	99 Es Einsteinium (252)	100 Fm Fermium (257)	101 Md Mendelevium (258)	102 No Nobelium (259)	103 Lr Lawrencium (260)

Geochemistry- Lecture 1

THE NATURE OF THE UNIVERSE

The earth is a unit within the solar system, which consists of the sun, the planets and their satellites, the asteroids, the comets, and the meteorites. The sun itself is only one star within our galaxy, which comprises probably more than 10^{11} stars and has a lens-like form with a diameter of about 70,000 light-years (1 light-year $\sim 10^{13}$ km). Beyond our own galaxy there is a very large number of other galaxies of approximately the same size. These systems, the extra-galactic nebulae, are scattered fairly uniformly through space, the nearest to us being the Andromeda nebula at a distance of about 1,000,000 light-years. From spectra of these extra-galactic nebulae we know that the universe is expanding. By extrapolation we infer an origin of the universe in a single spot that explosively disintegrated (the big bang). This means, all the matter in the universe was initially concentrated into a very small region.

THE SOLAR SYSTEM

The solar system can be treated as an isolated unit, and its age considered independently of the rest of the galaxy and the universe as a whole. The solar system is essentially a closed system, and its elemental composition the same as when it formed, except insofar as it has been modified by the conversion of hydrogen to helium in the sun and by the decay of radioactive elements:

In the study of geochemistry the solar system is of primary importance, although it is fairly unimportant within our own galaxy and insignificant in relation to the universe as a whole. Any satisfactory theory of the origin of the solar system must explain its regularities, the most important of which are the following:

1. The sun contains over 99.8% of the mass of the system.
2. The planets all revolve in the same direction around the sun in elliptical orbits, and these orbits all lie in practically the same plane.
3. The planets themselves rotate about their axes in the same direction as their direction of revolution around the sun and so do their satellites (except Uranus, which has retrograde rotation).
4. The planets show a rather regular spacing as expressed by Bode's law, and they form two contrasted groups: an inner group of small planets and an outer group of giant planets. A gap between Mars and Jupiter is occupied by the asteroid belt.

COMPOSITION OF THE SOLAR SYSTEM

Spectroscopic studies of the sun have been made over many years and many data have been accumulated. The spectra are produced in the outer part of the sun and give the composition of the solar atmosphere.

Our Sun is a typical star that is currently in the main sequence stage of evolution. It is not, however, a first-generation star, but instead is made up of matter produced by earlier stars. Almost all of the naturally occurring elements have been detected in the Sun's spectrum, with hydrogen and helium by far the most abundant, and there is no reason to conclude that any element is really absent. Those that are not observed are elements with very small abundance. The most striking feature is the extreme abundance of hydrogen and helium, a feature that is probably also characteristic of the larger planets, Jupiter, Saturn, Neptune and Uranus. The properties of the Sun indicate that its outer layers consist of about 73% hydrogen, 25% helium, 0.5% carbon, 0.5% oxygen, and 1% other elements.

The nine planets can be subdivided into the outer Jovian planets (Jupiter, Saturn, Uranus, and Neptune), the inner terrestrial planets (Mercury, Venus, Earth, and Mars), and the least known and outermost planet, Pluto. The Jovian planets have large masses and low densities, while the terrestrial planets show the reverse relationships. The major chemical difference among the planets lies in the abundance or scarcity of hydrogen and helium. The inner planets are small and do not have the gravitational fields to retain these gases. Also it seems likely that the inner planets were much hotter during their early stages of formation; as a result, hydrogen and helium were lost. The Jovian planets, on the other hand, are mainly composed of gaseous hydrogen and helium and of "ices" (frozen volatiles of H_2O , CH_4 , and NH_3). The sparse atmospheres that surround the terrestrial planets are composed primarily of more massive, slower-moving molecules such as carbon dioxide (CO_2), nitrogen (N_2), oxygen (O_2), and water vapor (H_2O). On the four Jovian planets, low temperatures and relatively strong gravity prevent even lightweight hydrogen and helium gases from escaping into space.

☼ **The inner, terrestrial, planets:** Mercury has no atmosphere, and its density indicates that it is probably similar in composition to the earth. Venus is our nearest neighbour, and has a very dense atmosphere, consisting almost entirely of carbon dioxide and nitrogen which conceals its surface. The size and mass of Venus suggest that its composition is probably much like that of the earth. Mars, the next planet beyond the earth, has an atmosphere that does not obscure the surface. However, clouds and dust storms have been observed on the face of Mars, and polar ice caps form in winter and melt in summer, showing that the atmosphere must contain some water vapour. The reflecting power of Mars indicates that its surface is largely composed of reddish rock. The size and mass of Mars indicate a composition probably similar to that of the earth. However, Mars seems of uniform chemical composition throughout and is not differentiated into an iron core and silicate mantle, as is the earth.

☼ **The Jovian planets,** Jupiter, Saturn, Neptune, and Uranus, have many features in common, in particular low densities and thick atmospheres that completely obscure their surfaces. The low densities and thick atmospheres are explained by an abundance of hydrogen and helium probably comparable with that in the sun. Much of the hydrogen is evidently present as methane and ammonia. The data we have on the major planets indicate that they have interiors similar to that of the earth but are covered with a great thickness of ice and condensed gases to form massive atmospheres.

☿ **Pluto** the distant planet similar in size to Mercury, is an enigmatic body of which we know very little; it appears to be without an atmosphere, and its albedo is like that of the moon, suggesting a surface of dark-coloured rock, possibly similar to basalt. It may have been a satellite of Neptune or a body captured by the solar system.

♄ **The asteroids** are located in a belt between the terrestrial and Jovian planets. These small bodies are believed to have undergone very little change since their formation at the same time as the planets formed. The compositions of the asteroids can be estimated from observing properties such as spectral reflectivities, and results indicate a regular change in composition with distance from the Sun. This result implies accretion of the asteroids from the solar nebula at their present location and it is consistent with models developed for formation of the planets over a period of time by accretion from a primordial solar nebula.

THE COMPOSITION OF METEORITES

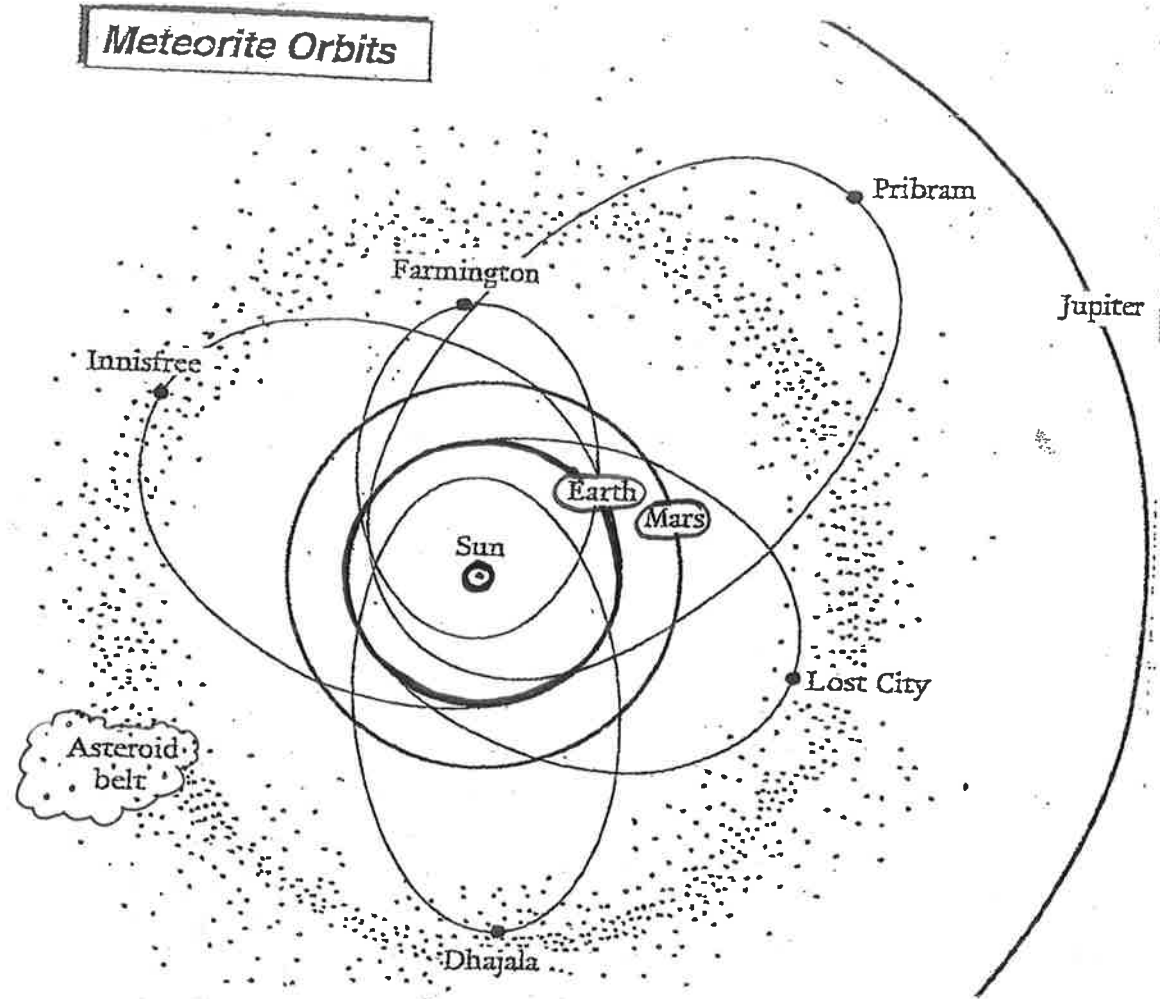
Our knowledge of the abundance of the elements in the universe comes from two major sources: (1) spectroscopic analyses of the light from our sun, other stars, and nebulae (particularly for volatile elements); and (2) meteorites (for non-volatile elements). The spectroscopic analyses involve comparisons of the intensities of elemental lines in stellar and nebulae spectra. Meteorites have become available in larger numbers in recent years due to the discovery and collection of a wide variety of meteorites in Antarctica. Most meteorites are probably fragments from the asteroid belt of the solar system. Their chemical variety indicates that they were once parts of several larger planetary bodies, each with its own unique chemical properties. Since spectrographic evidence tells us nothing about the composition of the interiors of the planets. We must fall back on analogies with our own planet and with the evidence provided by meteorites.

Meteoritic matter is continually falling on earth, mostly in the form of dust undetectable except by special means; it is estimated that the rate of meteoritic infall is between 1000 and 10,000 tons daily. Our knowledge of the composition of meteorites comes from the larger and more spectacular ones that are seen to fall or from objects that are recognised as meteorites by the special characters distinguishing them from terrestrial rocks.

Meteorites consist essentially of a nickel-iron alloy, of crystalline silicate, mainly olivine or pyroxene, or of a mixture of these. None resembling sedimentary or metamorphic rocks have been found. Many systems of classification have been devised for meteorites, but for our purpose they may be grouped as follows:

1. Siderites or **irons** (average 98% metal).
2. Siderolites or **stony irons** (average 50% metal, 50% silicate).
3. Aerolites or **stones** (silicate > metal).

Meteorite Orbits



Mer- cury	Venus	Earth	Mars	(Va- cant)	Jupiter	Saturn	Uranus	Neptune	Pluto
4	4	4	4	4	4	4	4		4
0	3	6	12	24	48	96	192		384
4	7	10	16	28	52	100	196		388

Actual distances of the planets from the sun in terms of the Earth's distance as 10

3.9	7.2	10	15.2	..	52	95	192	301	395
-----	-----	----	------	----	----	----	-----	-----	-----

✧ **The siderites, or iron meteorites**, consist essentially of a nickel-iron alloy (Ni is usually between 4 and 20%, rarely greater), generally with accessory troilite (FeS) and graphite. The metal generally shows a definite structure known as Widmanstätten figures. This structure consists of lamellae of kamacite (a nickel-iron alloy with about 60% Ni) bordered by taenite (a nickel-iron alloy with about 30% Ni). This structure is typical of exsolution in an alloy that has cooled very slowly from a high temperature.

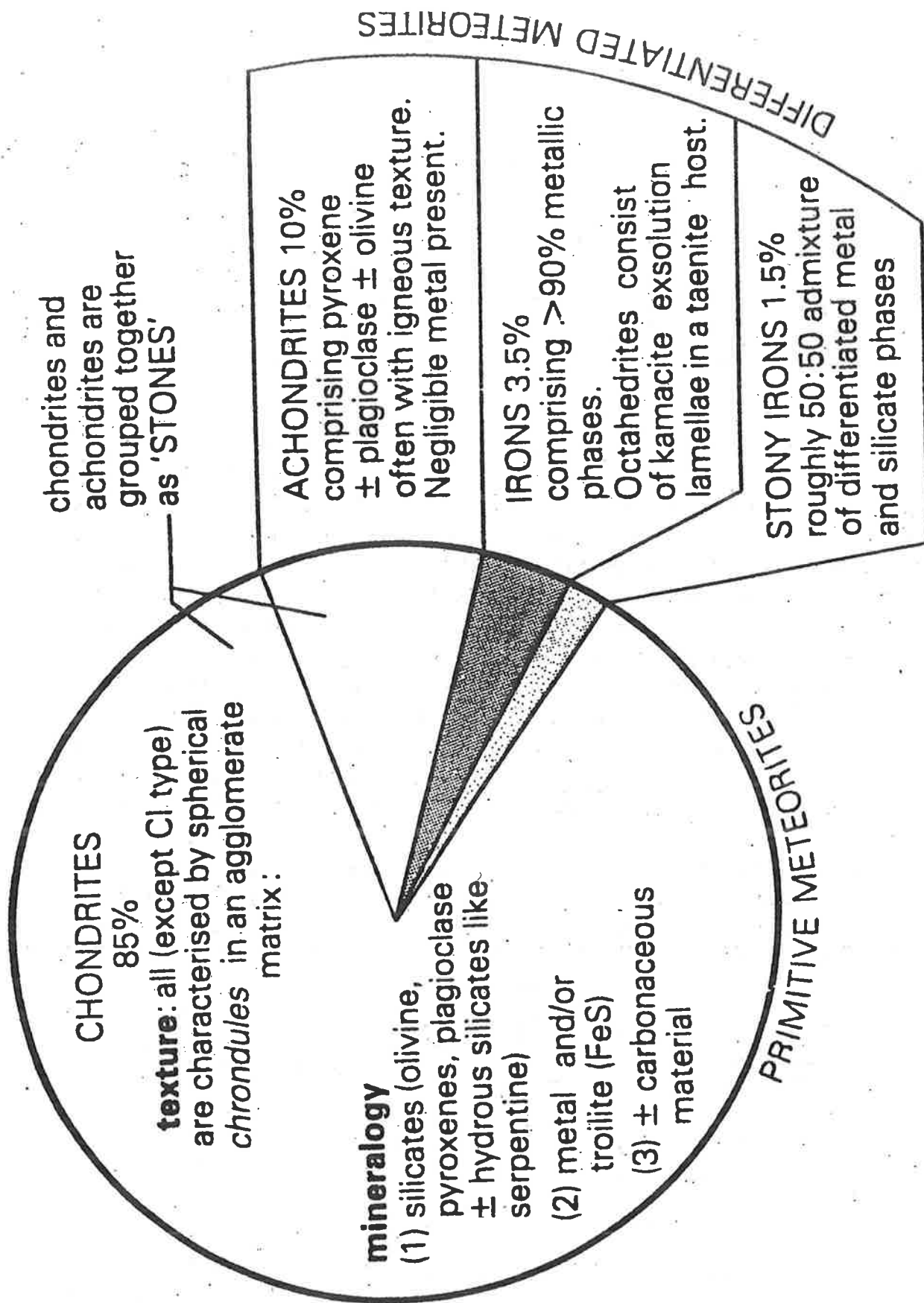
✧ **The siderolites, or stony-iron meteorites**, are made up of nickel-iron and silicates in approximately equal amounts. Two distinct groups, the pallasites and the mesosiderites, of different chemical and mineralogical composition, are recognised. The pallasites are made up of a continuous base of nickel-iron enclosing grains of olivine which often show good crystal forms. In the mesosiderites the metal phase is discontinuous and the silicates are mainly plagioclase feldspar and pyroxene.

✧ **The aerolites or stones** are divided into two groups, the *chondrites* and the *achondrites*.

■ **The chondrites** are so named because of the presence of chondrules, which are small rounded bodies (averaging 1 mm in diameter) consisting of olivine and/or pyroxene. Chondrules seem to be unique to these meteorites and have never been observed in terrestrial rocks, hence are probably significant in terms of the origin of such meteorites. The average composition of chondrites is about 40% olivine, 30% pyroxene, 1–20% nickel-iron, 10% plagioclase, and 6% troilite. One group of chondrites, the carbonaceous chondrites (C1 chondrites), is unique among meteorites in consisting largely of hydrated iron-magnesium silicate (serpentine or chlorite) and containing up to 10% of complex organic compounds. Inclusions in carbonaceous chondrites, which have a high content of refractory elements calcium, aluminium and titanium (CAIs), may represent the initial material formed from the solar system nebula. The origin of the organic compounds, whether the remains of extraterrestrial organisms or the products of nonbiological synthesis, has been argued for over a century and is still actively controversial. However, Miller showed in 1957 that all organic compounds in meteorites can be synthesised by inorganic means.

■ **The achondrites** are a diverse group of stony meteorites which do not contain chondrules and which are usually much more coarsely crystalline than the chondrites. Many achondrites resemble terrestrial igneous rocks in composition and texture, hence have probably crystallized from a silicate melt.

Another way to classify meteorites is as undifferentiated (chondrites) and differentiated (irons, stony irons, and achondrites). Their chemical compositions indicate that the parent bodies of chondrites have never been melted *and* fractionated, while the other meteorites reflect the result of melting prior to their formation. In other words, the parent bodies of differentiated meteorites separated into masses of varying composition and, as a result, these meteorites have compositions that are different from that of the solar atmosphere (which is believed to be representative of the nebula from which the solar system formed). Thus chondrites, with element ratios similar to those in the solar atmosphere, are believed to be representative of the primitive material from which the bodies of the solar system formed. Moreover, there is a close correspondence between the average composition of iron meteorites with the average



composition of the metal from chondrites, strongly suggesting a common source. The iron meteorites probably represent metal segregated by the partial or complete melting of material of chondritic composition (core of a planet).

There is general agreement that meteorites provide us with the best sample from which to derive the absolute abundances of the non-volatile elements. All meteorite types can plausibly be developed by the partial or complete melting and differentiation of material of chondritic composition. On this account the chemical composition of the chondrites has been the primary source of information regarding the absolute or cosmic abundances of the elements since they represent the non-volatile bulk composition of all of the inner planets including that of the sun.

ADDENDA: Eight achondrite meteorites have ages (about 1,300 million years) that are approximately 3,000 million years younger than those of all other meteorites. These stones are known as SNC meteorites. Recent research has shown that all the SNC meteorites have chemical and isotopic similarities (suggesting a common parent) and some of their chemical properties are similar to those found in studies of the atmosphere and soil of Mars. It is now generally accepted that these meteorites escaped from Mars as a result of impact on that planet of an asteroid or comet. The name SNC meteorites is from the names of the three meteorite classes to which they belong: shergottites, nakhlites, and chassignites. The three class names are from the localities where three of the achondrites fell: Shergotty, India; Nakhla, Egypt; and Chassigny, France.

FORMATION OF THE SOLAR SYSTEM

We can develop the following general model for the origin of the solar system. Approximately 4.6 billion years ago condensation began from a solar nebula made up mainly of gas. Solid material condensed from the gaseous mass as it cooled. This separation would tend to occur in a certain chemical order if simple condensation from a homogenous, totally gaseous nebula occurred. More recent studies of the solar nebula do not assume a high-temperature, homogeneous, wholly vaporised initial state. It is now believed that the vapour had some solid material containing pre-solar anomalies. Current models suggest a complex multistage history involving both partial evaporation and condensation; this seems to be required to explain the properties of meteorite chondrules and refractory inclusions. In addition, some mineral assemblages probably formed from gaseous material that differed from the initial material as a result of fractionation of portions of the original nebula. Thus it is currently accepted that there was not one unique, simple condensation sequence of minerals as cooling proceeded. This implies that different parts of the solar system have different histories of formation and thus somewhat different final compositions. If, as seems likely, aggregation of solid particles and masses began before the overall condensation process had run its full course, the initial accreting objects would receive an abundance of the early, high-temperature reaction products. All of the planets probably formed over a period of time by accretion of small masses into larger, kilometer-sized masses (planetesimals) and finally to their present size.

THE COSMIC ABUNDANCE OF THE ELEMENTS

On the basis of data on the composition of meteorites and of solar and stellar matter, Goldschmidt in 1937 compiled the first adequate table of cosmic abundances of elements and isotopes. The data on hydrogen and helium were derived largely from examination of the sun and stars, and the figures for most of the other elements were based on their relative abundances in meteoritic material.

In general, the agreement between the relative abundances determined in different regions of the universe seems reasonably good. For example, meteoritic and terrestrial matter differs from stellar material only in the relative scarcity of the gaseous elements. In recent years it has been found, however, that the abundance of heavy elements varies from star to star and is related to stellar age. This finding strongly suggests that these elements are synthesised within the stars and are distributed by stellar explosions.

The relative abundance of the elements, especially the lighter ones, varies considerably. An element may be a hundred or a thousand times more or less abundant than its immediate neighbour in the periodic table. Nevertheless, numerous regularities are found. These may be summed up as follows:

1. The abundances show a rapid exponential decrease for elements of the lower atomic numbers (to about atomic-number 30), followed by an almost constant value for the heavier elements.
2. Elements of even atomic number are more abundant than those of odd atomic number on either side. This regularity was first recognised independently by Oddo in 1914 and Harkins in 1917 and is referred to as the Oddo-Harkins rule.
3. The relative abundances for elements of higher atomic number than nickel vary less than those for elements of lower atomic number.
4. Only ten elements—H, He, C, N, O, Ne, Mg, Si, S, and Fe all with atomic numbers less than 27, show appreciable abundance; of these, hydrogen and helium far outweigh the other eight. A low-abundance gap between He and C exists (i.e. Li, Be, B).

Any attempt to explain the origin of the elements must therefore explain the following:

- a. The extreme abundance of hydrogen and helium (more than 99 percent of all atoms).
- b. The general decrease in abundance with increasing atomic number.
- c. The relatively low abundance of some elements (such as lithium, beryllium, boron, and scandium) and the relatively high abundance of other elements (such as iron, nickel, and lead).
- d. The greater abundance of even atomic number elements as compared to odd atomic number elements (shown by the zigzag pattern).

Several theories as to the mode of formation of the chemical elements have been proposed. One, which may be termed the equilibrium theory, proposes that the relative abundances of the elements are the result of a "frozen" thermodynamic equilibrium between atomic nuclei at some high temperature and density. By suitable assumptions as to the temperature, pressure, and density, good agreement with observed abundances is obtained for elements of atomic number up to 40. For elements of higher atomic number, however, these

assumptions lead to impossibly low abundances. Alternatively, theories have been proposed which consider the relative abundances of the elements as resulting from non-equilibrium processes; on this basis the light nuclei were built up by thermonuclear processes and the remaining nuclei by successive neutron capture. This theory predicts the general trend of the observed data but fails to explain some of the detailed features, particularly bridging of the gap caused by the non-existence of nuclei of atomic weights 5 and 8. The difficulty can be overcome by postulating the fusion of three He^4 nuclei to give C^{12} , thereby skipping the intermediate elements lithium, beryllium, and boron; these elements would be derived by secondary processes.

Formation of the elements, as part of stellar evolution, started well before the Earth solidified about 4.6 billion years ago and continues to the present time. Stellar evolution, starting about 15 billion years ago: A hot, dense early universe expanded and cooled so that it consisted of local concentrations of hydrogen and (to a lesser extent) helium. These concentrations grew and developed into galaxies, as stars began to form by gravitational collapse from clouds of gas and dust (nebulae). The centre of each stellar mass eventually became hot enough for hydrogen to fuse ("burn") to form helium. Energy is released by this reaction. Element building by such sequences (known as nucleosynthesis) continues to occur, billions of years after the "big bang". The hydrogen-burning stage of stellar evolution is called the main sequence stage. This stage ends when the inner core of hydrogen has been used up, resulting in expansion of the outer part and contraction of the inner part of the star. The product is a red-giant star. Eventually, the core becomes hot enough to start the burning of helium to produce carbon and oxygen. Once the hydrogen and helium in the core are used up, the outer part of a star again expands, along with further collapse of the inner part into the core area. Low-mass stars return to the red-giant stage. No other elements are produced in the lower-mass stars. In the larger stars the carbon-oxygen core gets hot enough to burn, producing elements such as magnesium, silicon, and sulphur. Further burning of these elements produces a core of iron and nickel. Continued collapse in the core area of the star produces a neutron star. In this type of star, addition of neutrons to iron in the core forms heavier elements up to at least plutonium. The reactions go through a series of steps in which elements of increasingly higher atomic number are produced.

The above description is for a first-generation star, one that forms from only hydrogen and helium. However, we know that a neutron star enters a supernova stage in which masses of material, including heavy elements, are expelled back into the interstellar medium. Thus second and later generations of stars form from material containing a small percentage of other elements, in addition to the main components hydrogen and helium. Such a starting material allows a greater variety of nuclear reactions during stellar evolution, and thus other elements and isotopes can be produced that were not produced during the evolution of a first-generation star. For instance, oxygen and carbon are more abundant than all other elements except hydrogen and helium because they are the final products of helium burning. Lithium, boron, and beryllium have a low abundance because their isotopes do not form in the normal chain of thermonuclear reactions. It is now thought that stable forms of these three elements formed later than those of most other elements by spallation (fragmentation) of still heavier elements as a result of cosmic ray effects.

Absolute abundances of the elements, in turn, depend on nuclear rather than chemical properties and are related to the inherent stability of the nuclei. Nuclei of the even N (neutron number) and even Z (proton number) are both more numerous and more abundant than nuclei of odd N. Nuclei of even N, odd Z and odd N, even Z are about equally numerous and abundant. Nuclei of the odd N and odd Z type are few in number (These features evidently reflect the nuclear binding energy, which is greatest for even N-even Z nuclei).

The most stable (and thus most abundant) nuclides have nearly equal and even (rather than odd) values of N and Z. Thus the iron nuclide $^{56}_{26}\text{Fe}$ is more stable and more abundant than $^{55}_{25}\text{Mn}$. Also the nuclide $^{55}_{26}\text{Fe}$ is unstable and does not occur in nature. The stability of a nuclide is related to the binding energy that holds its nucleus together. Calculations of the binding energies of the nuclides show an increase, as mass number increases to $^{56}_{26}\text{Fe}$, and then a steady decrease for higher mass numbers.

Summary of element formation:

Step 1. Hydrogen "burning" to produce helium.

Step 2. Helium "burning" to produce C^{12} , O^{16} , Ne^{20} , and perhaps Mg^{24} .

Step 3. Alpha-particle processes, in which Mg^{24} , Si^{28} , S^{32} , Ar^{36} and Ca^{40} are produced by successive additions of alpha-particles to O^{16} and Ne^{20} .

etc.

Correlating the processes of element formation with observed features of stellar evolution, all stars convert hydrogen into helium, but only the most massive stars produce the elements in the upper part of the periodic table. Certain heavy nuclides appear to be formed only under catastrophic conditions, such as the development of a supernova. A supernova is essentially a stellar explosion, the catastrophic disintegration of a star. Hence, all elements we are made of must have been part of a former, long gone, star! We are literally made of ancient star dust!



V.M. Goldschmidt and A. Einstein
on excursion near Oslo, 1940s.



V.M. Goldschmidt, 1930s

Annex: The Moon

The Moon is significantly different in composition from most other bodies of the solar system. It is strongly depleted (relative to Type 1 carbonaceous chondrites) in volatile elements such as potassium, more so than the terrestrial planets. And it seems to have an enrichment of refractory elements, such as uranium, compared to the rest of the solar system. Also the abundance values of other elements, such as iron, are unique to the Moon. Finally, the Moon's composition clearly does not match that of the Earth or of the primordial solar nebula (as represented by Type 1 carbonaceous chondrites). This geochemical evidence, along with other evidence, suggests a unique origin for the Moon.

The general geology of the Moon is simple: the relatively smooth, dark maria and the more rugged, lighter highlands. The maria consist of a wide variety of basaltic rocks, while the highlands are composed of anorthosite and related rocks. (The lunar surface is covered with a blanket of debris formed by meteorite impacts, and outcrops of bedrock are rare.) The highland rocks are as old as 4.5 billion years, while the maria basalts are as young as 3.0 billion years.

Overall, the Moon is thus not a primitive, relatively unchanged mass similar in composition to carbonaceous chondrites. The lunar crust represents strong chemical fractionation, with a chemical composition distinctly different from the bulk lunar composition. We know less about the Moon's mantle, but several types of data suggest the mantle is heterogeneous and surrounds a small core. The various hypotheses for formation of the Moon include: capture of an originally independent body, formation from material of the Earth's mantle by fission, formation from a ring of accreting material surrounding the newly formed Earth, and impact with the Earth by a Mars-sized planetesimal. The impact hypothesis, with the material making up the Moon coming mainly from the impacting body, is one of the best of the current explanations for the chemical composition and physical properties of the Moon. According to this hypothesis, the impact, which produced a mass of partly vaporised material in orbit around the Earth, occurred shortly after the Earth accreted from a population of planetesimals.

Taylor (1987) gives the following sequence for the evolution of the Moon. After the impact described above, the material of the Moon accreted and became partially or completely molten (forming a magma ocean). Differentiation of the molten mass resulted in a feldspathic crust and a fractionated lunar mantle. The mantle probably surrounded a small metallic core. Crystallization of the magma ocean produced residual melts of various types, some of which later invaded the crust. This stage concluded at about 4.4 billion years and was followed by partial melting (due to radioactive heating) of the mantle and ejection of the basaltic lavas of the maria from 4.2 to 3.0 billion years ago. No further igneous activity occurred after this time.

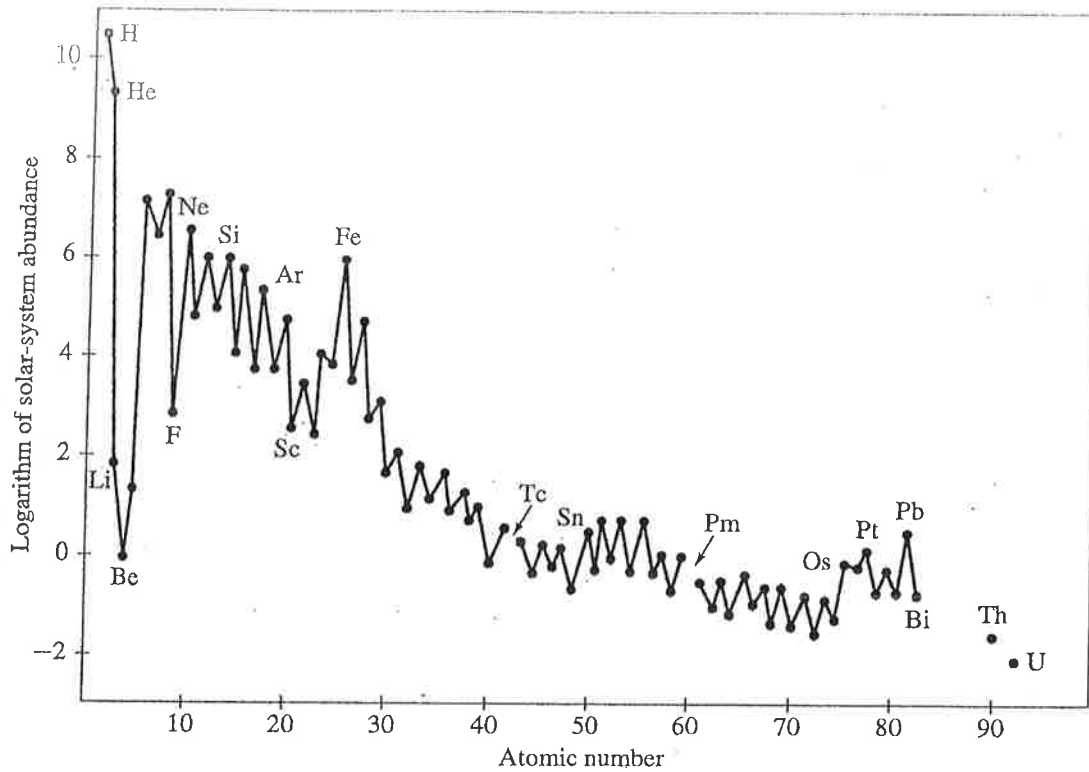
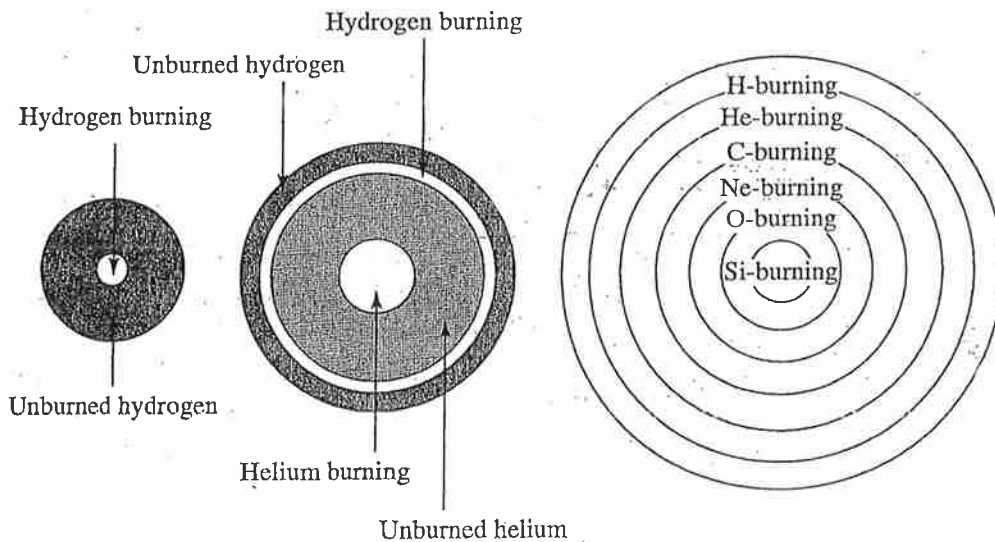


Figure Plot of the abundance of the elements in the solar system versus their atomic number. The abundances are expressed as the logarithm of the numbers of atoms of each element relative to 10^6 atoms of silicon. (After G. Faure, *Principles of Isotope Geology*, 2d ed. Copyright © 1986 by John Wiley & Sons. Reprinted by permission of John Wiley & Sons, Inc.) Data from Anders and Ebihara (1982).



Name of process	Fuel	Products	Temperature
Hydrogen-burning	H	He	60×10^6 K
Helium-burning	He	C, O	200×10^6 K
Carbon-burning	C	O, Ne, Na, Mg	800×10^6 K
Neon-burning	Ne	O, Mg	1500×10^6 K
Oxygen-burning	O	Mg to S	2000×10^6 K
Silicon-burning	Mg to S	Elements near Fe	3000×10^6 K

Figure Three stars with progressively hotter nuclear fires. Like our Sun, the star at the left burns hydrogen to form helium in its core; this core is surrounded by unburned fuel. The middle star is burning helium to form carbon and oxygen in its core. This core is surrounded by a layer of unburned helium. Outside of this is a layer in which hydrogen burns to produce helium. Finally there is an outer layer of unburned hydrogen. The star on the right has a multilayered fire.

Geochemistry Lecture 2

The solar system and formation of the Earth

The Earth is part of the Solar system and is believed to have formed simultaneously with the other planets of the system, hence all planets in the Solar System are related.

Following accretion of the Earth by (a) accretion of molecules to form planetesimals, (b) collection of these to form proto-planets, and (c) the addition of elements by meteorite bombardment, its composition was modified by radioactive decay, so that certain elements present at the early stage were converted to more stable ones. This process together with the potential energy of the accreted particles provided sufficient heat energy for the primary melting of the Earth, starting a process of redistribution of elements ultimately producing the layered structure of the Earth we know today.

Knowledge from the deeper regions than the crust is largely inferential. Igneous activity samples the lower crust and the upper mantle. Information on the composition of the core is based on geophysical evidence (mass balance suggests the core to be very dense).

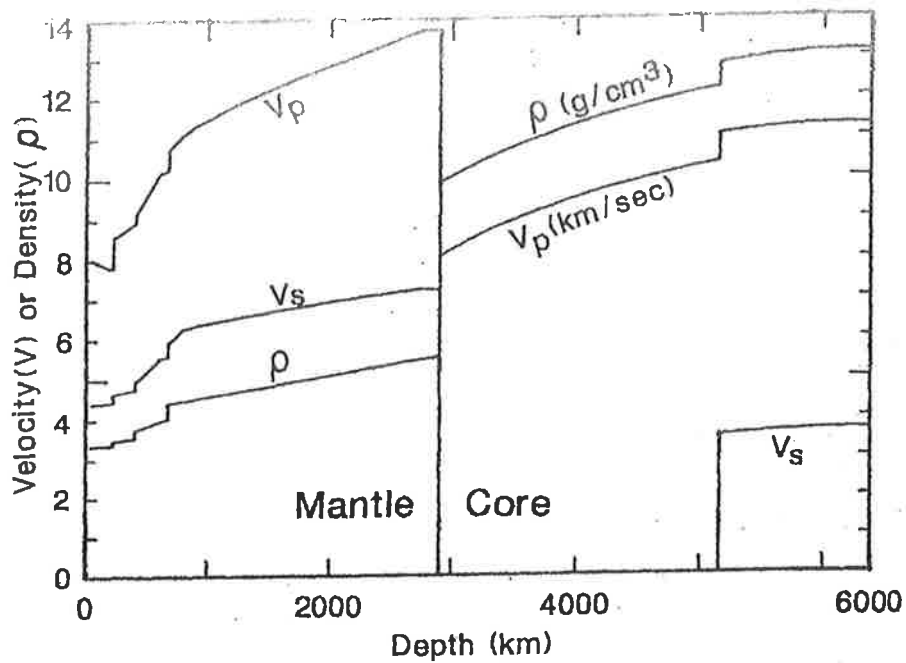
In theory the Earth has a "chondritic" composition, but in a globe that was modified with time, no single part of the Earth now corresponds directly to a chondrite. However, recent research revealed that there may be some "super-chondritic" remnants present in the lower mantle.

The Earth's structure

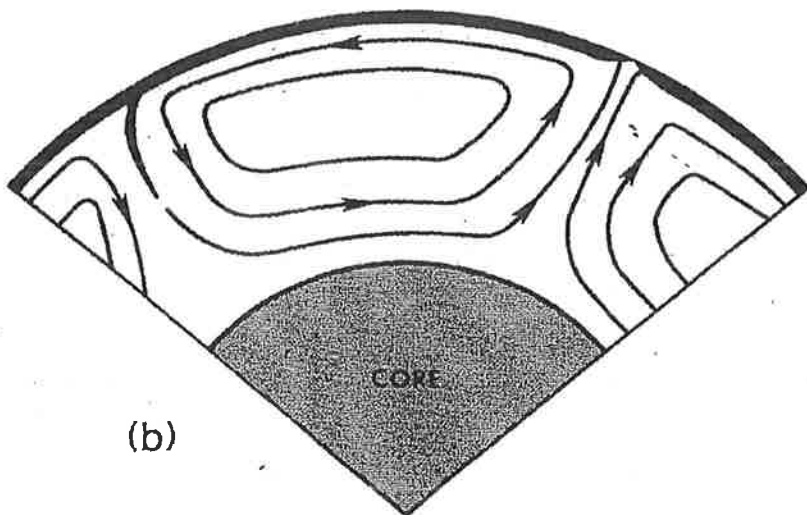
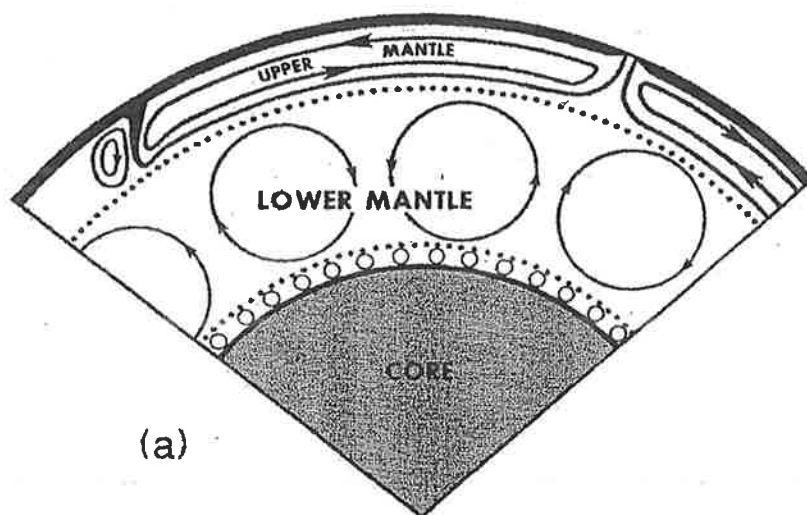
The Earth has a layered structure (chiefly core, mantle and crust) that formed after accretion of the Earth. Since all mantle derived materials have much lower Fe concentrations than chondrites we invoke segregation of an iron rich core.

Possible scenarios:

Elsasser model: Temperature of the Earth's interior just after accretion was too cold for melting Mg-silicates. But at the outer periphery, radioactive decay and meteorite bombardment allowed temperatures $>$ than the solidus of iron. Thus Fe phases will have melted and (since specifically more dense) will have sunk until the viscous resistance of the cooler silicate matrix will have forced the Fe-rich droplets to crystallise, thus transporting heat toward the lower regions of the



Seismic compressional velocity (V_p ; km/sec), shear velocity (V_s ; km/sec), and density (ρ ; g/cm³) as a function of depth according to the Preliminary Reference Earth Model (PREM) of Dziewonski and Anderson (1981).



Models of the thermal convection in the mantle. (a) Convection cells confined within the upper and lower mantles. (b) Convection cells extending through the entire mantle (after Richter, 1979; Basaltic Volcanism Study Project, 1981).

planet. This eventually started a convection process in the mantle (aided by radioactive decay), which promoted further melting in the top 100 km. This caused a convective chain reaction with small scale convection in the outer rim and increasingly large scale convection in the mantle. A thin crust developed that was broken up into pieces by convective motion underneath and thickened by underplating of rising differentiated melts (start of plate tectonics ?).

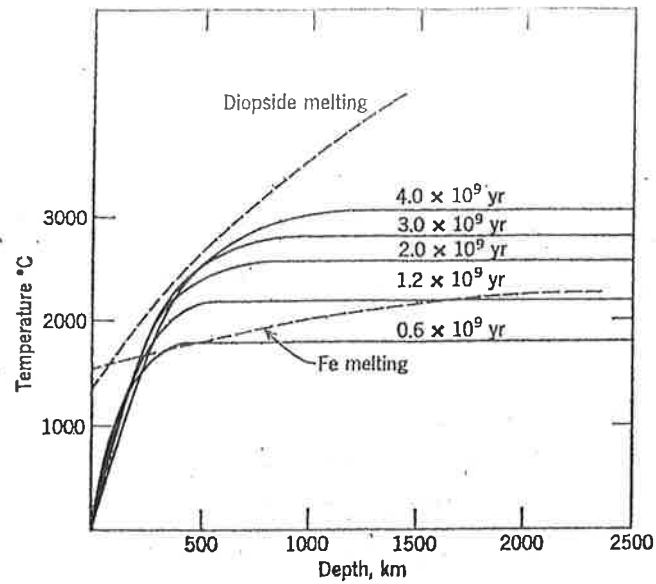
Fukai and Suzuki model: (a) Proto Earth started as a cold planetesimal of chondrite composition (except for atmophile elements. (b) When it grew in size it captured (gravitationally) all gas that was released by the impact of accreting material to form the atmosphere. (c) Because of the blanketing effect of the atmosphere, the impact energy of accreting material was trapped and heated the surface above the melting point of Fe-FeS and possibly some silicates. The molten Fe-FeS was gravitationally segregated from the silicate. (d) As the molten Fe-FeS grew larger a physical instability eventually broke up the cold chondritic core to form (e) the Fe-FeS core, the mantle and later the crust.

In any event it is unlikely that *major* segregation of the crust from the mantle began before the end of meteorite bombardment (ca. 3.9Ga ago). The outer skin must have contained a lot of meteorite derived material, but by then evolution of the mantle had already started. The oldest preserved crust (e.g. in Greenland and other continental cratonic nuclei) was already in a state of advanced evolution. Evidence for earlier crust is lacking, although it appears plausible that it existed.

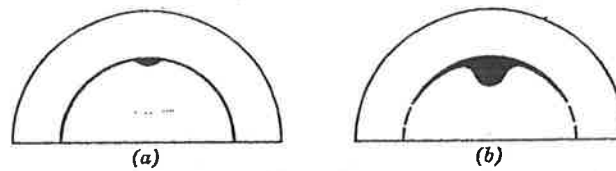
Chemical composition of the Earth

Assuming the Earth to be made of cosmic dust (chondritic composition) a systematic pattern of the Earth's composition relative to average chondrite composition should be present. There is a particular pattern of atomic number (AN) vs. abundance in chondrites. Elements with even ANs are more abundant than those with odd ANs. Oddo Harkins Rule: Energy required to produce elements with odd ANs was much higher than the energy to form elements with even atomic numbers.

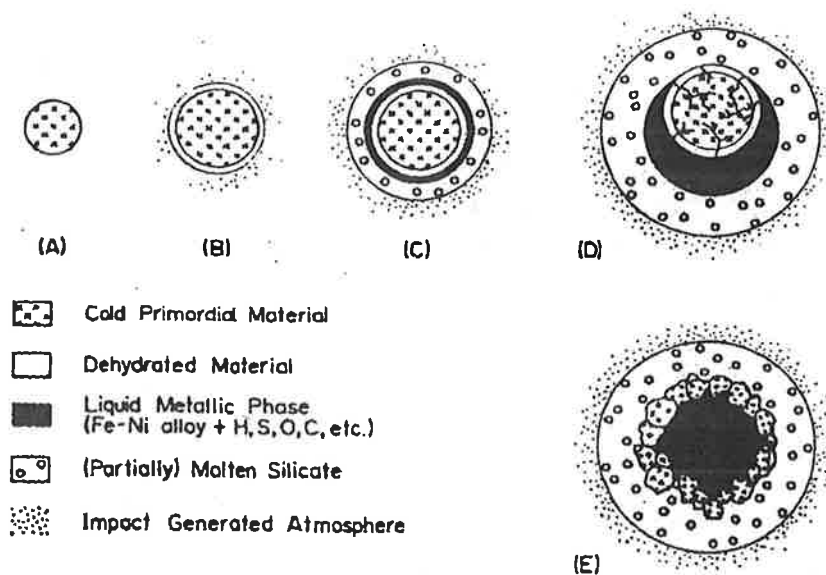
In the Earth, this pattern is retained in inter-element abundances, supporting the theory that the Earth is (was) of chondritic bulk composition. Accepting this theory, deviations of the Earth's composition from chondrite composition should then reveal the large scale losses and gains since the time the earth formed from the cosmos.



Temperatures in a homogeneous Earth heated by the radioactivity of the average chondrite. (MacDonald)



Stages of drop formation from a heavy liquid layer. (Elsasser, 1963)



Schematic of the formation processes of Earth's core (Fukai and Suzuki, 1986). See the text for details.

- Losses:** Volatile elements (e.g. F, Cl, Br, Hg, etc) → lost during early stages.
 Radioactive elements (e.g. Rb, K) → lost due to radioactive decay.
- Gains:** Daughter products of radioactive decay (e.g. Sr).
 Addition of cosmic dust (permanent process) (e.g. Be).

Radioactive daughter elements → Increase as a function of the age of the planet rather than initial composition!

However, elements are not evenly distributed as layering/differentiation of the Earth redistributed the elements into core, mantle and crust. Since visible already in chondrites, it appears that certain elements partition preferentially in three co-existing phases :

Siderophile: affinity for metallic phases

Chalcophile: affinity for sulphide phases

Lithophile: affinity for silicate phases

Atmophile: affinity for gaseous state

This was first realised by the Norwegian geochemist *V.M. Goldschmidt* and is therefore referred to as the Goldschmidt classification. The theoretical basis for this classification is the structure of the atoms - primarily the electron configuration - and their effect on bonding (bond strength and bond type) and is closely related to the position of an element in the Periodic table.

Lithophile: elements which readily form ions with a complete outermost shell containing 8 electrons (affinity with oxygen): Al, Na, K, Ca, etc.

Chalcophile: elements which have 18 electrons in the outermost complete shell (affinity with sulphur): Cu, Se, As, Zn, Cd, etc.

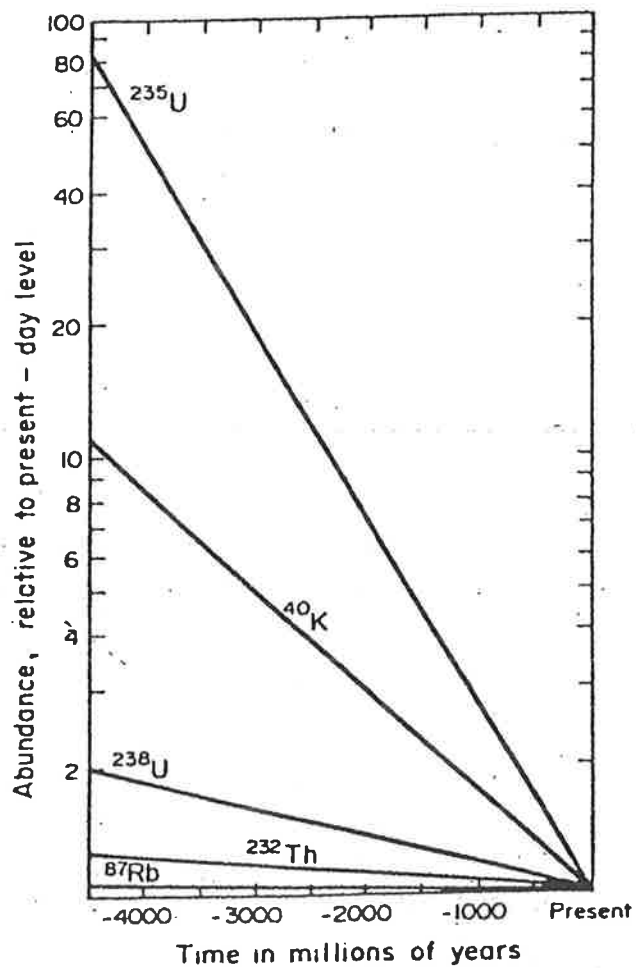
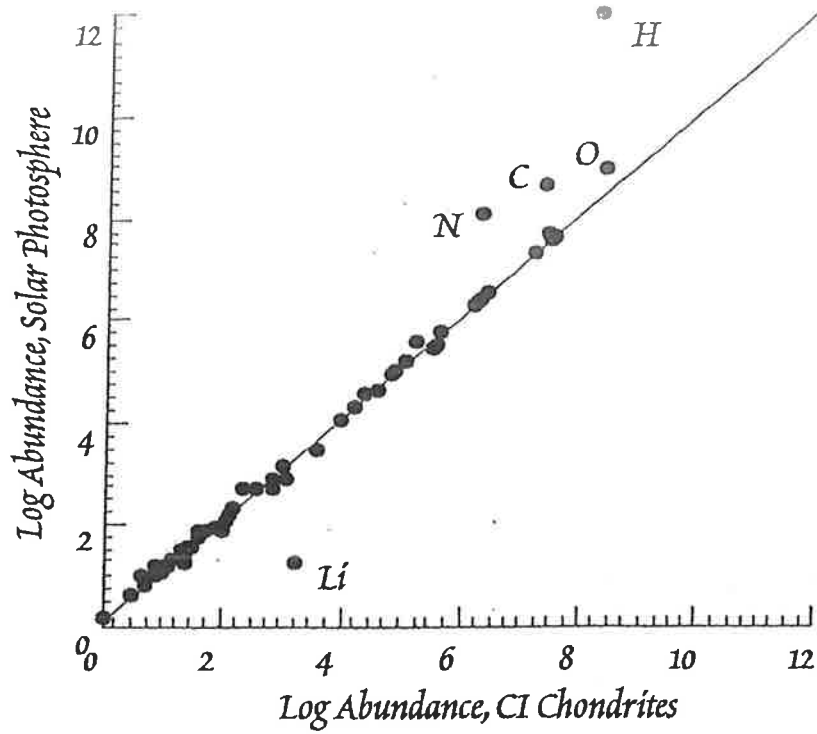
Siderophile: Group VIII + neighbouring elements with incompletely filled outermost shells (don't combine, remain isolated): Fe, Ni, Pt, Co, Au, etc.

Goldschmidt not only setup a classification for elements but also produced rules which enable the geochemist to determine the sequence in which various minerals crystallise and thereby redistribute the elements during e.g. magmatic processes.

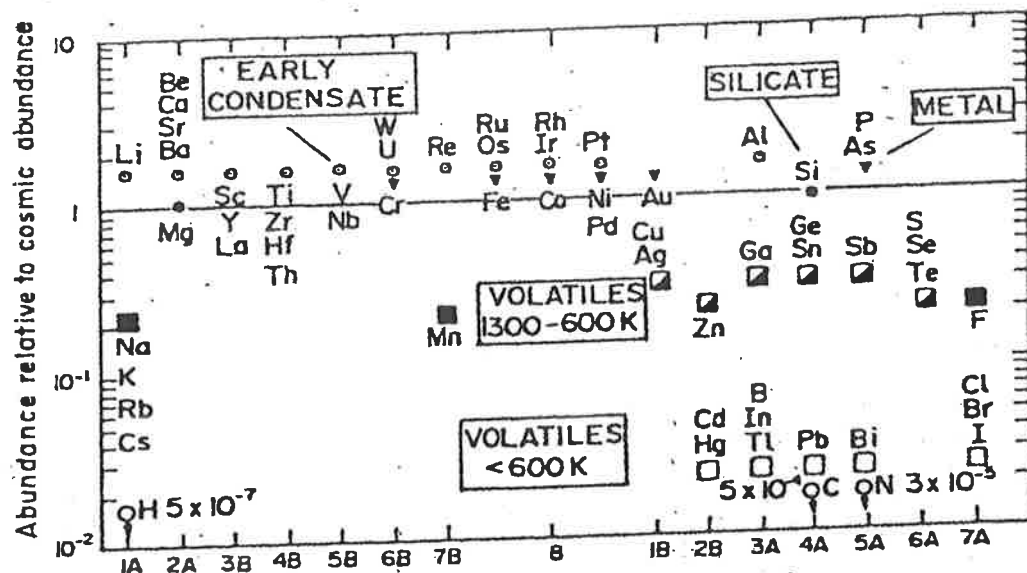
The rules are based on the reactivity and an elements "affinity" depends on

(a) the electronic structure of the atom

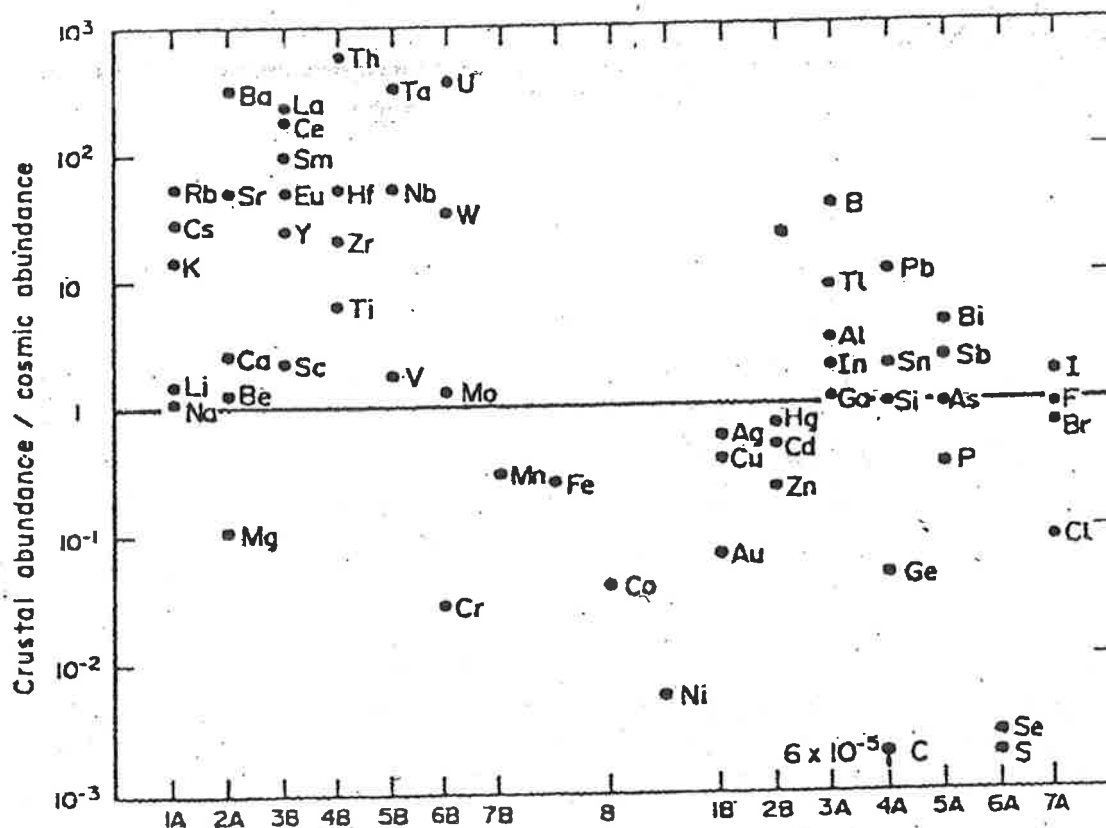
(b) the firmness to which the outer electrons are bound to the nucleus



Relative changes (log scale) in the abundances of some radioactive isotopes in the Earth over 4500 million years.



Model composition of the Earth, relative to cosmic abundances. It is based on the assumption that each component contains its cosmic complement of trace elements. The ordinate is divided according to the chemical groups of the periodic table. (After Ganapathy and Anders, 1974)



Composition of the crust, normalized to cosmic abundances of the elements and to Si = 10^6 atoms. The diagram is in the same format as Fig. 4.3, with which it may be compared

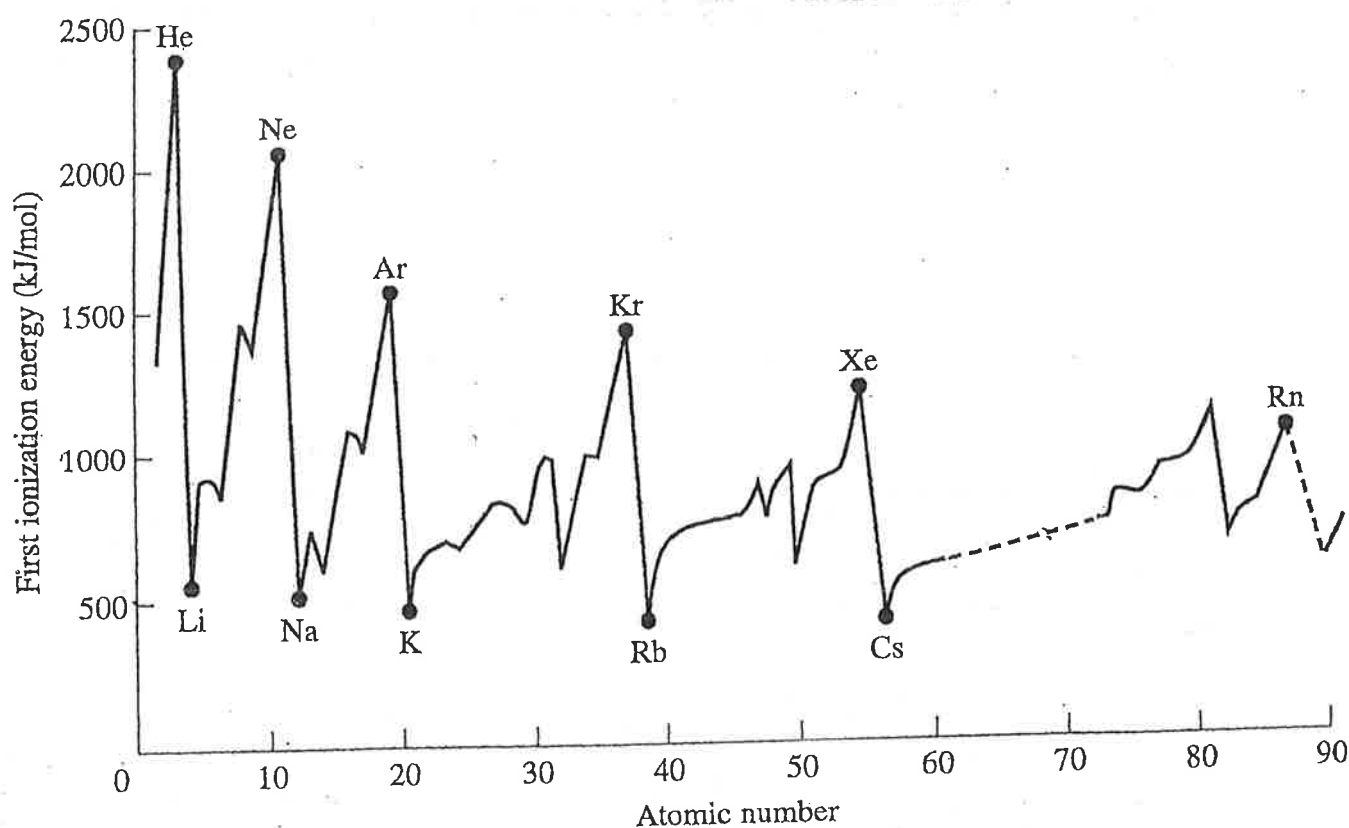
Geochemical Classification of the Elements (based on distribution in meteorites)

Siderophile	Chalcophile	Lithophile	Atmophile
Fe* Co* Ni*	(Cu) Ag	Li Na K Rb Cs	(H) N (O)
Ru Rh Pd	Zn Cd Hg	Be Mg Ca Sr Ba	He Ne Ar Kr Xe
Os Ir Pt	Ga In Tl	B Al Sc Y La-Lu	
Au Re† Mo†	(Ge) (Sn) Pb	Si Ti Zr Hf Th	
Ge* Sn* W†	(As) (Sb) Bi	P V Nb Ta	
C‡ Cu* Ga*	S Se Te	O Cr U	
Ge* As† Sb†	(Fe) Mo (Os)	H F Cl Br I	
	(Ru) (Rh) (Pd)	(Fe) Mn (Zn) (Ga)	

*Chalcophile and lithophile in the earth's crust.

†Chalcophile in the earth's crust.

‡Lithophile in the earth's crust.



Variation of the first ionization potential with atomic number. Note that the noble gases have high ionization energies, whereas the alkali metals and alkaline earth metals have low ionization energies. (After R. Chang, *General Chemistry*, p. 262. Copyright 1986 by McGraw-Hill, Inc. Used with permission of McGraw-Hill, Inc.)

The affinity will be governed by the relative reactivities of an element with oxygen or sulphur. (a)+(b) are inter linked. (b) Depends on (a) because the variation in effectiveness with which given arrangements of electrons shield the outer electron depends on the charge of the nucleus. If the screening by inner electrons is efficient, outer electrons are loosely held and are thus available for chemical reaction, and vice versa. The energy to completely remove an electron from an atom is called "Ionisation Potential" (in eV). The energy required to remove the first electron is termed the first Ionisation Potential (I_1). The energy required to remove a second electron the second Ionisation Potential (I_2), and so on.

Low Ionisation potential: electrons are removed easily = chemically active.

High Ionisation potential: electrons are removed with difficulty = chemically inactive

EXAMPLE: Na and Cu:

Both are in group I of the Periodic Table (Na in Ia; Cu in Ib). Atoms of both Na and Cu contain a single ~~atom~~ ^{electron} outside a so called closed shell of electrons. 8 in Na and 18 in Cu. The similarity of the structure is shown in the near identical ionic radii ($\text{Na}^+ = 0.97 \text{ \AA}$, $\text{Cu}^+ = 0.96 \text{ \AA}$). However, the first Ionisation potential of Na = 5.1 eV, whereas that of Cu = 7.7 eV. Hence, the single outer electron is more firmly bound in Cu and thus Cu is chemically less active. This has an effect on the siderophile, chalcophile and lithophile tendencies.

Group Ia		Group Ib	
Element	I_1 (eV)	Element	I_1 (eV)
Li	5.3		
Na	5.1		
K	4.3	Cu	7.7
Rb	4.1	Ag	7.5
Cs	3.9	Au	9.2

Note the striking difference between the I_1 's of the two groups.

Au-anomaly: generally there is a trend of falling I_1 with increasing atomic weight in each group. Au, however, does not follow this trend. Au holds valency electrons so firmly that it reacts with virtually no other element.

From this the character of an element (affinity) can be predicted, i.e., Li, Na, K, Rb and Cs are lithophile, Cu and Ag are chalcophile and Au is siderophile.

Geochemistry- Lecture 3

Secondary Element Distribution-Magmatism

Major elements in magmatic processes

The discussion so far has concerned the way ions group together according to their affinities (i.e. siderophile, lithophile, calcophile and atmophile). The evolution of the Earth, however, proceeded very rapidly and a differentiated planet was formed. In this process, ions in the lithosphere (the lithophile elements) that make up the vast bulk of the mantle and the crust were again redistributed, this time from the primitive mantle into the developing crust.

The principal mechanisms involved were (1) melting of the mantle and (2) differentiation of the melt produced this way.

(1) Mantle melting: redistribution between solid and liquid phases where elements partitioned themselves between the residual solids and the mantle melt.

(2) Mantle melts then ascend towards the Earth surface where they undergo differentiation and/or crystallisation, redistributing again elements between the solid and the liquid phase.

Redistribution implies that the relative proportions (concentrations) of the elements change during these processes, so that the resultant solids and liquids have different compositions than the starting compositions. This can be expressed by **distribution coefficients** (K_D). Distribution coefficients are controlled by:

★ **The structure** of the ions and molecules in solids and liquid and their relative energies and stabilities.

★ **Thermodynamics.** The inherent activity of elements under various equilibrium conditions and the energy states that exist in the liquid or the solid phase.

★ **Kinetics:** this involves

- a) the generation of magma – rate and extent of melting and separation of liquid from the solid
- b) the transport of magma – degree of fractionation or separation during transport, mixing or mode and rate of accumulation.
- c) consolidation of magma – rates of cooling and fractionation etc. and the openness of the system (e.g. volatile loss).

Kinetics: The process of crystallisation from a melt can be linked to a sieving process whereby the various elements are preferentially extracted in a sequence by which, with falling temperature, successive elements are progressively fixed in solid crystals. Conversely in the case of melting from a solid polycrystalline mantle elements are preferentially fixed in a sequence by which, with rising temperature successive elements are progressively released from the solid.

Thermodynamics: The thermodynamic approach to the process envisages that the crystallisation takes place at equilibrium, and the process can be viewed in terms of escaping tendencies, i.e. the tendency for each constituent to escape from one phase to another. Quantitatively this is expressed by the chemical potential or fugacity (gases) and the deviation from ideal behaviour in solution, the activity coefficient.

Structural considerations are very significant because the abundance of Si^{4+} , a strongly lithophile element which rapidly bonds to oxygen to form SiO_4 complexes which exist in tetrahedral clusters in the melt. These clusters polymerise to networks and orient themselves to form regular crystal lattices. The networks and lattices provide sites for the remaining cations which then compete for the appropriate spaces in the structures. Here we come back to the distribution coefficient. The success of a cation in getting a place in the "secure harbour" of a crystal lattice is quantitatively expressed by the partition or distribution coefficient (K_D), indicating the degree to which an element is depleted in the liquid and enriched in the solid or vice versa.

$$K_D = C_M / C_L = \text{conc. in the mineral} / \text{conc. in the solid}$$

$K_D > 1 \rightarrow$ strong enrichment in the solid i.e. the element is compatible in the crystal.

$K_D < 1 \rightarrow$ strong enrichment in the liquid, i.e. the element is incompatible in the crystal.

Most rock forming minerals are solid solutions i.e. they contain varying proportions of end members (remember Lecture 2) and the partition coefficients show that Mg is for example incorporated first in the olivine lattice, Fe follows later. A tendency characteristic for magmatic evolution. Such a pair of ions which substitute in the structure are known as diadochs and the process is called ionic substitution.

Goldschmidt's Laws for Ionic substitution

These laws give good guidelines for major elements, though they are too simplistic for most trace elements. However, they still provide good approximations for them.

1) Two ions of equal radius and charge substitute with equal facility.

\rightarrow equal chance to enter the solid phase, i.e. neither will be enriched or depleted in the liquid.

Example zircon: Zr^{4+} (0.79 Å) and Hf^{4+} (0.78 Å)

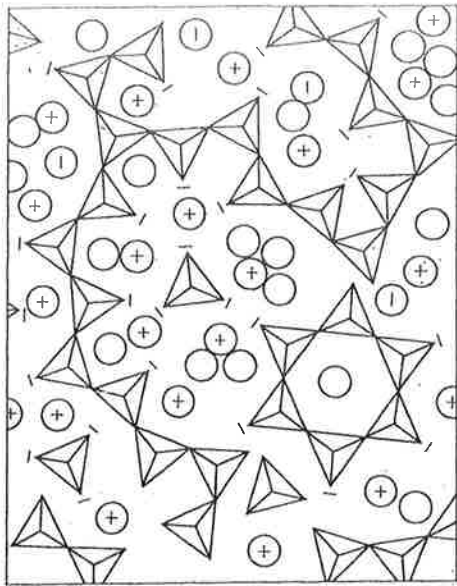
2) Two ions of the same charge but different radius – the smaller ion is preferred in the solid.

Example: olivine Mg^{2+} (0.66 Å) and Fe^{2+} (0.74 Å)
or Ni^{2+} (0.69 Å) and Fe^{2+} (0.74 Å)

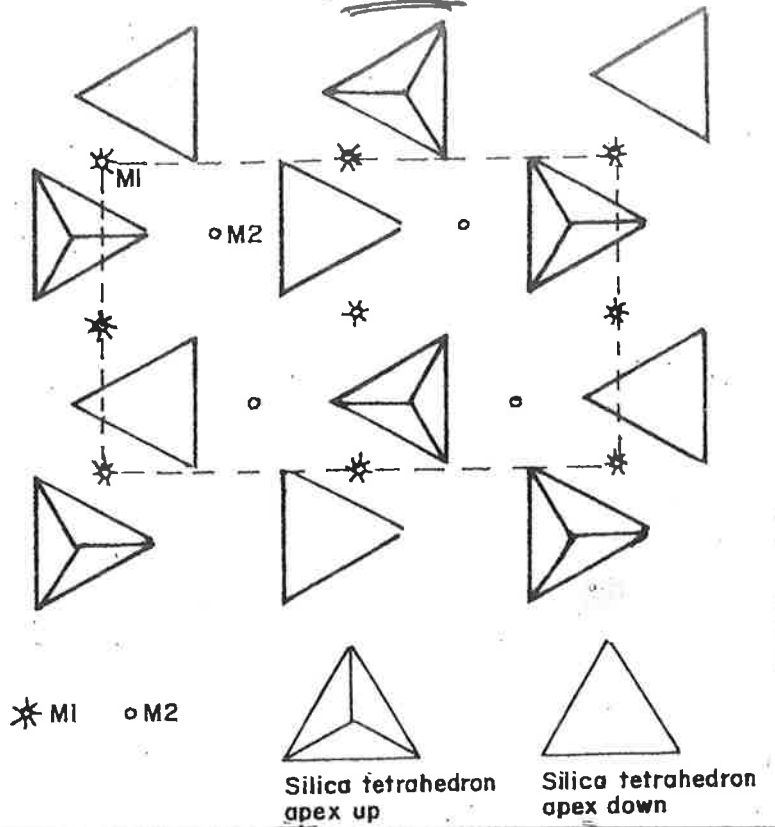
3) Two ions of the same radius but different charge – the higher charge is preferred in the crystal

Example: plagioclase Ca^{2+} (0.99 Å) to Na^+ (0.97 Å)
 Sc^{3+} (0.81 Å) to Mg^{2+} (0.66 Å)

Melt

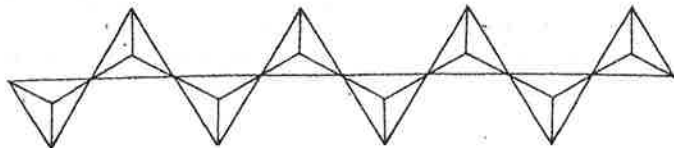


Olivine



PYROXENE

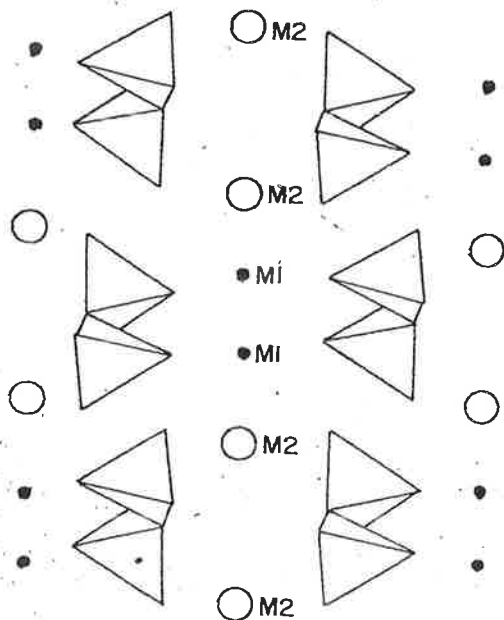
(a) Single chain



Plan view

$(\text{SiO}_3)_n^{2n-}$

End view



Goldschmidt's
Radius - ratio - rule

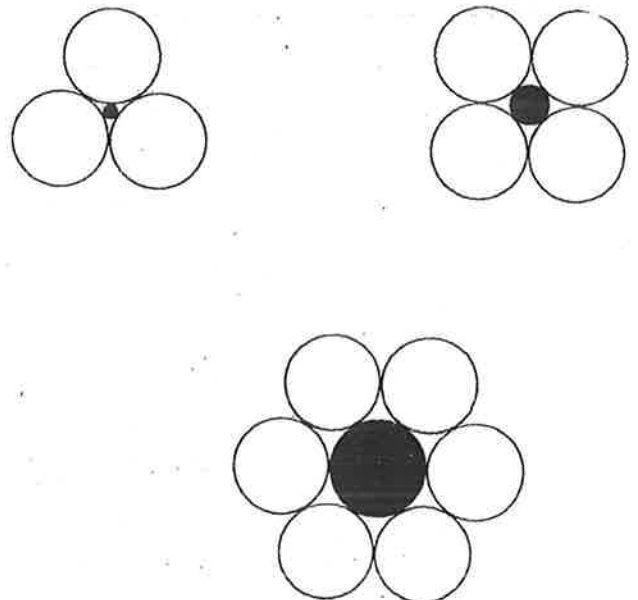


Figure 4.2 Planar representation of the relationship between radius ratio and coordination number.

The significance of ion size becomes clear when we consider that the ions have to be accommodated in the silicate structure which is dominated by SiO_4 tetrahedra and their bonding can only take place when the co-ordination number is acceptable to the sites available. Hence:

Goldschmidt's radius ratio rule which shows, if the relative sizes of cation and anion are known, then the number of anions that can pack around the cation can be determined. In fact diadochic replacement can only occur between elements of the same co-ordination number with oxygen. e.g. substitution with Si (4-fold elements), with Al (4 or 6 fold elements), with Ca (6 or 8 fold elements and with K (8 or 12 fold elements). The charge required is linked with this – in any site the available cation charge must be distributed amongst the anions around it and the ions which can produce stronger bonds will be preferred within these limits.

During the crystallisation of a silicate melt, the structures which form become larger and more complex as crystallisation proceeds; this is because there is only a finite number of oxygen ions and as these are used up as SiO_4 bonds (4 oxygens to each silicon) it becomes necessary for the remainder to be shared. Hence, larger cations tend to be incorporated later in the sequence (K^+ 1.33 Å) doesn't appear till late (K-fsp) whereas Na^+ (0.97 Å) enters early (plag, px).

Another element whose fate in evolving magmas is a very important petrological indicator is Al. Al^{3+} can occupy either Y-sites (substitute for Mg, Ca in 6-fold co-ordination) or Z sites (for Si in 4-fold co-ordination). To occupy Z-sites a complex Si-O structure is necessary but where this is available (e.g. in plag) the structure with Al^{3+} is thermally more stable because the Al^{3+} uses up less of the available O_2^- charges and gives stronger bonded structure. Hence, the high temperature plag is anorthite ($\text{CaAl}_2\text{Si}_2\text{O}_8$) rather than albite ($\text{NaAlSi}_3\text{O}_8$).

Trace elements in magmatic processes

A trace element can be defined as an element present in a rock in concentrations < 0.1wt% (<1000ppm). Sometimes trace elements will form minerals on their own (e.g. zircon), but more commonly they substitute for major elements in rock forming minerals. Trace elements have become extremely useful in discriminating between different magma series, between different magma sources and between different magmatic processes because they obey Henry's law at very low concentrations (activity is proportional to their concentration at equilibrium conditions) and can thus be modelled mathematically, allowing quantitative testing of petrological models, especially crystal-liquid equilibria. Another advantage of trace elements is that many of them are fairly insensitive to surface weathering and retain their inter-element ratios even in altered rocks. These elements are known as immobile trace elements. Trace elements in combination with isotope studies have become the most important aids to identifying and defining the chemical/petrological nature of the mantle and the sources of magmas plus the processes of magma evolution (differentiation, assimilation, magma mixing etc.).

Geochemical behaviour of trace elements

The behaviour of trace elements is generally described as a preference for the melt (liquid) or the crystal (solid). Those elements that are partitioned into the crystal phase at any given equilibrium state are compatible, those that are partitioned into the liquid are incompatible.

Incompatible elements are the last to be extracted from a melt during crystallisation, i.e. they will be concentrated in the melt during fractional crystallisation. They will also be the first to enter the melt when solid rock is heated. Then they will be highly concentrated in a very small degree of partial melt.

The degree of compatibility varies of course between melts of different compositions and between different minerals. Goldschmidt's rules still have a value for these elements being used in subdivision on the basis of charge and size, often called field strength (electrostatic charge per unit area of surface of the cation or ionic potential). Ions with similar charge and size show similar geochemical behaviour.

Small highly charged cations are HIGH FIELD STRENGTH elements or HFSE (ionic potential >2). Large low charged cations are LOW FIELD STRENGTH elements, commonly known as large lithophile elements LILE.

Distribution coefficients

Trace element behaviour can be modelled assuming them to obey Henry's law at equilibrium, i.e. the activity is directly proportional to the concentration $a_{TE} = K_{TE} \cdot X_{TE}$, where a is the activity, K the Henry's law constant and X the composition of an element. This clearly shows a compositional control to the behaviour of a trace element. Trace elements do thus enter a mineral in an amount that can be calculated given that K is known. As long as Henry's law is obeyed the distribution coefficient between mineral and melt gives a measure for the tendency of an element to enter a solid. This partition coefficient or distribution coefficient (remember $K_D = C_M/C_L$) can be measured for most minerals in volcanic rocks by analysis of the concentration of an element in the crystal and in the surrounding glass. Then a $K_D > 1$ implies the element is compatible, a $K_D < 1$ implies it is incompatible.

When an element critically exceeds the concentration of the ppm level or is very low ($< 10\text{ppm}$) the distribution coefficient is no longer directly proportional to the composition and the mineral/glass ratio no longer reflects the distribution behaviour accurately. For example in accessory REE-minerals some elements are strongly concentrated, although they are present at trace element concentrations in the liquid. (e.g. Zr in titanite, monazite, and of course in zircon).

1	H	2	He																														
3	Li	4	Be																														
11	Na	12	Mg																														
19	K	20	Ca																														
37	Rb	38	Sr	39	Y	40	Zr	41	Nb	42	Mo	43	Tc																				
55	Cs	56	Ba	57	La	58	Ce	59	Pr	60	Nd	61	Pm	62	Sm	63	Eu	64	Gd	65	Tb	66	Dy	67	Ho	68	Er	69	Tm	70	Yb	71	Lu
87	Fr	88	Ra	89	Ac																												
Rare earth elements																																	
Platinum group elements																																	

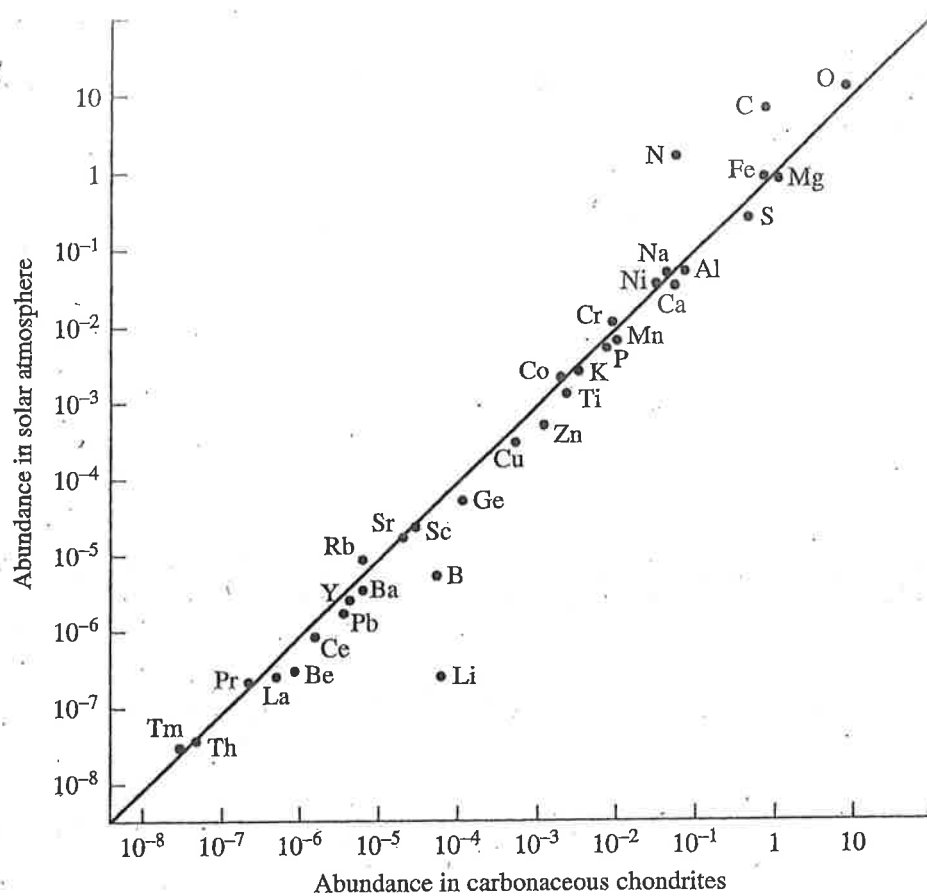


Figure 1-8 Comparison of abundances of elements in Type 1 carbonaceous chondrites with abundances in the solar atmosphere. In both cases, abundances are in terms of atoms per silicon atom. Type 1 carbonaceous chondrites are chondrites with volatile elements in approximately the same proportions as in the Sun. They are representative of primitive material from which the solar system formed. (After Wood, J. A., *The Solar System*. Copyright © 1979. p. 103. Adapted by permission of Prentice Hall, Inc., Upper Saddle River, NJ.)

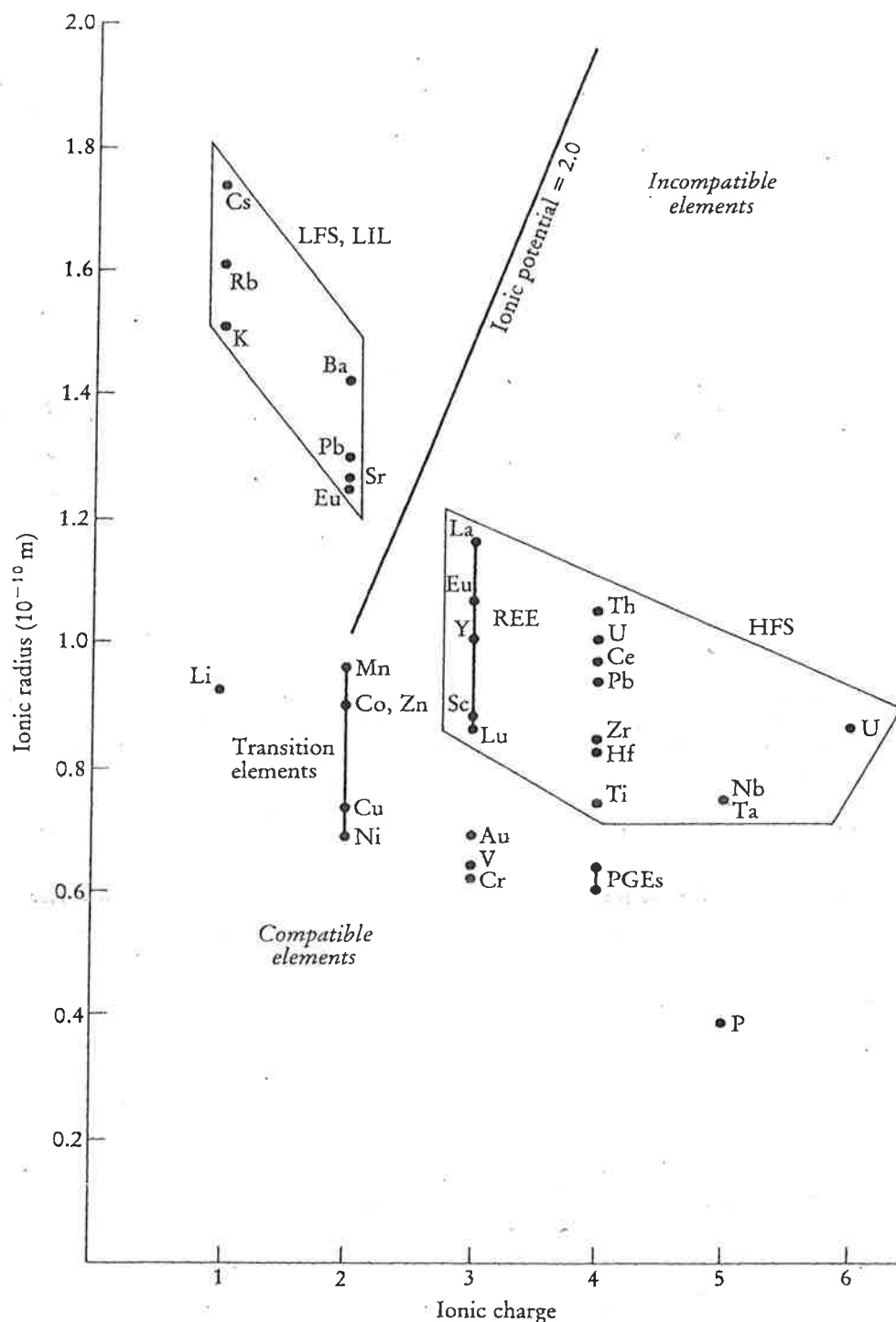
Cosmic Abundances of the Elements

(atoms per 10,000 atoms Si)*				
Z	Element	Abundance	Z	Element
1	H	4.0×10^8	44	Ru
2	He	3.1×10^7	45	Rh
3	Li	1.0	46	Pd
4	Be	0.20	47	Ag
5	B	0.24	48	Cd
6	C	35,000	49	In
7	N	66,000	50	Sn
8	O	215,000	51	Sb
9	F	16	52	Te
10	Ne	86,000	53	I
11	Na	440	54	Xe
12	Mg	9100	55	Cs
13	Al	950	56	Ba
14	Si	10,000	57	La
15	P	100	58	Ce
16	S	3750	59	Pr
17	Cl	90	60	Nd
18	A	1500	61	Pm
19	K	32	62	Sm
20	Ca	490	63	Eu
21	Sc	0.28	64	Gd
22	Ti	24	65	Tb
23	V	2.2	66	Dy
24	Cr	78	67	Ho
25	Mn	69	68	Er
26	Fe	6000	69	Tm
27	Co	18	70	Yb
28	Ni	270	71	Lu
29	Cu	2.1	72	Hf
30	Zn	4.9	73	Ta
31	Ga	0.11	74	W
32	Ge	0.51	75	Re
33	As	0.04	76	Os
34	Se	0.68	77	Ir
35	Br	0.13	78	Pt
36	Kr	0.51	79	Au
37	Rb	0.07	80	Hg
38	Sr	0.19	81	Tl
39	Y	0.09	82	Pb
40	Zr	0.55	83	Bi
41	Nb	0.01	90	Th
42	Mo	0.02	92	U
43	Tc	—		

* After Suess and Urey, *Rev. Mod. Phys.*, **28**, 53-74, 1956.

Abundances of Elements in the Solar Atmosphere

Element	Atomic number	Abundance (atoms/ 10^4 atoms Si)
H	1	3.2×10^8
He	2	0.5×10^8
C	6	166,000
N	7	30,000
O	8	290,000
Na	11	630
Mg	12	7900
Al	13	500
Si	14	10,000
S	16	6300
K	19	16
Ca	20	450
Sc	21	0.2
Ti	22	15
V	23	1.6
Cr	24	33
Mn	25	25
Fe	26	1200
Co	27	14
Ni	28	260
Cu	29	35
Zn	30	8



Figure

Plot of ionic radius vs ionic charge for trace elements of geological interest. An ionic potential (charge/size ratio) of 2.0 subdivides the incompatible elements into low field strength (LFS) elements, also known as large ion lithophile elements (LIL) and high field strength elements (HFS). Compatible elements are placed towards the bottom, left-hand corner of the diagram. The ionic radii are from Shannon (1976) and are quoted for eight-fold coordination to allow a comparison between elements. Some of the first transition series metals (transition elements) and the PGE elements, are quoted for six-fold coordination.

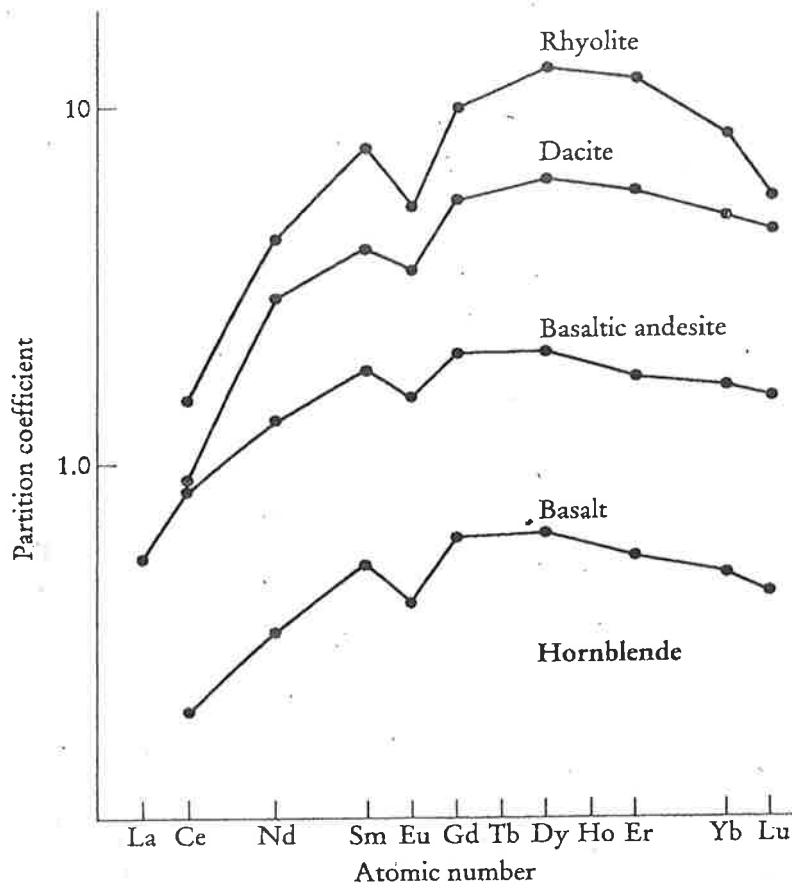
Bulk distribution coefficient (D)

Since a magma usually contains more than one phenocryst phase a trace element is removed from the melt relative to the types of minerals crystallising and their amount. This can be expressed in the bulk distribution coefficient D_{TE} with $D = \sum_i W_i K_{Di}$. D is the bulk distribution coefficient reflecting how much of an element is removed by the sum of all minerals crystallising, with each mineral showing a different partition coefficient at the given equilibrium state.

D is sensitive to a number of controls:

- ✱ Firstly it is of course composition dependant. It varies with magma type, i.e. with changing liquid and mineral composition. D in basic magmas are often an order of magnitude lower than in associated acidic magmas.
- ✱ The crystal structure is a further variable. Different minerals accommodate different elements in different concentrations.
- ✱ D is also temperature dependant. E.g. Sr distribution in plagioclase is a log function of T between 1100°C and 1400°C.
- ✱ Another control is the fugacity of oxygen in the magma (the partial pressure of oxygen in the melt, i.e. is the system oxygen rich or poor, oxidising or reducing). This influences not only iron Fe ($Fe^{2+} \rightarrow Fe^{3+}$) but also in elements such as Eu. At low f_{O_2} Europium occurs as Eu^{2+} , whereas at high f_{O_2} it occurs as Eu^{3+} . This has a major impact on whether Eu is accommodated in Plagioclase and ferromagnesian phases. Plagioclase incorporates Eu^{2+} but ferro-magnesian phases do not. This means Eu is incompatible during olivine and pyroxene crystallisation but becomes compatible when plagioclase starts to crystallise (under normal low f_{O_2} conditions). During advanced differentiation f_{O_2} increases and Eu becomes increasingly incompatible again. This behaviour of Eu is therefore used to evaluate plagioclase fractionation which produces a negative anomaly on a spider plot.

Next lecture we will explore the influence of various D's during magmatic processes in a quantitative way. You should therefore be fairly familiar with the principles we discussed today. The best summary of the topic is probably given in Rollinson, "Using Geochemical Data" !!! Maybe you also want to check in Klein and Hurlbut "Manual of Mineralogy."



A plot of the partition coefficients for the rare earth elements between hornblende and melt (log scale) vs atomic number (normal scale) in basalt, basaltic andesite, dacite and rhyolite. There is a clear increase in partition coefficient with increasing silica content of the melt, amounting to an order of magnitude difference between basaltic and rhyolitic melts.

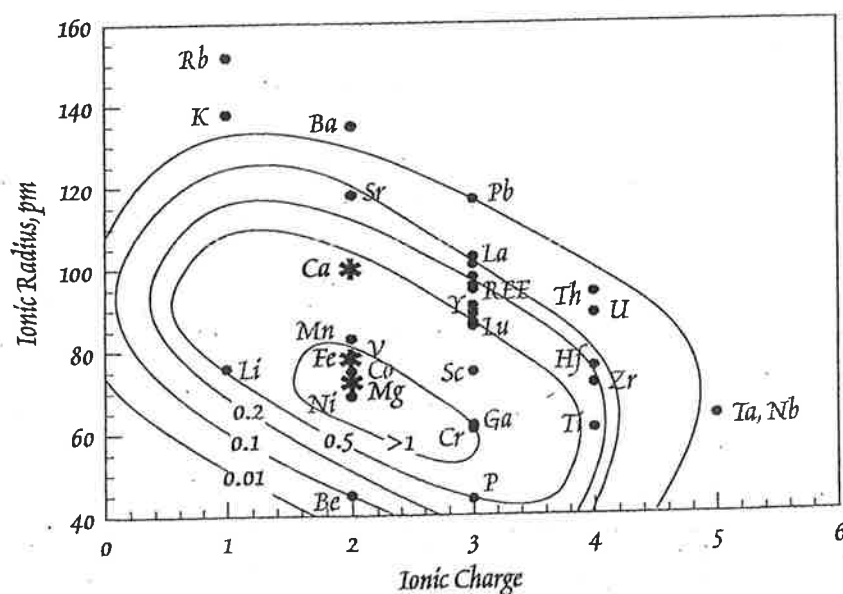
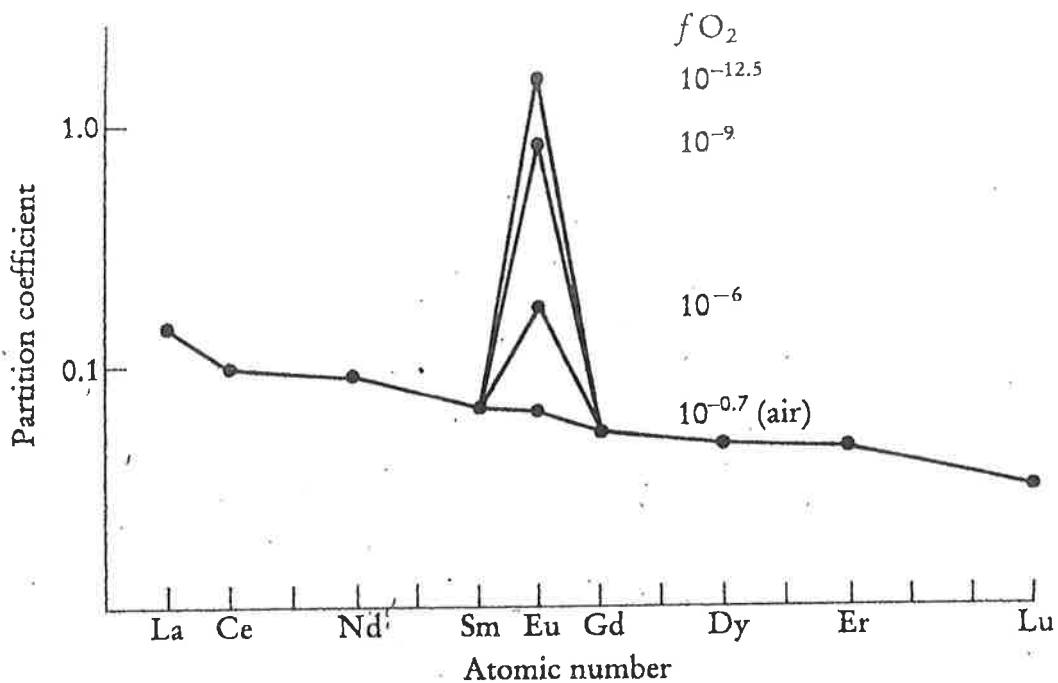
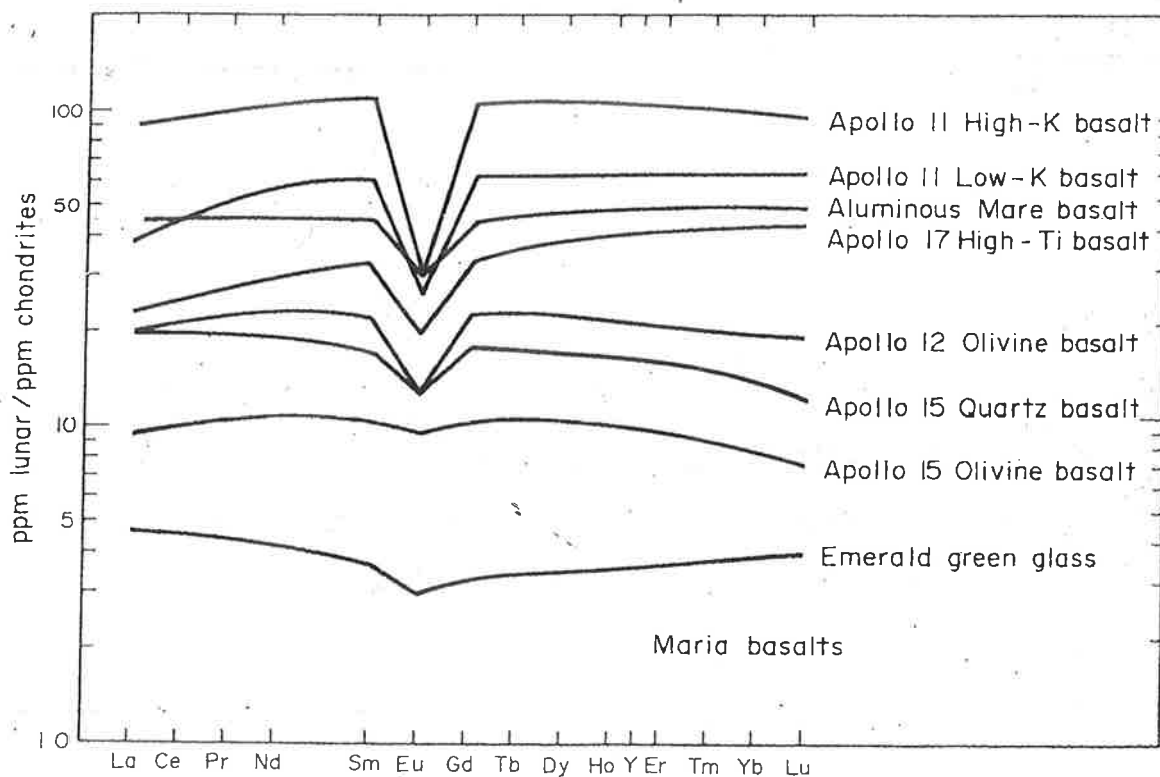


Figure 7.10. Ionic radius (picometers) vs ionic charge contoured for clinopyroxene/liquid partition coefficients. Cations normally present in clinopyroxene are Ca^{2+} , Mg^{2+} , and Fe^{2+} , shown by * symbols. Elements whose charge and ionic radius most closely match that of the major elements have the highest partition coefficients.



The partition coefficient for Eu between plagioclase and a basaltic melt plotted as function of oxygen activity (fO_2) compared with other REE (after Drake and Weill, 1975)



Element abundance patterns, normalized to abundances in chondrites, for maria basalts. (After Taylor, 1975)

Ytterby is a village on the Swedish island of Resarö, in Vaxholm Municipality in the Stockholm archipelago.

Lending its name to a famous quarry where many rare earth minerals have been discovered, the small village has been the inspiration for naming four chemical elements on the Periodic Table: Yttrium(Y), Ytterbium(Yb), Terbium(Tb) and Erbium(Er).

Three other elements also trace their origin to the Ytterby quarry: Gadolinium (Gd) (named after gadolinite, which is named after Professor Johan Gadolin), Holmium (Ho) (from the Latin name for Stockholm), and Thulium (Tm) (Thule is an old Latin word for the Nordic countries).

(From wikipedia)

Ytterby mine in Resarö delivered feldspar and quartz for the glass and porcelain industry until the 18th century.

All of the elements discovered, except Thulium and Gadolinium(!), were initially extracted from the mineral Gadolinite.

Gadolinite is a mineral of a nearly black color and vitreous luster, and consisting principally of the silicates of cerium, lanthanum, neodymium, yttrium, beryllium, and iron with formula: $(\text{Ce,La,Nd,Y})_2\text{FeBe}_2\text{Si}_2\text{O}_{10}$. Called gadolinite-(Ce) or gadolinite-(Y) depending on the prominence of the variable element composition (namely, Y if it has more yttrium, and Ce if it has more cerium).

Gadolinite is fairly rare, but it forms attractive crystals that some collectors desire. Its hardness is between 6.5 and 7, and its specific gravity is between 4.0 and 4.7. It fractures in a conchoidal pattern. The mineral's streak is grayish-green.

Gadolinite was named in 1800 for Johan Gadolin, the Finnish mineralogist- chemist who first isolated an oxide of the rare earth element yttrium from the mineral in 1792. The rare earth gadolinium was also named for him. However, gadolinite does not contain more than trace amounts of gadolinium.

(From wikipedia)



hydrogen 1 H	lithium 3 Li	beryllium 4 Be																	boron 5 B	carbon 6 C	nitrogen 7 N	oxygen 8 O	fluorine 9 F	helium 2 He
1.0079	6.941	9.0122																	10.811	12.011	14.007	15.999	18.998	4.0026
Li	Be	Mg																	B	C	N	O	F	Ne
11	12	24.305																	13	14	15	16	17	18
Na	Mg																		Al	Si	P	S	Cl	Ar
22.990																			28.982	28.086	30.974	32.065	35.453	39.948
potassium 19	calcium 20	calcium 20																	gallium 31	germanium 32	arsenic 33	selenium 34	bromine 35	krypton 36
K	Ca	Ca																	Ga	Ge	As	Se	Br	Kr
39.098	40.078	40.078																	69.723	72.61	74.922	78.96	79.904	83.80
rubidium 37	strontium 38	strontium 38																	indium 49	tin 50	antimony 51	tellurium 52	iodine 53	xenon 54
Rb	Sr	Sr																	In	Sn	Sb	Te	I	Xe
85.468	87.62	87.62																	114.82	118.71	121.76	127.60	126.90	131.29
caesium 55	barium 56	barium 56																	thallium 81	lead 82	bismuth 83	polonium 84	astatine 85	radon 86
Cs	Ba	Ba																	Tl	Pb	Bi	Po	At	Rn
132.91	137.33	137.33																	204.38	207.2	208.98	209	210	222
francium 87	radium 88	radium 88																	unquadium 114	Uuq				223
Fr	Ra	Ra																	Uuq					

Key:
 element name
 atomic number
 symbol
 atomic weight (mean relative mass)

lanthanum 57 La	cerium 58 Ce	praseodymium 59 Pr	neodymium 60 Nd	promethium 61 Pm	samarium 62 Sm	europium 63 Eu	gadolinium 64 Gd	terbium 65 Tb	dysprosium 66 Dy	holmium 67 Ho	erbium 68 Er	thulium 69 Tm	ytterbium 70 Yb
138.91	140.12	140.91	144.24	144.91	150.36	151.96	157.25	158.93	162.50	164.93	167.26	168.93	173.04
La	Ce	Pr	Nd	Pm	Sm	Eu	Gd	Tb	Dy	Ho	Er	Tm	Yb
89	90	91	92	93	94	95	96	97	98	99	100	101	102
Ac	Th	Pa	U	Np	Pu	Am	Cm	Bk	Cf	Es	Fm	Md	No
227	232.04	231.04	238.03	237	244	243	247	247	251	252	257	258	259

*lanthanoids

**actinoids

The use of distribution coefficients in Melting and Crystallisation models.

Simple models have been devised to quantify changes in trace element concentrations during both partial melting and fractional crystallisation.

1. Partial Melting

Batch melting

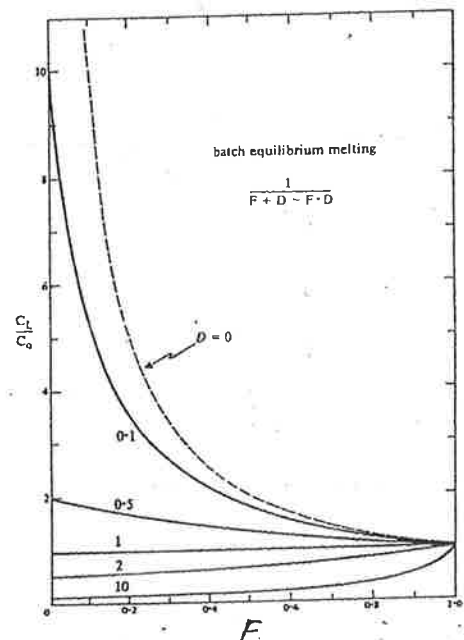
The simplest model is for Equilibrium Batch Melting. The liquid remains at the site of melting and is in equilibrium with the solid residue until mechanical conditions allow it to escape as a "batch" of primary magma. Here the concentration of an element in the liquid (C_L) is related to the concentration (C_0) in the original source material (mantle or lower crust) by the expression:

$$C_L / C_0 = 1 / (F + D - FD)$$

where F = wt. fraction of melt formed ($F = 0$ = solid; $F = 1$ = liquid) and D = bulk distribution coefficient for residual solids at the moment the melt is removed.

To determine D , one must calculate the proportions of the residual minerals. We can see that the enrichment of incompatibles ($D \ll 1$) in the magma approaches $1/F$ (since $D - FD$ is almost zero for very small D) and this enrichment factor can be very high for small degrees of partial melting where F is very small.

The maximum limit is $1/D$ when F nears zero (i.e. very small degree of melting \rightarrow e.g. for $D=0.1$, $1/D=10$). This is reached when F is infinitesimally small, i.e. the very first drops of melt. (Note: $D=0$ when nothing enters crystal or leaves melt). One important use for this model is in constraining the trace element composition of the source rock to a magma.



Example 1: consider a partial melt from a mantle peridotite ($D_{Ce} = 0.012$). Then the maximum enrichment of Ce in the melt can be $1/D = 1/0.012 = 80$ for very small degrees of melting. Increasing degrees of melting will reduce the enrichment. In any case Ce will be strongly enriched in the melt.

Example 2: consider a partial melt ($F=0.2$) from a mantle peridotite ($D_{Ni} = 2$). $\rightarrow 1/(0.2+2)-(0.2 \times 2) \rightarrow 1/2.2 - 0.4 \rightarrow 1/1.8 = 0.55$. Hence the concentration of Ni is higher in the solids than in the liquid defining Ni to be compatible in mantle rocks

NOTE: We know that alkali basalts have high REE (e.g. Ce) contents - up to 100 x chondrite. From the model - even with a very small degree of partial melt - the theoretical maximum enrichment from a chondrite is x 80, hence the source of alkali basalt magma cannot have a primitive chondrite composition. It must have been already the product of an event that enriched Ce in mantle peridotites! Kay and Gast (1973) proposed that the mantle source for alkali basalts must have had 2-5 x chondritic REE abundances - and even then the basalt magma would only be a 2% partial melt. As this seems to be too small a fraction to be efficiently extracted it has been assumed that either:

- 1) the magma was subsequently enriched in REE by crystal fractionation
- 2) the mantle source is LIL enriched - for example by volatile metasomatism

Incremental Batch Melting

Incremental Batch Melting models repeated extraction of melts each from the same source under equilibrium conditions. This produces a more rapid rate of depletion of incompatibles, which means that *late liquids* might have even lower incompatible element concentrations than the original source, since almost all has been extracted already.

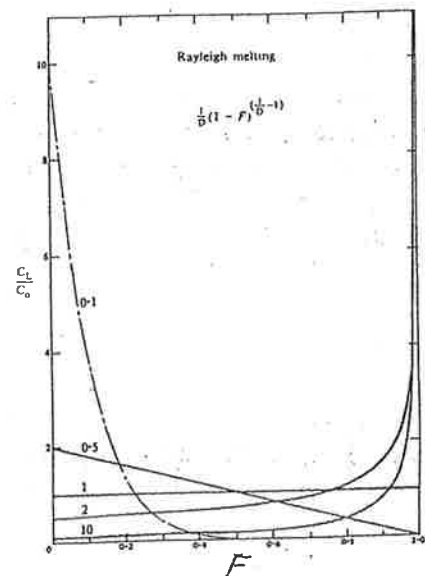
This could be important in assessing the source of MORB tholeiitic basalts. These rocks are depleted in LILs, and in particular the ratio of LREE to HREE is quite different to chondritic meteorites. The answer seems to be that the mantle source for MORB has already been depleted by the removal of a small-degree partial melt which has taken out much of the LIL's, especially the LREE's.

Rayleigh Melting

Rayleigh Melting models an infinitely small amount of liquid formed in equilibrium with the residue, then removed from the system. This gives the limiting extreme to changes in trace element content where the melt migrates faster than diffusion in the solid phases. It produces changes even more extreme than batch melting.

$$C_L/C_0 = 1/D (1-F)^{(1/D-1)}$$

Example : consider a partial melt from a mantle peridotite ($D_{Ce} = 0.012$) and a degree of melting of 0.1. For batch melting $C_L/C_0 = 9$. Using the same parameters but Rayleigh melting the resultant $C_L/C_0 = 0.02$, suggesting that most of the Ce was already removed during the very early liquid parcels that were removed, depleting the source and the later melts in this component. Such a scenario may be applicable to MORB melts that appear to be depleted relative to OIB melts possibly as the result of large degrees of melting of a source from which previously melt had already been extracted.



2. Crystal Fractionation.

Many basalts have compositions rather different from that of the initial partial melt - they have evolved, and this has been achieved by the removal of crystalline solids (mainly olivine) during the ascent and evolution of the magma.

The model is concerned with the magma evolution, which is really the reverse of the partial melting since it starts with all liquid and by removing crystals reduces the amount of liquid, so the extreme concentration of incompatibles occurs at the end, not the beginning.

C_0 = initial concentration of element in **starting magma**

C_L = present concentration of element in **remaining liquid**

If all crystals remain in equilibrium with the magma, we have a simple reversal of batch melting. But this is unlikely as evidenced by e.g. zoning, gravity settling, etc. In fact the better

model is **Rayleigh Crystal Fractionation**. The simplest case is magma isolated in a chamber with continuous crystal fractionation: $C_L/C_0 = F^{(D-1)}$

Note: starting composition $C_L/C_0 = 1$; fully crystallised daughter rock $F = 0$.

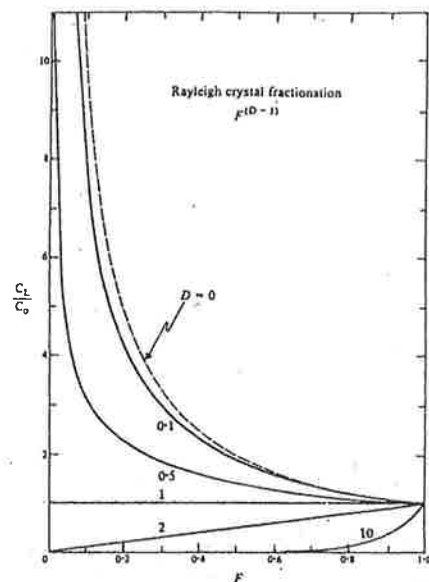
Limiting case is $D = 0$ (all stays in liquid) - completely incompatible

Then $C_L/C_0 = F^{-1} = 1/F$ (e.g. 10% solidification $\rightarrow C_L/C_0 = 1/0.9 = 1.11$; 90% solidification $\rightarrow C_L/C_0 = 1/0.1 = 10$).

The enrichment of incompatibles in the remaining liquid closely resembles that if equilibrium melting until more than 75% Of magma has been crystallised, then there is a rapid approach to $1/F$ (limit $D = 0$).

If $D > 1 \rightarrow$ an element is compatible and enters the solid. The compatibles however behave differently to the equilibrium model. They are removed even more rapidly in the early formed minerals so their concentration in the liquid soon falls below $1/D$.

Example: Ni- $D_{Ni}=7$; initial Ni concentration will fall by ~50% in 10% crystallisation and by 98% by 40% crystallisation. Late crystallising cumulates will thus be strongly depleted in compatible elements such as Ni



Rayleigh fractionation describes a simple system with an emphasis on the process of fractional crystallisation. Other models exist that describe for example in situ crystallisation where crystals form at the side-walls of a magma chamber and it is the liquid that is removed rather than the crystals. In situ crystallisation commonly produces less extreme enrichment results and therefore Rayleigh fractionation is still used as the process reflecting the range of what is possible during crystal-liquid separation.

Natural systems, however, may require more complex models since neither partial melting nor fractional crystallisation are likely to occur in a completely closed systems. O'Hara (1977, Nature 266, 503-7) has shown a complex model based on open system crystal fractionation in which periodically a small proportion of the liquid is drawn off as a erupting lava, while the chamber is periodically replenished by new unfractionated magma. This is known as the RTF model (periodically Replenished, periodically Tapped, continuously Fractionated magma chamber).

Further applications of trace elements in high-T Geochemistry

X-Y Plots

Given that two trace elements show rather similar geochemical behaviour i.e. similar D's in a magma, a x-y plot of element A vs. element B should always produce a straight line that passes through the origin. The best example for this is the widely used Zr vs. Nb plot. Any deviations from a straight line or a y-axis intersect through the origin can be interpreted as an additional process to pure fractional crystallisation that influenced the petrogenesis of a rock suite.

Element ratio vs element ppm plot

This type of plot is used where two elements behave similarly in magmatic differentiation, although their content in the magma will change due to e.g. crystal fractionation. Widely used are Rb/Sr vs. Sr ppm or Pb/Ce vs. Ce ppm. This type of plot helps evaluating the relationship between two elements during e.g. fractional crystallisation and produces for most cases a curved line as the two elements under study will have slightly varying D's at different stages of magmatic evolution.

Enrichment-depletion plot

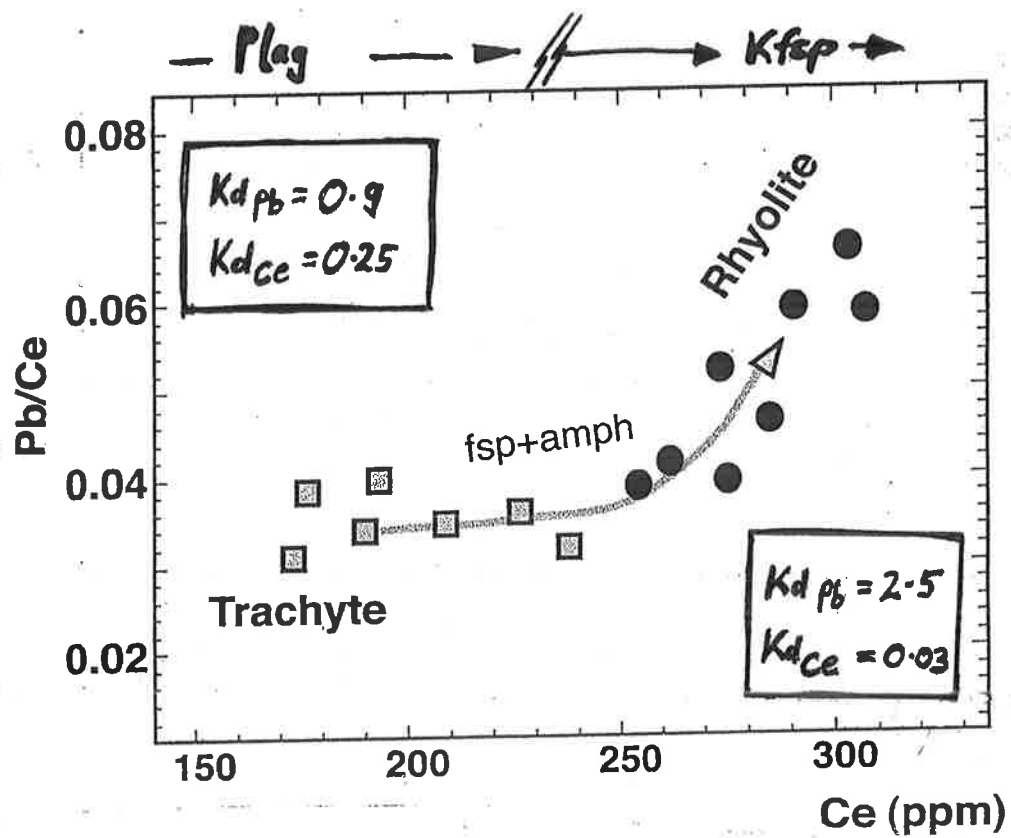
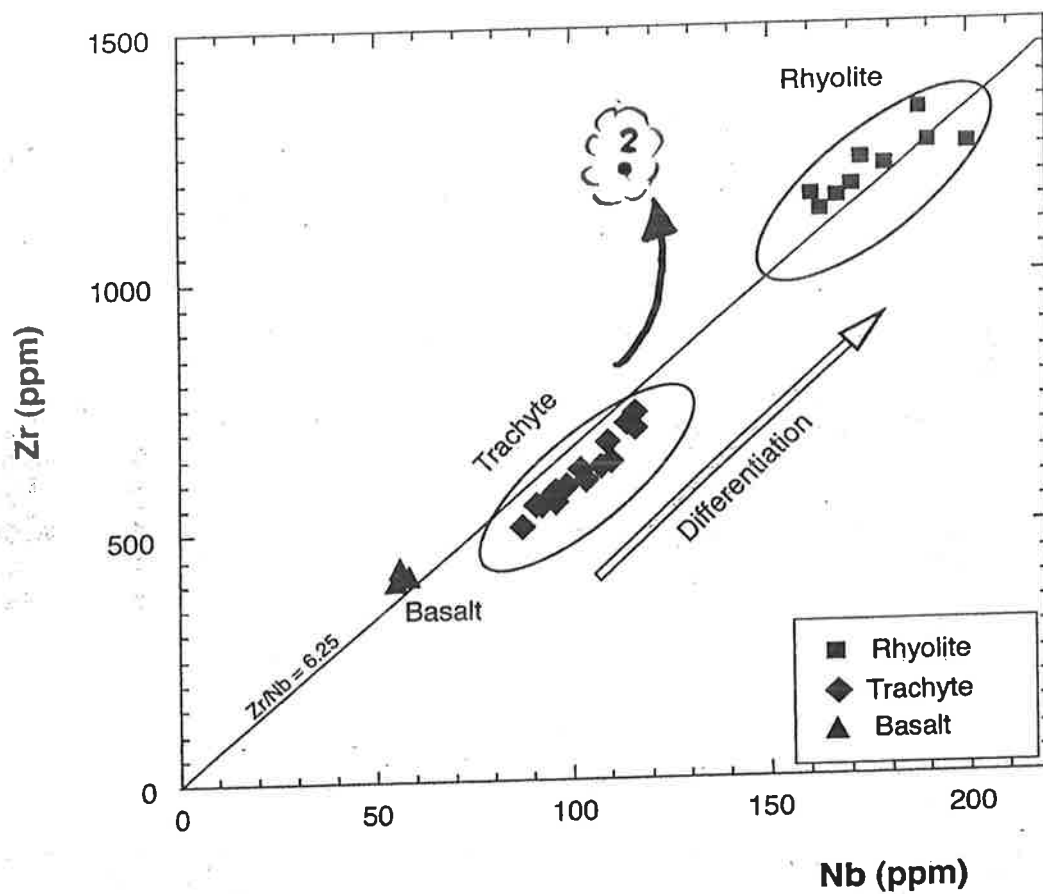
This type of plot compares - for example - the abundance of elements in vertically zoned igneous deposits as is common in ash-flow tuffs (ignimbrites). As fractionation in magma chambers tends to produce more evolved magma that segregates at the chamber top, early erupted parts of a unit often show enrichment in incompatible elements, whereas later erupted parts of a unit are relative to the early parts depleted in these elements. For compatible elements this trend is reversed.

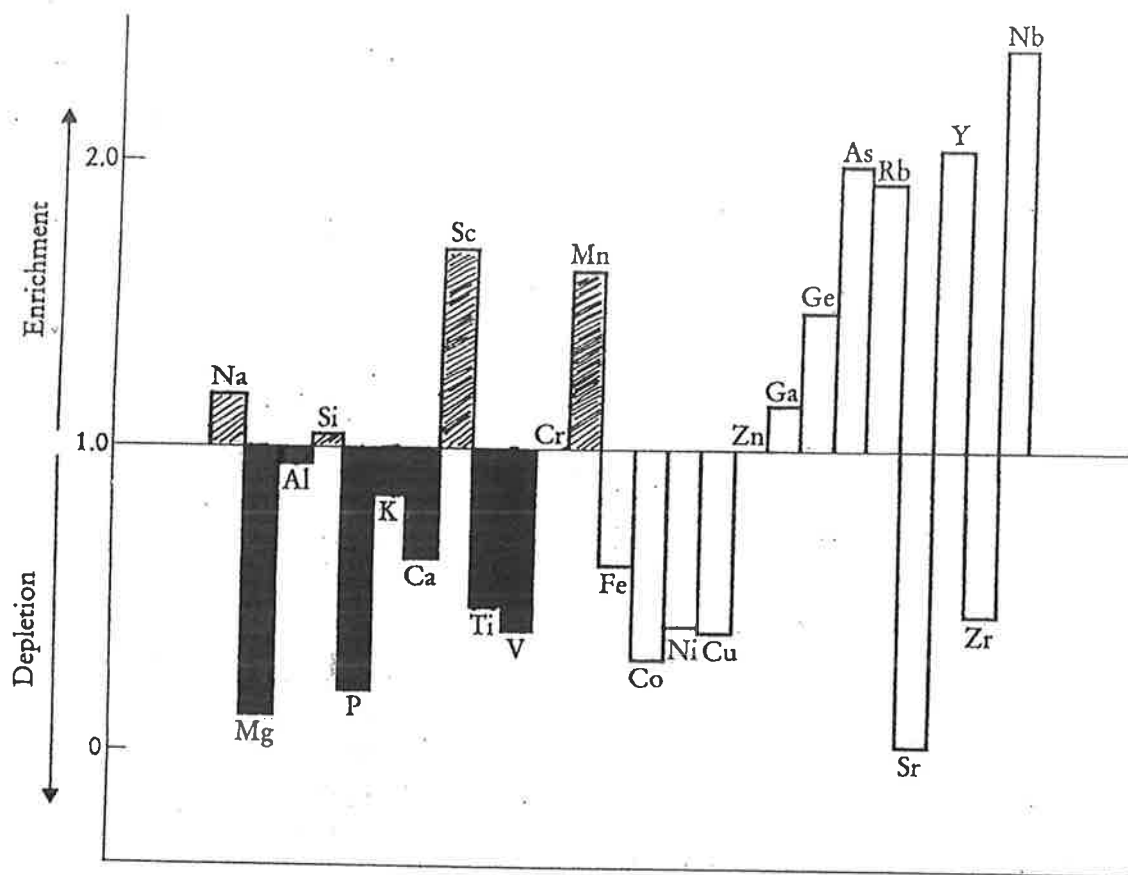
Chondrite normalised spider plots

Element concentrations are normalised to average "chondrite" or "primitive mantle" to evaluate the enrichment or depletion relative to a known standard (chondrite in this case) and are plotted vs. element abundance on a log scale. These diagrams are very useful for comparing factors of enrichment and may even be used for discriminating the source/tectonic setting of an igneous rock suite.

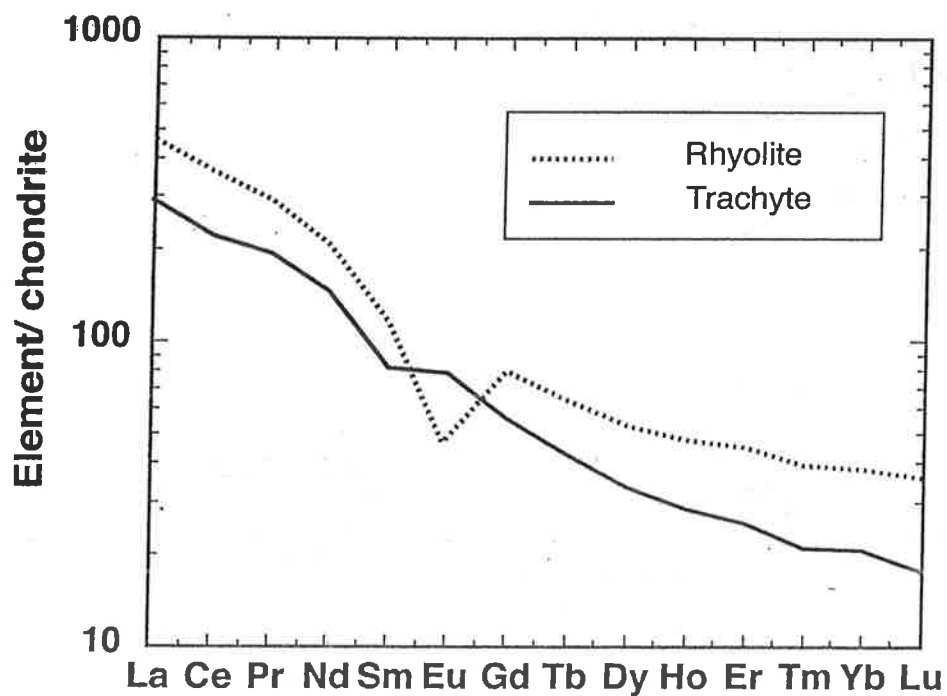
Discrimination diagrams

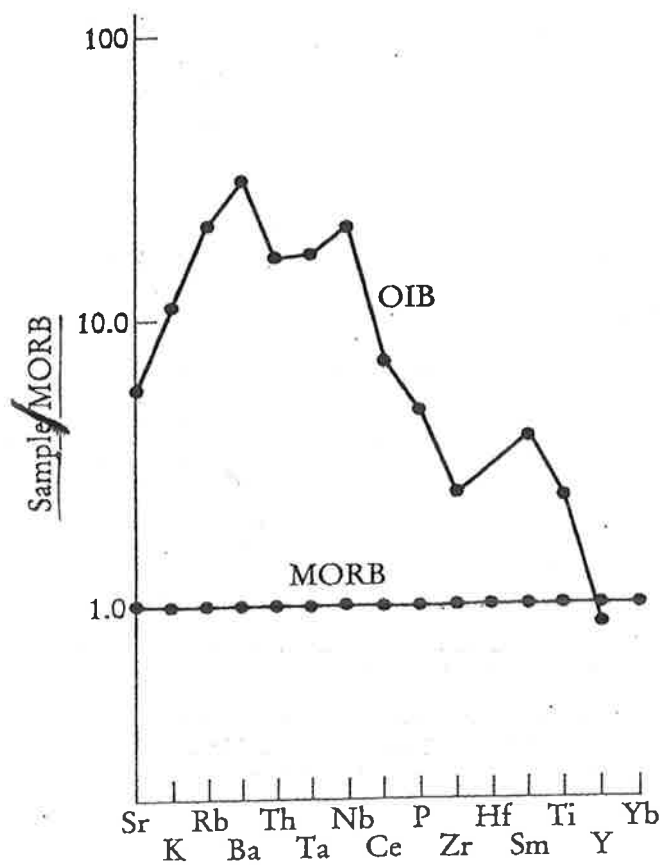
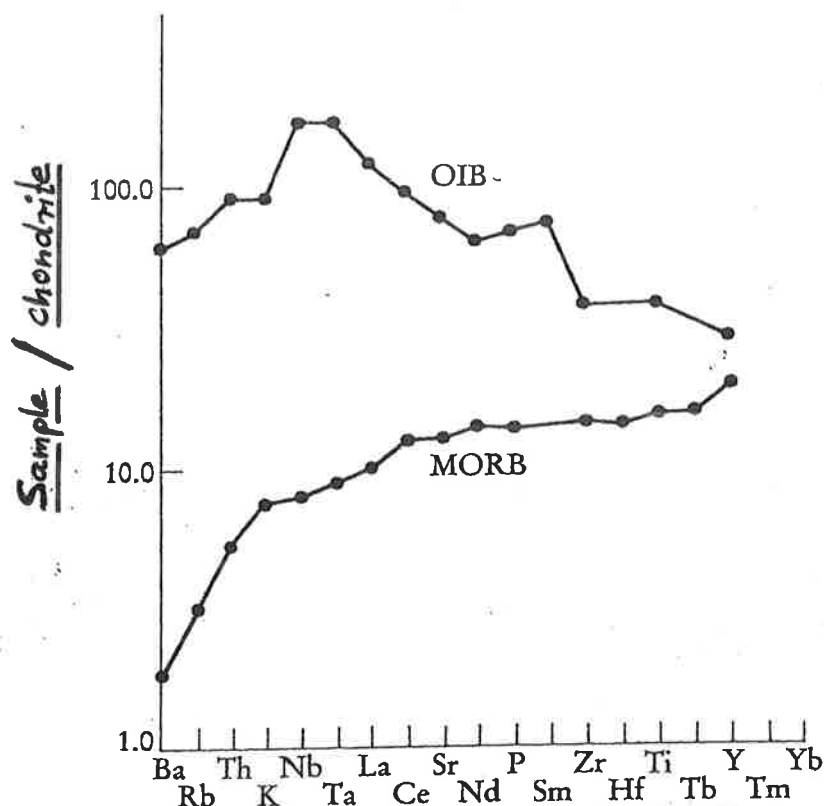
This type of trace element diagram aims to discriminate between different tectonic settings and is based on empirical relationships of various trace element concentrations in rock suites that occur different tectonic settings. The use of discrimination diagrams enables the geochemist to reconstruct the tectonic provenance of a rock suite and is especially helpful for altered and ancient sample suites where field relations are obscured by subsequent events.

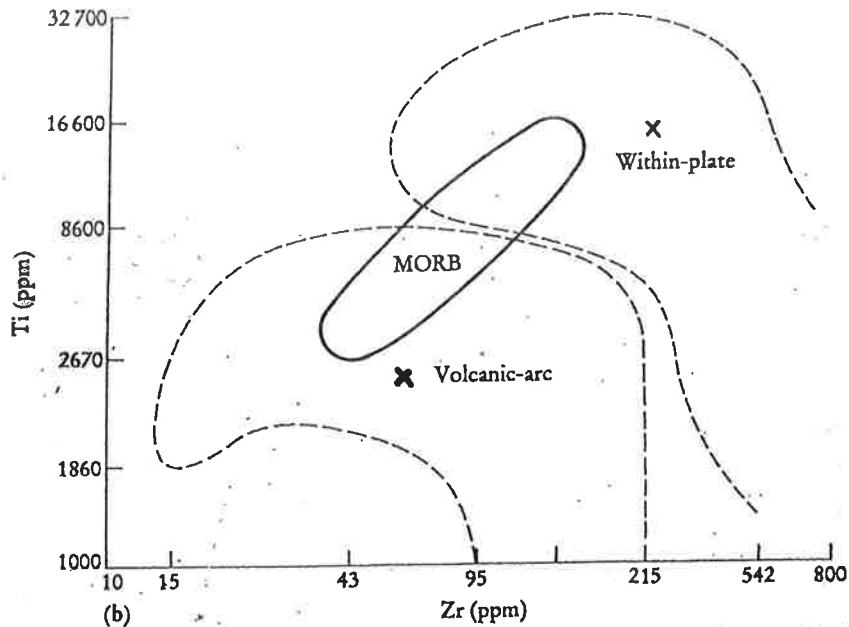




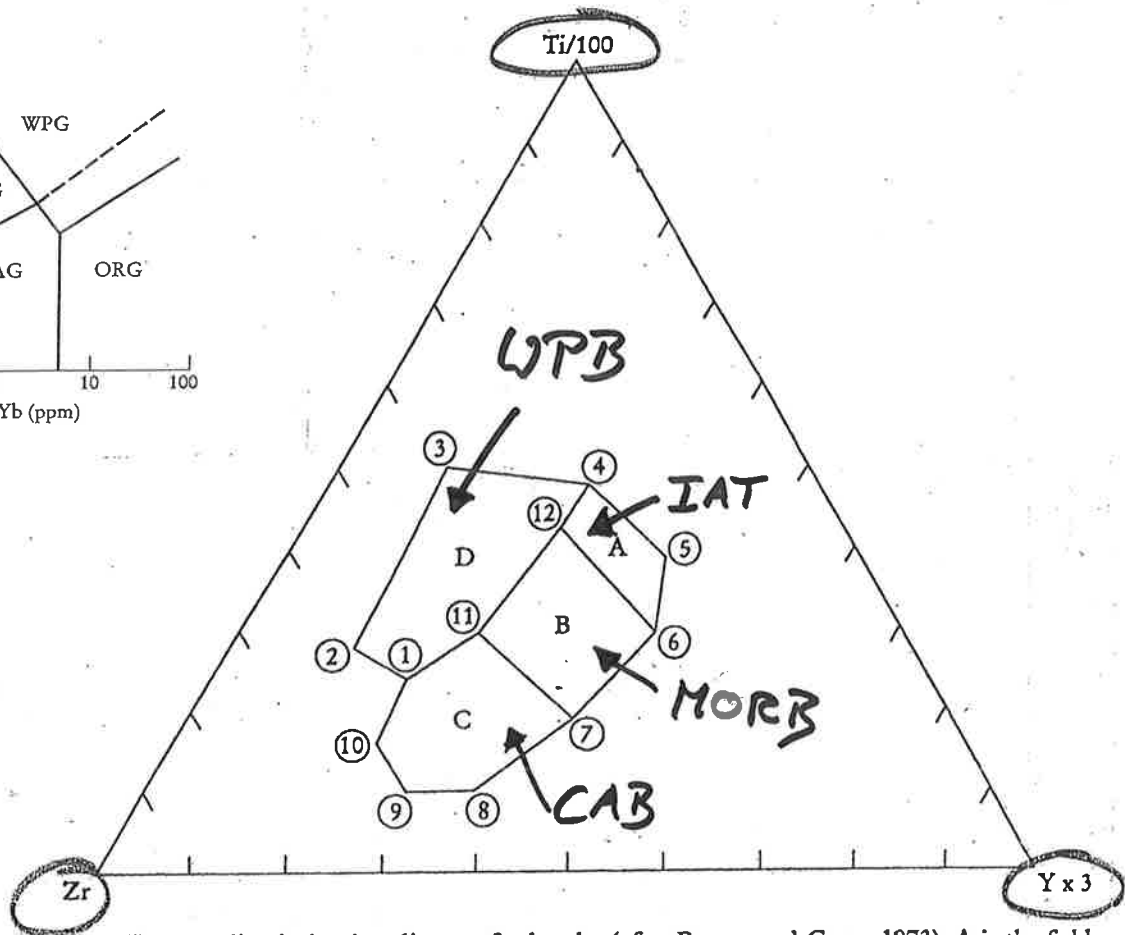
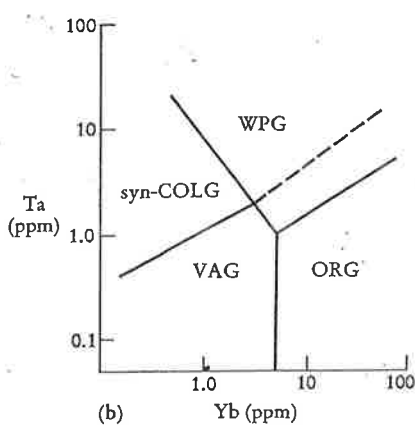
Enrichment-depletion diagram showing the enrichment factors for selected major and trace elements from the Bishop's tuff, arranged in order of increasing atomic number. The diagram compares the relative concentrations of the early and late members of the Bishop's tuff and is thought to be a measure of the zonation of the magma chamber. Data from Hildreth (1981).







Discrimination diagrams for basalts based upon Ti-Zr variations. (a) Linear scale (after Pearce and Cann, 1973); the fields are as follows: A, island-arc tholeiites; B, MORB, calc-alkali basalts and island-arc tholeiites; C, calc-alkali basalt; D, MORB. The plotting coordinates (extracted from Pearce and Cann, 1973 — Figure 2) are as follows:



The Ti-Zr-Y discrimination diagram for basalts (after Pearce and Cann, 1973). A is the field of island-arc tholeiites, C the field of calc-alkali basalts, D is the field of within-plate basalts and B is the field of MORB, island-arc tholeiites and calc-alkali basalts. Rocks which plot in field B give an ambiguous result but can be separated by plotting on a Ti-Zr diagram (Figure 5.2) or if unaltered on a Ti-Zr-Sr diagram (Figure 5.3). The plotting coordinates, extracted from Pearce and Cann (1973 — Figure 3)

L5: Radiogenic Isotopes

A. Radioactive decay can be expressed by the change of number of nuclei through time following a constant decay rate:

$$dN/dt = -\lambda N \quad \text{or} \quad dN/N = -\lambda dt$$

Integrated this yields:

$$\ln N_t/N_0 = -\lambda t \quad \rightarrow \quad N_t/N_0 = e^{-\lambda t} \quad \rightarrow \quad \underline{N_t = N_0 e^{-\lambda t}} \quad (1)$$

where N_t = the number of nuclei present at the time t , N_0 = the number of nuclei to start with and λ = the decay constant.

B. From equation (1) we can derive the half life of an isotopic decay series:

$$1/2 = 1 e^{-\lambda t} \rightarrow \ln 1/2 = 1 (-\lambda t) \rightarrow \ln 2 = \lambda t_{1/2} \quad \rightarrow \quad \underline{t_{1/2} = \ln 2 / \lambda} \quad (2)$$

The number of **daughter products (D)** from the decaying nuclei at a given time is:

$$\underline{D_t = N_0 - N_t} \quad (3)$$

Rearranging equation (1) yields: $N_0 = N_t e^{\lambda t}$

$$\text{Equation (1) in equation (3) yields } D_t = N_t e^{\lambda t} - N_t \rightarrow \underline{D_t = N_t (e^{\lambda t} - 1)} \quad (4)$$

With this expression we can now evaluate how much daughter nuclei formed during a given time span when we know the present abundance of mother nuclei in the system.

C. This, however, assumes that at t_0 no daughter nuclei were present in the system whatsoever. To evaluate the number of initially present daughters in the system at the time the radioactive clock started ticking we use the expression:

$$\underline{D_t = D_0 + N_t (e^{\lambda t} - 1)} \quad (5)$$

which is simply equation (4) plus the amount of initially present daughter nuclei (D_0). We can now calculate the initial isotope composition of a system at the time it formed !

Most widely used are the isotope systems Sr, Nd, and Pb.

Sr-Nd systems

Strontium

The $^{87}\text{Sr}/^{86}\text{Sr}$ ratios in any rock depend on the initial $^{87}\text{Sr}/^{86}\text{Sr}$ plus the addition of ^{87}Sr from the decay of ^{87}Rb ($^{87}\text{Rb} \rightarrow ^{87}\text{Sr}$), whereby ^{86}Sr is the stable non-radioactive Sr isotope.

Hence,

$$^{87}\text{Sr} / ^{86}\text{Sr} = (^{87}\text{Sr} / ^{86}\text{Sr})_0 + (^{87}\text{Rb} / ^{86}\text{Sr}) (e^{\lambda t} - 1)$$

Rb is more lithophile than Sr (i.e. bigger) and has therefore a lower bulk distribution coefficient than Sr. In other words, Rb is more incompatible. Hence, Rb (parent or mother) will more readily enter the melt fraction during mantle melting. This caused the concentration of Rb in the crust to increase, whereas the concentration in the mantle decreased with time ($\text{Rb/Sr}_{\text{crust}} > \text{Rb/Sr}_{\text{mantle}}$). Due to the radioactive decay of Rb to Sr the continental crust has now a far higher $^{87}\text{Sr}/^{86}\text{Sr}$ ratio due to addition of ^{87}Sr produced by radioactive decay.

Neodymium

^{143}Nd is produced by the α decay of ^{147}Sm . The stable Nd isotope that is not produced by radioactive decay is ^{144}Nd . The system Sm/Nd works essentially the reverse way than Rb/Sr. Sm has a higher bulk distribution coefficient than Nd, i.e. Nd is more incompatible (Nd has a smaller bigger than Sm!). Thus, a mantle melt will have more Nd than the source. This means a lower Sm/Nd ratio and hence the melts that make it to the crust have a slower growing $^{143}\text{Nd}/^{144}\text{Nd}$ ratio than the mantle. After a period of time the $^{143}\text{Nd}/^{144}\text{Nd}$ crustal ratio will therefore be substantially lower than the corresponding mantle ratio.

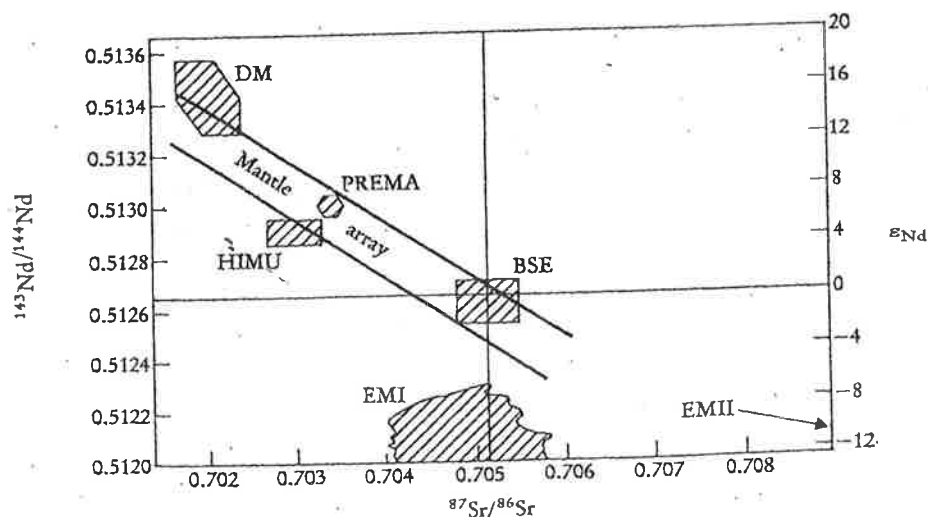
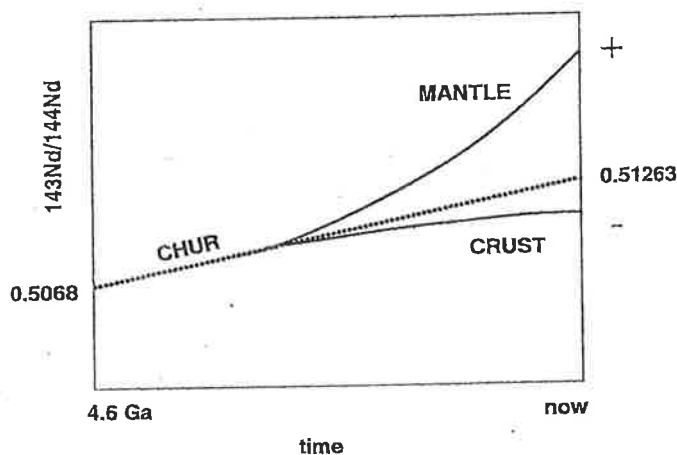
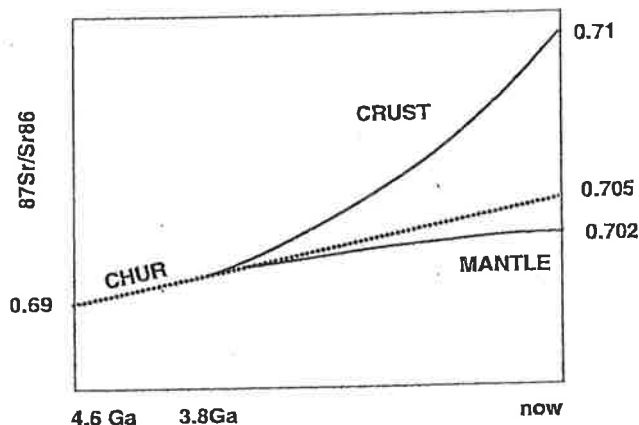
Sr-Nd correlation

If the two systems ratios are plotted on a x-y diagram, the "isotopic reservoirs" of the depleted mantle and that of the crust are clearly distinguished, with a bulk Earth composition that plots in-between. It can be seen that present day MORB is away to the top left of Bulk Earth - ie has evolved to higher Nd and lower Sr ratios - the opposite of the crustal composition. This is termed depleted and enriched, respectively.

The Bulk Earth composition (BSE) has been calculated from the original chondrite composition. It represents the estimated present day Sr and Nd ratios of the whole mantle+ crust - which means the initial chondrite ratio plus the decay contributions of Rb and Sm over a period of 4.6Ga. One consequence of this is that MORB cannot be separated from CHUR (Chondrite Uniform Reservoir) and originates from a *depleted* mantle.

Note: Radiogenic isotopes do not change by physical influence ($\Delta P, T$) or fractional crystallisation, because the mass difference between (say) ^{143}Nd and ^{144}Nd is too small to influence the partitioning of the two isotopes, i.e. they behave the same way. Hence, their ratio always reflects their source or a mixture of the source and any component that was added subsequently to a magma or a rock (e.g. by assimilation or weathering).

Parent isotope	Decay constant	Daughter isotope	Half-life (years)
K^{40}	$5.543 \times 10^{-10}/\text{yr}$	Ar^{40} & Ca^{40}	1.25×10^9
Rb^{87}	$1.42 \times 10^{-11}/\text{yr}$	Sr^{87}	48.8×10^9
Sm^{147}	$6.54 \times 10^{-12}/\text{yr}$	Nd^{143}	106×10^9
Th^{232}	$4.948 \times 10^{-11}/\text{yr}$	Pb^{208}	14.0×10^9
U^{235}	$9.848 \times 10^{-10}/\text{yr}$	Pb^{207}	0.70×10^9
U^{238}	$1.551 \times 10^{-10}/\text{yr}$	Pb^{206}	4.47×10^9
Lu^{176}	$1.94 \times 10^{-11}/\text{yr}$	Hf^{176}	35.7×10^9
Re^{187}	$1.61 \times 10^{-11}/\text{yr}$	Os^{187}	43.0×10^9



$^{143}\text{Nd}/^{144}\text{Nd}$ vs $^{87}\text{Sr}/^{86}\text{Sr}$ isotope correlation diagram, showing the main oceanic mantle reservoirs of Zindler and Hart (1986). DM, depleted mantle; BE, bulk silicate Earth; EMI and EMII, enriched mantle; HIMU, mantle with high U/Pb ratio; PREMA, frequently observed PREvalent MANTle composition. The Mantle array is defined by many oceanic basalts and a bulk Earth value for $^{87}\text{Sr}/^{86}\text{Sr}$ can be obtained from this trend.

Distribution of isotopic reservoirs in the Earth and their use as isotopic traces

Analysis of MORB basalts throughout the geological column - as far back as the Archaean - show that this depletion in incompatibles has existed through most of the Earth's history. According to O'Nions et al 1979 (J. Geophys. Res., 84) the depletion is due to the extraction of continental crust, much of which segregated from the mantle at a very early stage in Earth history.

The source for Ocean Island Basalts (OIB's) has unusually higher radiogenic Sr and less radiogenic Nd than MORB. However, the compositions span a wide array, suggesting an inhomogeneous mantle that was partly depleted by melting but partly enriched by e.g. metasomatic processes. Nevertheless the composition of OIB's more closely reflects that of the BSE composition (i.e. of chondrite composition), implying that there is a possibility for unmodified chondritic compositions in the mantle or that a depleted source got intermixed with crustal material due to e.g. crustal recycling as a result of subduction.

Island arc systems and continental arcs show a compositional range that extends well into the field for continental crust, pointing towards a crustal component picked up by these magmas during ascent.

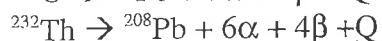
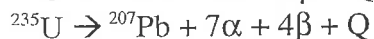
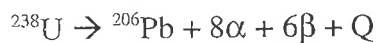
Further isotopic reservoirs commonly used in isotope geochemistry are:

EM I - mantle enriched in incompatibles especially LILE

EM II - mantle enriched in incompatibles especially LREE

HIMU - (high μ) - mantle with high mother Uranium ($^{238}\text{U}/^{204}\text{Pb}$)

U-Th-Pb systems



whereas ^{204}Pb is the stable non-radioactive Pb isotope

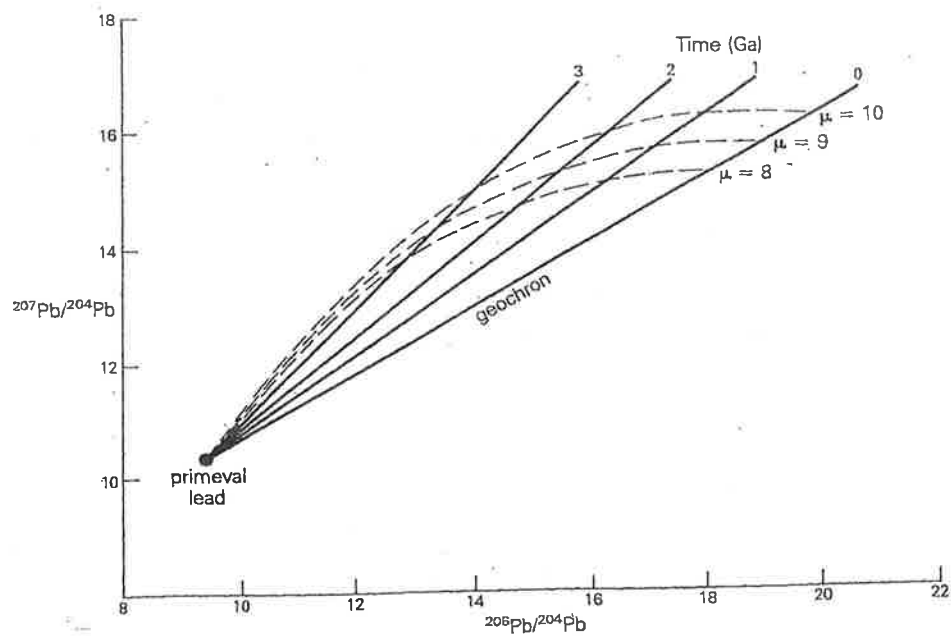
The initial isotopic composition in a rock can be calculated using equation (5):

e.g. for $^{206}\text{Pb}/^{204}\text{Pb}$:

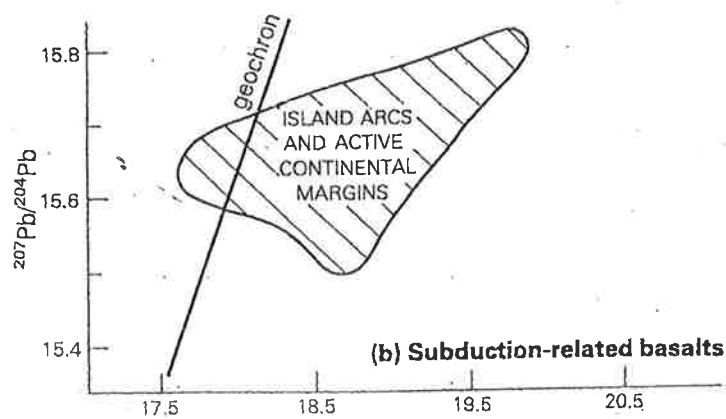
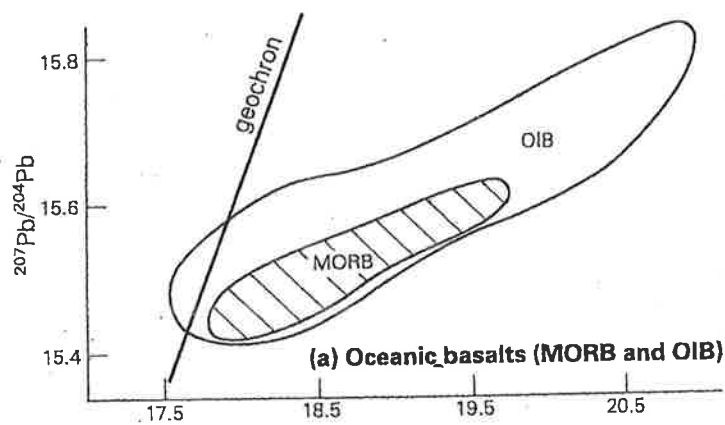
$$^{206}\text{Pb}/^{204}\text{Pb} = (^{206}\text{Pb}/^{204}\text{Pb})_0 + ^{238}\text{U}/^{204}\text{Pb} (e^{\lambda t} - 1)$$

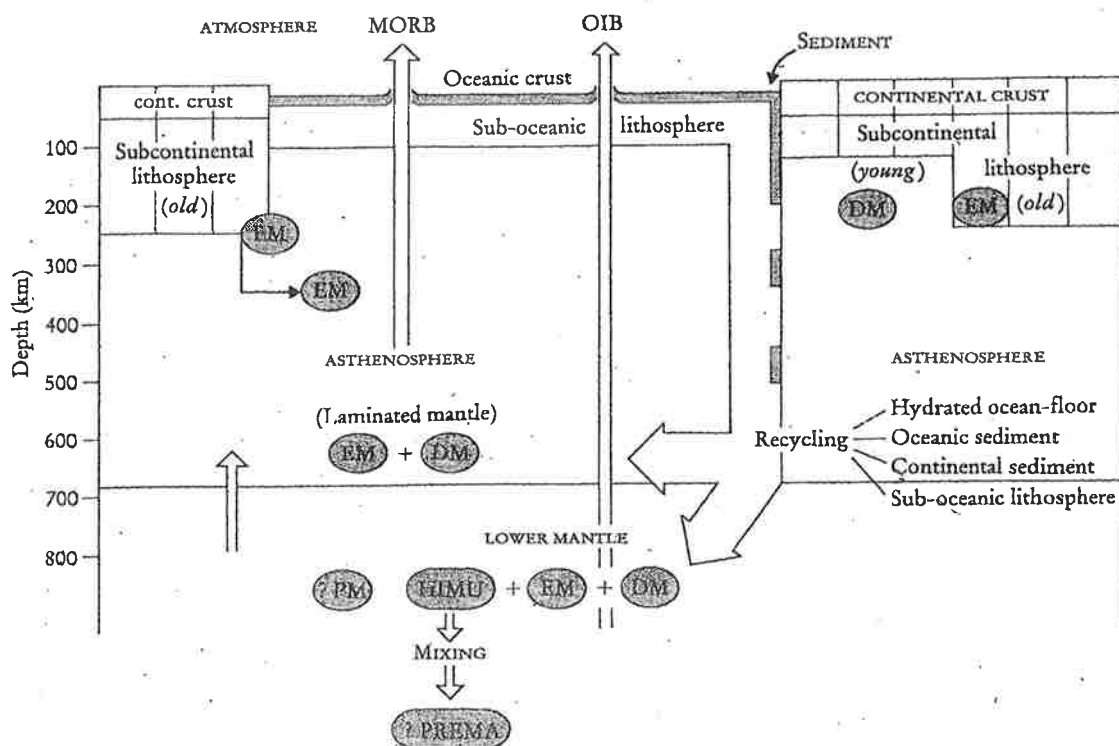
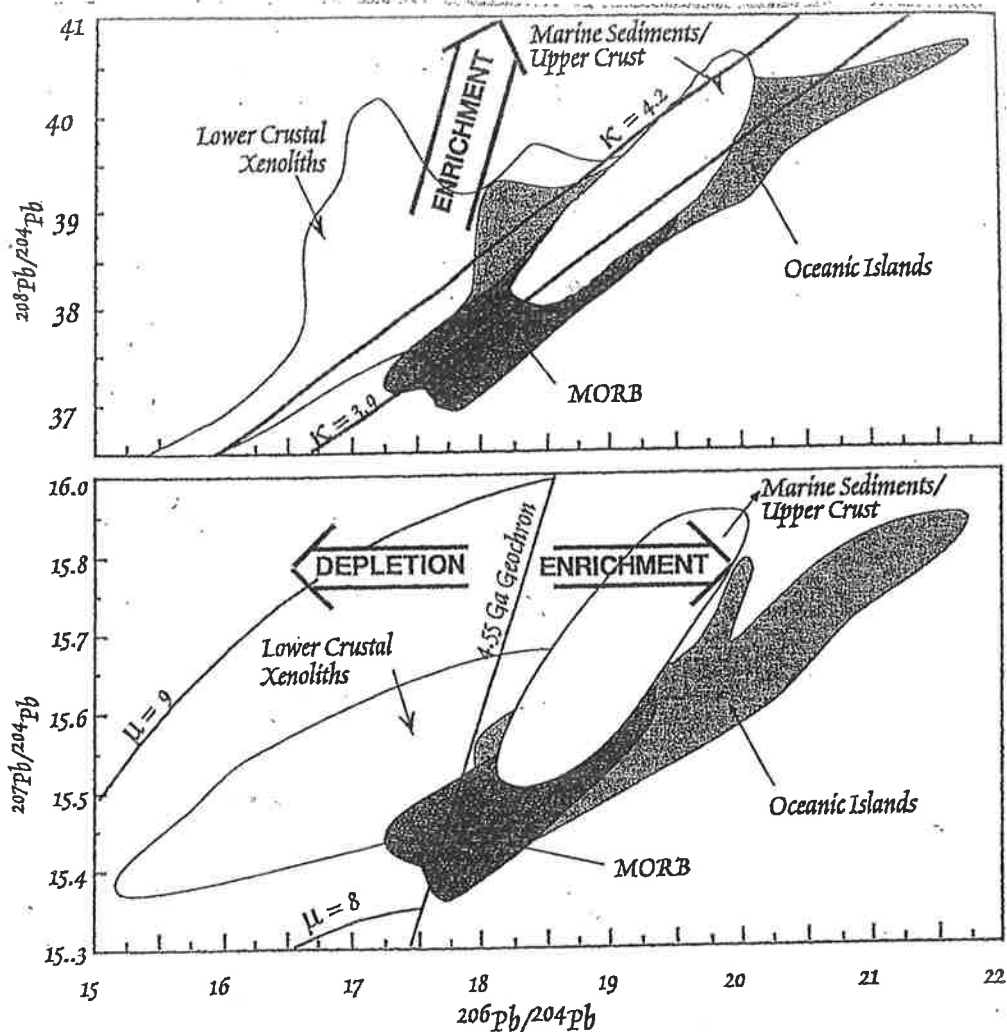
Following the same logic as for the Sr and Nd systems, the isotopic composition of the Earth should be the same as that in meteorites. Meteoritic values are: $^{206}\text{Pb}/^{204}\text{Pb} = 9.307$; $^{207}\text{Pb}/^{204}\text{Pb} = 10.293$; $^{208}\text{Pb}/^{204}\text{Pb} = 29.475$.

U and Th are preferentially concentrated in the melt (i.e. more lithophile) relative to Pb and consequently the U/Pb and Th/Pb ratios of crustal rocks are higher than those of the mantle. Since the different lead isotopes are produced from different parent elements, their amount of increase depends on the concentration of parent isotopes in a system and on the decay rate. Hence, the growth curves of daughter products fan out on a $^{206}\text{Pb}/^{204}\text{Pb}$ vs. $^{207}\text{Pb}/^{204}\text{Pb}$ plot (^{235}U decays faster than ^{238}U , but has a



Growth curves showing the isotopic evolution of Pb in the Earth. The dashed curved lines are lead growth curves for U-Pb systems having present-day μ values of 8, 9 and 10. The straight solid lines are isochrons for ages 0, 1, 2 and 3 Ga.





Cartoon diagram showing the different crust and mantle reservoirs and the possible relationships between them, based upon the observations of isotope geochemistry. The mantle reservoirs are identified using the nomenclature of Zindler and Hart (1986): EM, enriched mantle; DM, depleted mantle; HIMU, mantle with high U/Pb ratio; PREMA, prevalent mantle; PM, primitive mantle.

shorter half life, i.e. is used up more quickly). Straight lines on this plot are isochrons for ages 0, 1, 2, 3 Ga. All single-stage leads that were removed from their source at time t must lie on these isochrons. the line for $t=0$ is called the geochron and all modern single stage isotope ratios lie on this line (e.g. the Earth as a whole). Magmas have, however, experienced multi-stage history and most modern igneous rocks do not plot on the geochron.

If a system has experienced a decrease in U/Pb at some point in the past (depleted in U), its Pb composition will lie to the left of the Geochron. If a system experienced an increase in U/Pb (enriched in U) its present Pb isotope composition will lie to the right of the Geochron.

Upper continental crust rocks plot to the right consistent with U enrichment as a result of crustal segregation. Lower crustal xenoliths plot mostly to the left, pointing towards melt extraction (U depletion) in the lower crust.

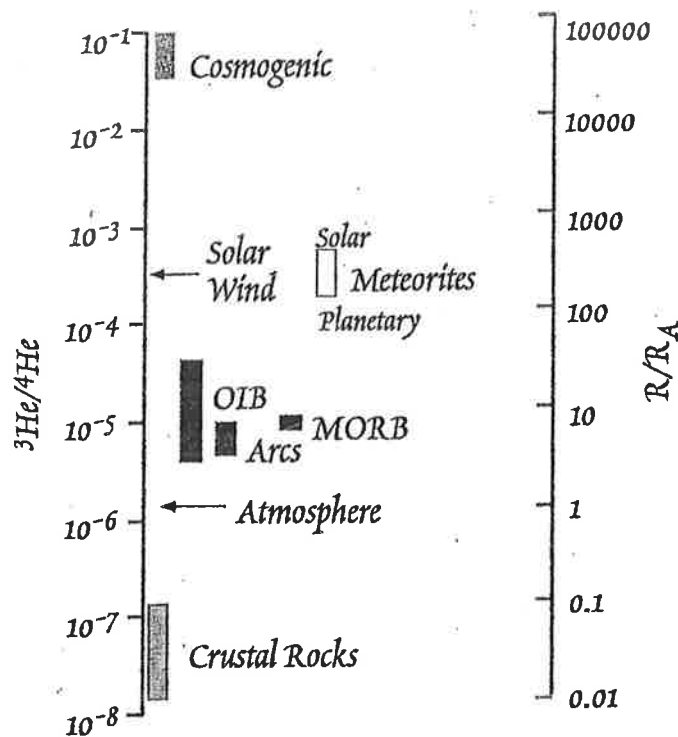
Subduction related "arc-basalts" plot also mainly to the right of the geochron which has been attributed to mixing of mantle components with subducted components (Pb is fluid-mobile). Basalts from intra-continental settings display a wide range of compositions likely to be also a function of crustal contamination as magma is passing through the crust

Surprisingly, MORB and OIB's plot also to the right, defining marked linear arrays, although they should be derived from the (depleted) mantle. This observation is known as the *Pb-paradox*. The cause for this is controversial. Clearly the upper mantle is not homogeneous in terms of Pb composition. One hypothesis states that U in the mantle increased due to metasomatic activity. Another hypothesis – which is probably closer to the truth as far as we know at the present day – is that the mantle experienced an input of crustal Uranium by subducted crustal rocks.

Helium Isotopes

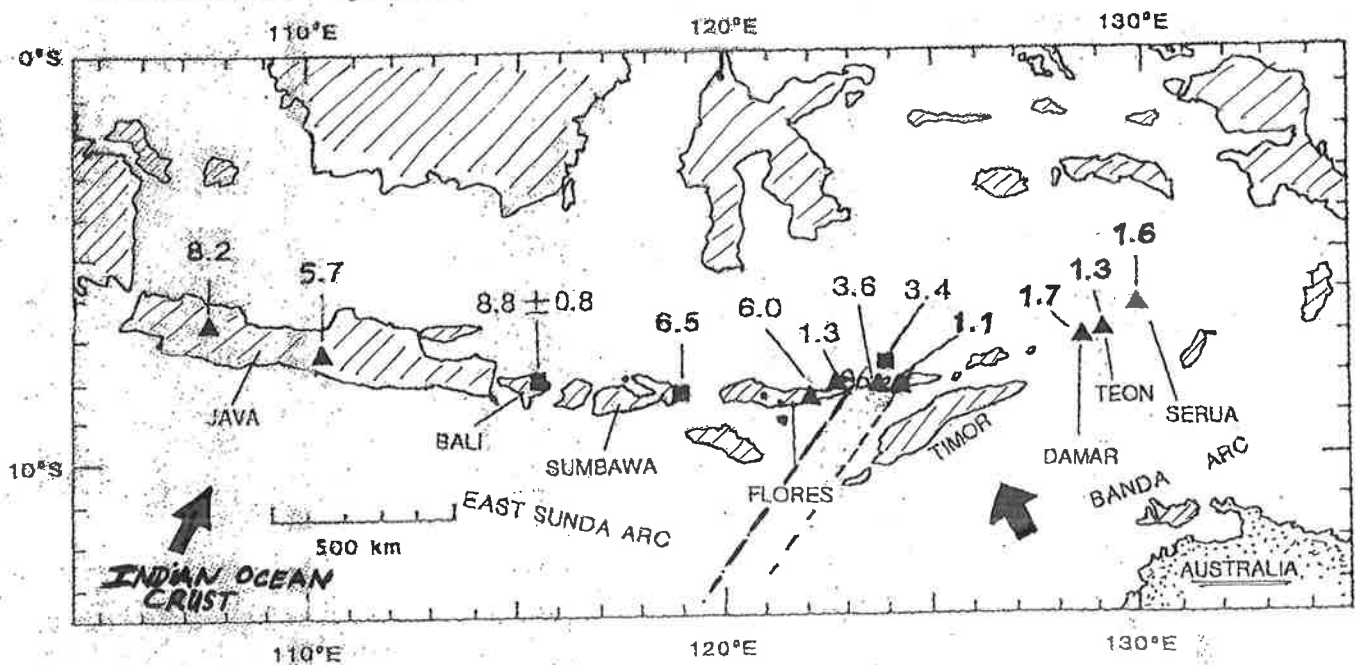
^4He are permanently produced in the Earth by α decay of e.g. U and Th. ^3He , on the other hand is the stable isotope of helium. Helium is a noble gas, contrasting Sr, Nd and U which are lithophile elements and this has a major influence on the helium isotope systematics and its use in geochemistry. Noble gases do not combine with any other chemical component and they are atmophile, meaning they tend to be lost from Earth and escape into the cosmos. Therefore, He is not stored on the Earth, rather it finds its way to the atmosphere and from there into the cosmos because of its low mass preventing gravitational attraction by the Earth. The ratio of ^3He (the stable isotope that represents the relict helium from the formation of our planet) to ^4He (that is produced by radioactive decay) is therefore very small. In the atmosphere this ratio is $^3\text{He}/^4\text{He} = 1.38 \times 10^{-6}$. The atmospheric ratio (due to common availability) is used as a He standard, where a rock or water $^3\text{He}/^4\text{He}$ ratio is divided by the atmospheric He ratio ($R_{\text{sample}}/R_{\text{atmosphere}} = R/R_A$).

In the continental crust R/R_A is 0.1 to 0.001, contrasting meteorites where R/R_A is ca. 200. Only very recently Lupton and Craig (1975) discovered that in MORB glasses extremely high R/R_A ratios occur being on the order of 8-9. From this they concluded that some primordial ^3He is still trapped in the Earth interior and is constantly escaping through magmatic activity. Subsequent studies have shown that R/R_A ratios on ocean islands are even higher values reaching up to about 24. This implies that OIB's are derived from a less degassed and thus more primordial source than MOR basalts. Island arc basalts, in turn show R/R_A values roundabout 5 reflecting a mixture of mantle and crustal components.



He isotope ratios in various terrestrial and solar system materials. "Solar" and "Planetary" refer to the solar and planetary components in meteorites. "Crustal rocks" shows the values expected for *in situ* production from α decay and neutron-induced nuclear reactions.

$^3\text{He}/^4\text{He}$ in volcanic gases:



Hilton et al., 89
NATURE

Exercise – Radiogenic Isotopes

You are provided with a table of isotopic compositions of the Inner Hebridean island of Rum in Scotland. Rum is dominated by Pre-Cambrian metamorphic and sedimentary rocks and Tertiary igneous rocks. Among the Tertiary rocks (60 Ma), the most abundant are granite intrusions, rhyodacite tuffs and an ultrabasic intrusive complex of cumulate peridotites, plagioclase-rich gabbros and gabbros from a basic-ultrabasic magma.

The granitic and felsic igneous rocks (rhydacites) provide the most evolved spectrum of igneous compositions on Rum, whereas the basalts and ultrabasic cumulate gabbros provide an approximation of the isotopic sources of the Tertiary volcanism.

1. Plot a Sr-Nd isotope diagram, marking well known reference points and fields, such as BSE and the MORB domain.
2. Using the full set of data provided. Propose a model that explains the petrogenesis of the granitic and felsic igneous rocks.
3. Consider what mantle sources might be involved in generating the mafic parental magmas.

Table 1. Isotope ratios of Rum rocks

	$^{87}\text{Sr} / ^{86}\text{Sr} (60 \text{ Ma})$	$^{143}\text{Nd} / ^{144}\text{Nd} (60 \text{ Ma})$
Basalt dyke	0.7029	0.5130
Ultrabasic cumulate	0.7037	0.5127
Western granite	0.7122	0.5122
Rhyodacite	0.7126	0.5121
Torridonian Sst	0.7130	0.5132
Lewisian gneiss	0.7184	0.5118

Radiogenic Isotopic Tracers
in Geochemical Modelling
of Igneous Petrogenesis

Referring to Dr. G McNeill

by V Troll
(1997)

Isotopic tracers in geochemical modelling of igneous petrogenesis

Radiogenic isotopes are used in geochemistry in two principal ways. Historically they were first used to determine the age of rocks and minerals. More recently they have been used in petrogenetic studies to identify geological processes and sources. The latter is commonly known as isotope geochemistry (Rollinson 1995).

Unfortunately it is beyond the scope of this work to explain also the stable isotope systems, even when their use is of essential importance in some respects of geochemical modelling. Therefore it is referred to in Faure 1993, who provides a good introduction.

Isotopic systems

There are three important radiogenic isotope systems with which are dealt with in this work, and therefore a brief introduction of these systems will be provided.

-> Rb- Sr system: The β^- decay of ^{87}Rb to the radiogenic isotope of Sr (^{87}Sr) is called a mother/ daughter relation. The half-life of this system is approximately 48.8 Ga. The comparison of this ^{87}Sr to the stable ^{86}Sr allows the determination of the age of the rock.

The fact that ^{87}Sr has a smaller ionic radius and is, relative to its size, slightly heavier than its mother leads to a more lithophilic behaviour of ^{87}Rb and hence an enrichment of ^{87}Rb in the continental crust. The smaller Sr is less enriched in the continental crust and stays preferentially in the mantle, thus a comparison of the naturally occurring ^{86}Sr to the ^{87}Sr formed by the radioactive decay of ^{87}Rb allows definition of different isotopic environments. The mantle shows high abundance of ^{86}Sr but low abundance of ^{87}Rb and hence low ^{87}Sr . This leads to lower values of the $^{87}\text{Sr}/^{86}\text{Sr}$ ratio in the mantle than in the crust, where the lithophilic Rb is enriched and enhances the $^{87}\text{Sr}/^{86}\text{Sr}$ of the continental crust with continuous decay.

-> Sm- Nd system: The α^- decay of ^{147}Sm to the radiogenic ^{143}Nd is a mother/ daughter relation where the daughter is bigger in size and relatively light in weight compared to the mother. The half- life time of this system is approximately 106 Ga. The comparison of ^{143}Nd to the stable ^{144}Nd shows thus a reverse trend to the Rb- Sr system because Nd has a more lithophilic character than Sm. As a consequence Sm stays preferentially in the mantle and Nd in the crust. Hence the abundance of radiogenic Nd produced by Sm in the mantle is higher than in the crust and therefore the $^{143}\text{Nd}/^{144}\text{Nd}$ ratios of the mantle are higher relative to the $^{143}\text{Nd}/^{144}\text{Nd}$ ratios of the continental crust. Epsilon notations (CHUR normal.) are common.

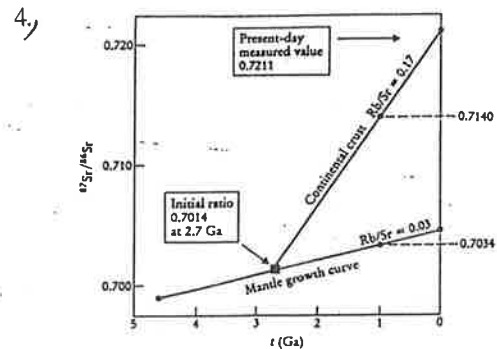
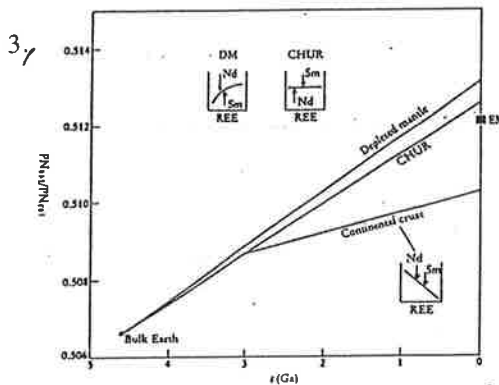
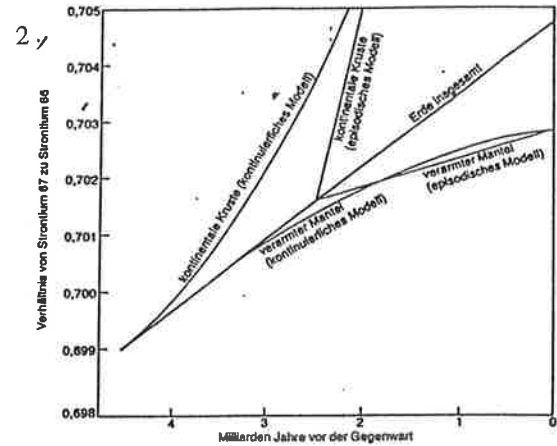
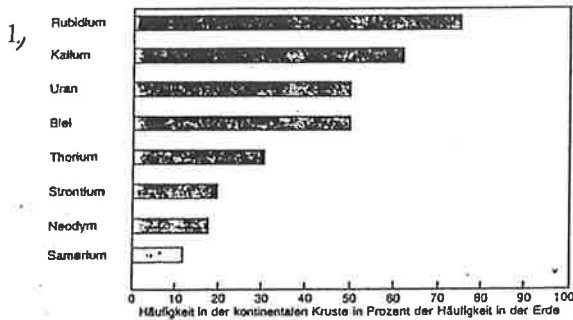
-> Re- Os system: The β^- decay of ^{187}Re to ^{187}Os shows basically the same mechanism as the Rb- Sr system, since the differentiation between Re and Os leads to an enrichment of the mother isotope ^{187}Re and thus of ^{187}Os within the crust. This partitioning is far less obvious than in the Rb- Sr system because as well the mother as the daughter show generally siderophile- chalcophile character and are therefore assumed to be of high abundance in the core. Just ppb of Re and Os can be measured in the crust, but the enrichment factor of Re to Os in some igneous rocks is up to 300 times whereas mantle peridotites show characteristics similar to chondrites. The fact that the mantle shows initial chondritic values (bulk values) is surprising, since the siderophile character should result in a Re- Os enrichment in the core and thus to depletion in the mantle. An accretion of chondritic material to the earth after the formation of the core is suggested which can account for the bulk ratios in the mantle (Dickin 1995). The strong signatures provided by the ^{187}Os to the stable ^{186}Os ratios make the system valid as a tracing tool. An Os ratio notation based on their percentage deviations (gamma) from the chondritic reference is often used, even when the zero point of this notation is unlikely to represent the bulk earth of $^{187}\text{Os}/^{186}\text{Os}$ composition (core abundance is uncertain), as it does the epsilon notation in the Rb- Sr and Sm- Nd system.

Evolution of present isotopic distribution

Assuming an initially heterogeneous distributed element abundance within the planetary body of the earth after the accretion of particles originally condensed out of the solar nebula, the question of the development to the present isotopic reservoirs arises. A melting stage, probably caused by short lived radioactive decay is assumed causing a differentiation of elements. This differentiation was resulting in the formation of the first kratons roughly 3.8Ga ago. Assuming a slow growth of these early continents, a slow differentiation of the isotopic mother/ daughter systems should be coeval. An increasing grade of differentiation with time and with respect of the relative mass and radius difference would lead to an enrichment of the slightly more lithophilic end members in the continental crust. A straight forward explanation for the degree of differentiability of the different systems is the relative differences in weight and ionic radii. However this explanation can account for Rb- Sr (Rb is bigger with almost the same weight) and in a reverse way for Sm- Nd (Nd is bigger and lighter), but the Re- Os system must be considered as exceptional. The Re enrichment factor in some basalts and granites is up to 300 and the weight difference is minor (Allegre 1980). This strong relative enrichment of Re to Os is supported by the fact that Re is considered as almost completely incompatible in mantle minerals, whereas Os is compatible (Dickin 1995).

Diag.1 shows the relative abundance of some elements in the continental crust compared with their abundance on the earth as a whole.

Present models differ in whether the differentiation degree has grown gradually (continuous model) or whether it started at a particular point (episodic model). Mathematical reconstructions can account for both theories, since the samples of rocks with ages of about 3 Ga are limited no definite answer can be given. In the diagrams 2 to 4. mathematical models which try to reconstruct the differentiation history according to the sampled isotopic ratios are illustrated. NB the degree of rising Sr ratios is higher than the dropping Nd ratios.



Referring to these models, the first significant differentiation should have occurred between 3 and 2.5 Ga in the episodic model and gradually in the continuous model since roughly 4.3 to 4.1 Ga. This is the base for the theory that the major REE depletion took place at a time between 3- 2.5 Ga (Rollinson 1995). Diagram 5. illustrates depletion trend of the mantle indicated by rising Nd ratios based on igneous rock samples with corresponding ages. The initial ratio of the average chondritic ratio of 0,5075 is assumed. An extrapolation of the line leads to the average Nd ratios for the earth at the present day (Bulk Earth). In diagram 6.) a development for osmium ratios in the mantle is shown, demonstrating an extrapolation for present day Os mantle ratios, based on igneous rocks which are supposed to be mantle derived. However there is little variation, even when the strongly rising line indicates a significant evolution, because the ratio is just above one for today and with an initial chondritic ratio of just over 0.8. Nevertheless, an evolution can be shown even when such big magnifications need to be used. These changes demonstrate furthermore the huge reservoir of Re- Os in the mantle when extraction of Re into the continental crust has caused only such little evolution. A bulk ratio for Os isotopes cannot be provided, since the abundance in the core is uncertain and the mantle distribution is assumed to be not a fractionation result (Dickin 1995).

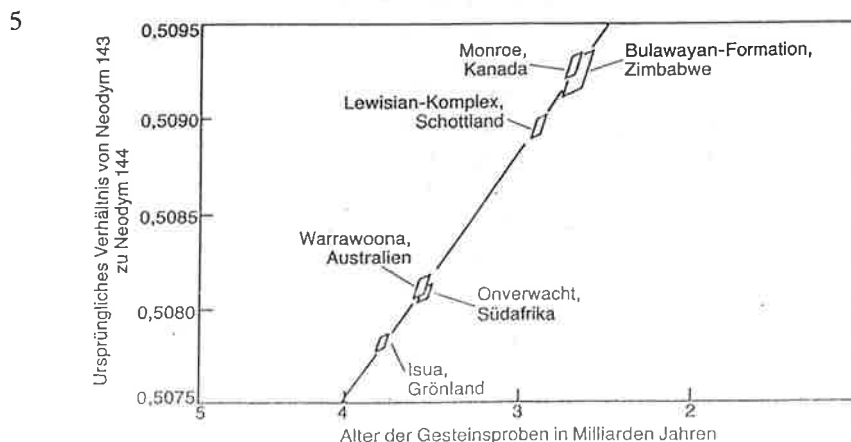


Diagram 7. shows the increase of radiogenic Os within the continental crust for the geological record. A rock which would have formed at 3.8 Ga ago (could have been recycled) indicated by the shaded are signed with b.) and rocks at a direct differentiate out of the mantle at particular times, carrying the time specific mantle signatures indicated with a.). The numbers in-between these two extremes allow to model a possible source of an igneous rocks suite by mixing or contamination of these two end members. NB the area a.) represents the whole range illustrated in diagram.6.

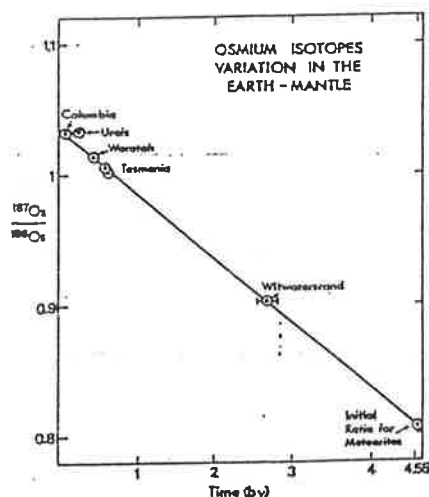


Fig. 6 The diagram shows the variations of $^{187}\text{Os}/^{186}\text{Os}$ with time in different Os-rich samples which are probably derived from mantle materials.

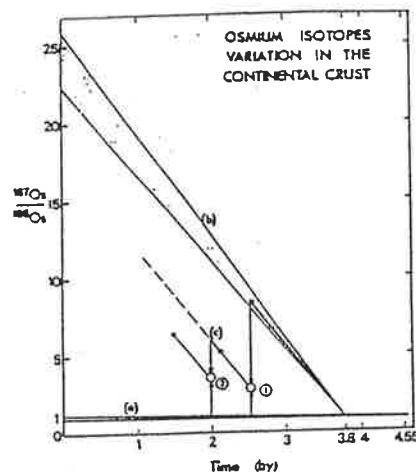


Fig. 7 Theoretical initial osmium isotopic $^{187}\text{Os}/^{186}\text{Os}$ ratio evolution diagram for the continental crust in the case of various models. a = continental crust continuously derived from mantle material (mantle evolution curve) ($^{187}\text{Re}/^{186}\text{Os} = 3.2$). b = continental crust continuously recycled from a primitive crust differentiated at 3.8 by. ($^{187}\text{Re}/^{186}\text{Os} = 400$). c = mixing model: in (f) formation of a granite from a mixture of old continental crust and new mantle material; in (2) formation of a granite from a mixture of new crust formed in (f) with new mantle material.

Isotopic Reservoirs

The fractionation of the earth lead to the evolution of distinct isotopic reservoirs. This evolution (see above) allows to define significant isotopic signatures for specific environments and thus the modelling of possible sources in petrogenesis. A description of the main isotopic reservoirs (based on a huge amount of samples) and a brief geological background will be provided as follows:

--> **Depleted Mantle (DM):** is characterised by high $^{143}\text{Nd}/^{144}\text{Nd}$ (>0.5133) and low $^{87}\text{Sr}/^{86}\text{Sr}$ (<0.7025). The $^{187}\text{Os}/^{186}\text{Os}$ values are assumed to represent a fairly closed system within the mantle and range from 0.85 to 1.05, whereas the Rb- Sr and Sm- Nd systems are considered as relatively open systems, because of the enrichment of e.g. Rb in the cont. crust. The depleted mantle is furthermore assumed to be the source of the oceanic crust which results in progressing depletion, since REE pattern are usually slightly enriched in MORB compared to the DM (Wilson 1989). Hence MORB show roughly the isotopic source signature of DM with slightly higher values for the more lithophilic isotopic elements, resulting in ratios closer to bulk earth.

--> **Enriched Mantle (EM):** is characterised by low $^{143}\text{Nd}/^{144}\text{Nd}$ (<0.5123) and relatively variable $^{87}\text{Sr}/^{86}\text{Sr}$ values. $^{187}\text{Os}/^{186}\text{Os}$ values of about 1.05 are assumed to be representative. The enriched mantle is often divided into EMI and EMII with EMI as subduction related material and EMII as metasomatically enriched oceanic crust.

--> **HIMU Mantle:** shows Nd ratios between 0.5128 and 0.5130 coupled with Sr ratios of about 0.7030 and Os ratios of about 1.25 ($\gamma > +20$). The HIMU mantle is supposed to be slightly enriched because of alteration or minor mixing with cont. crust.

--> **PREMA Mantle:** is characterised by Nd ratios of about 0.5130 and Sr ratios of 0.7033. Os ratios rise to a maximum of +5. This prevalent mantle is assumed to be a possible source for OIB and some IAB. With an assumed existence of such an reservoir the mixing theories of e.g. OIB would be invalid.

--> **Bulk Earth (BE)**: is defined by Sr ratios of about 0.7048, Nd ratios of about 0.5127 and uncertain Os ratios (estimation by Dickin 1995 1.08 to 1.18). Theoretically, the possibility of a mantle reservoir with bulk earth isotopic signatures is given. This would represent a residue mantle prior to the evolution of the cont. crust. Some authors assume that there is no reservoir with this composition and explain rocks with these signatures as mantle derived with different degree of contamination by cont. crust.

--> **Cont. Crust**: is characterised by Sr ratios > than at least 0.71 and variable Nd ratios roughly lower than 0.5128. The Os ratios are high depending on the age of the crust from 10 up to 25, but always significantly higher than the mantle range. Continental crust is assumed to be an accumulation of lithophilic elements and thus an enrichment in the more lithophilic isotopes of the mother/ daughter systems defines the cont. crust.

Figures 8,9 illustrate the distinct isotopic reservoirs. In 8.) defined by $^{87}\text{Sr}/^{86}\text{Sr}$ versus $^{143}\text{Nd}/^{144}\text{Nd}$ (Hall 1989) and in 9.) by epsilon Nd and gamma Os values. NB in fig 9.) the black points indicating a mixing sequence of a mantle plume with lower lithospheric mantle for Karoo basalts after Dickin 1995.

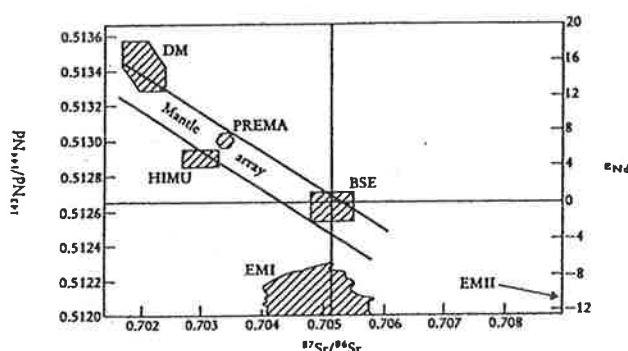


Fig. 8

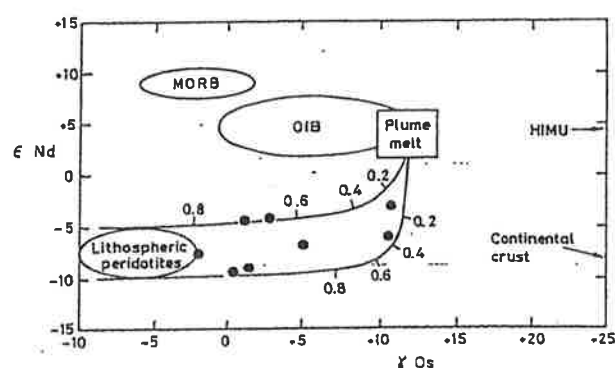


Fig 9

Isotopic Modelling of Petrogenesis

The range of possibilities to use radiogenic isotopes in geochemical modelling is even at the present stage of research hardly exhausted. Therefore just a selection of possible usages is provided below.

--> **Discrimination of tectonical environment**: Tectonical environment can be correlated to specific magma types, such as subduction related calcalkaline IAB. Thus a discrimination of tectonical setting can be strongly supported by isotopic evidence. This is already indicated in Fig. 8+9. NB in Fig 9. that the Karoo basalts can be discriminated as plume related magmas and furthermore it can be interpreted that these magmas had to pass the continental crust and carry therefore signatures of the lower lithosphere. Another example could be the tracing of a MORB as a partial melt of depleted mantle material simply by comparing the isotopic signatures. If the measured values plot in the empirically established MORB field the rock can be considered as mid-ocean rift related and hence be correlated with a tectonical graben structure.

--> **Fractional Crystallisation**: Since the nonradiogenic and the radiogenic isotopes of a specific system are almost not fractionable, an igneous rock suite would always carry the isotopic characteristics of the source. Hence, independently of the silica content of a single sample out of a magmatic fractionation series, the isotopic ratio would be the same. Consequently a change in the isotopic ratios indicates a change in the magma composition by an open system process, such as magma mixing or AFC (assimilation and fractional crystallisation). Fig.10 suggests an FC process for a calcalkaline suite from the Solomon Islands (Rollinson 1995). Fig.11 indicates as well ATA (assimilation while turbulent ascent) as FC and AFC processes for particular stages of a magmatic evolution from the lava succession on the Isle of Mull rock; The contaminant is supposed to be the Lewisian crust (triangles) (Kerr 1995). This correlation of Nd ratios versus Nd in ppm is based on the fact that an FC process would enhance the Nd ppm values but would not change the Nd ratios.

Fig. 11 Plot of $^{143}\text{Nd}/^{144}\text{Nd}$ versus Nd, showing trends for fractional crystallisation (FC), AFC, and assimilation during turbulent ascent (ATA). (Solid squares - MPG basalts, hollow squares MPG basaltic-hawaiites, triangles Lewisian crust from Tíree, P probable composition of primitive uncontaminated MPG magma). Several of the MPG lavas plotted on this diagram are from Carter et al. 1978.

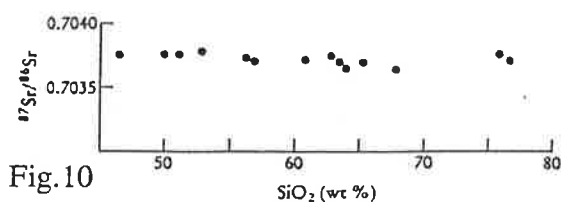


Fig. 10

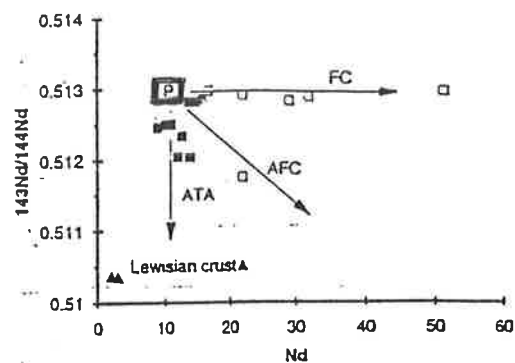


Fig. 11

-> **Contamination:** Any significant chemical change in magma composition does necessarily always change the isotopic signatures (open system), and therefore interpretations of a possible contaminant can be made. For example magma mixing with an influx of a different magma into the magma chamber is assumed for the Bushveld complex in South Africa resulting into a gradual change of the isotopic signatures towards the isotopic signatures of the contaminant and shows even the occurrence of a major pulse of magma influx in the main zone (Fig.12). AFC processes can be similarly modelled by observing the change in isotopic signatures on a Sr ratio versus Nd ratio diagram, which should result in a change at a particular stage of the magmatic evolution rather than, in a gradual change as observed in the case of magma mixing (Fig.13 shows an example from the massiv central after Wilson 1989).

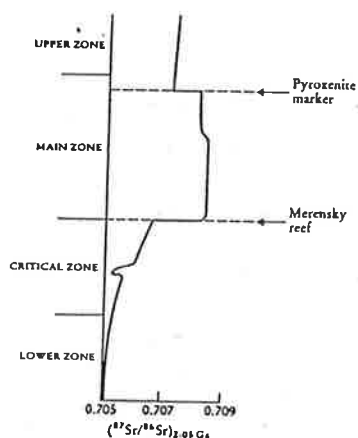


Fig. 12

Change in $^{87}\text{Sr}/^{86}\text{Sr}$ with stratigraphic height in the Bushveld intrusion, South Africa. The gradual increase in $^{87}\text{Sr}/^{86}\text{Sr}$ with stratigraphic height reflects the addition and mixing of a magma with a higher $^{87}\text{Sr}/^{86}\text{Sr}$ ratio. The marked increase in isotopic composition between the pyroxenite marker and the Merensky Reef marks the influx of a new pulse of magma

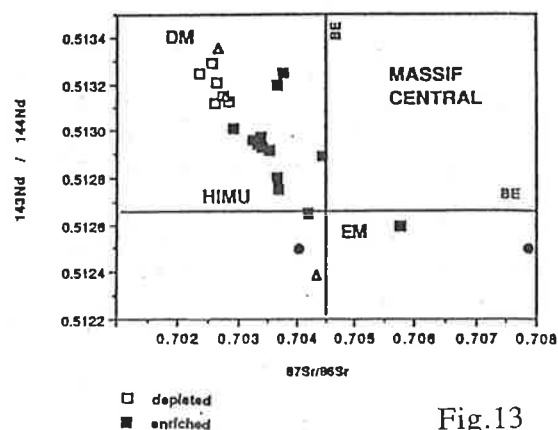


Fig. 13

Correlation of different isotopic systems can be used to model contamination. Two examples are provided in Fig.14. and 15.) Fig 14 shows the general mixing theories concerning the Sr ratio versus Nd ratio diagram (DePaolo 1988) and Fig 15. illustrated the three dimensional model when an additional system (in this case Pb) is taken into account in this case for an OIB from Hawaii. The possibility to determine contamination is furthermore supported by the correlation of Sr ratios with stable oxygen isotope values, which allow to interpret a possible contaminant and the possible kinds of contamination (Fig.16)

Other possibilities such as the contamination of a rock by sea water can be determined since sea water has a homogenous Sr ratio of 0.70924 (Rollinson 1995/Veizer 1989).

Fig.14.

Curves showing the isotopic composition of Nd and Sr in mixtures of the substances 1 and 2. For this calculation it is assumed that the Nd concentration in substance 2 is ten times greater than that of substance 1. The parameter X_2 is the weight fraction of substance 2 in the mixture. K is the ratio of the Sr/Nd ratios in substances 1 and 2, as shown

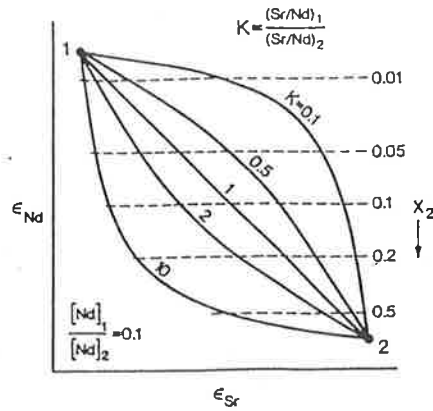
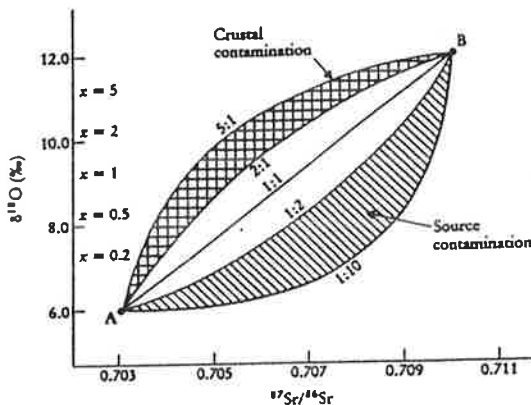
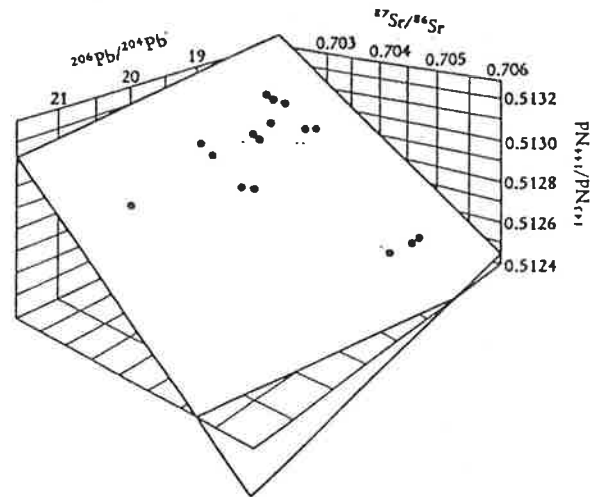


Fig 15.

Three-dimensional plot of average $^{206}\text{Pb}/^{204}\text{Pb}$, $^{143}\text{Nd}/^{144}\text{Nd}$ and $^{87}\text{Sr}/^{86}\text{Sr}$



(Fig.16)

Hypothetical mixing diagram (James, 1981) illustrating the effects of source contamination and crustal contamination on Sr and O isotope concentrations in a mantle melt. The mantle source (A) has $^{87}\text{Sr}/^{86}\text{Sr} = 0.703$ and $\delta^{18}\text{O} = 6.0\text{‰}$; the contaminant (B) has $^{87}\text{Sr}/^{86}\text{Sr} = 0.710$ and $\delta^{18}\text{O} = 12\text{‰}$. The values on the curves show the relative proportions of (Sr in mantle):(Sr in contaminant). In the case of source contamination (diagonal ruling) the ratio (Sr in mantle):(Sr in contaminant) < 1.0 giving rise to a convex-down mixing curve in which a large change in $^{87}\text{Sr}/^{86}\text{Sr}$ is produced by a small amount of contaminant. Where there is crustal contamination (cross-hatching) the (Sr in melt):(Sr in crust) ratio may be > 1.0 and the mixing curve is convex-upward. x indicates the proportion of contaminant (B) to mantle (A).

Conclusion

Radiogenic isotopic systems, such as the Rb- Sr, Sm- Nd and Re- Os systems are able to provide many possibilities for modelling the differentiation of the earth through geological time and the petrogenesis of igneous rocks. The specific characteristics of each of these systems can be used as a powerful tool in distinguishing between geological processes.

Nevertheless radiogenic isotopic tracers should always compared to other evidence such as major oxides and trace elements. Only if all analytical data are consistent a postulated theory can be assumed as valid. Radiogenic isotopes on their own cannot be seen as valid to base complete interpretations on, but they can allow further views into the nature of geochemical problems and enhance or weaken the quality of a geological and geochemical model.

References

- Allegre C (1980)/*Osmium Isotopes as Petrogenetic and geological tracers*/ EPSL;48,p 148
- Chappel B (1996)/ *Magma Mixing and Compositional variation*/ Jour. Petro.; Vol37, p 449
- DePaolo D (1988)/ *Neodymium Isotope Geochemistry*/ Springer Verlag; Berlin
- Dickin A (1995)/*Radiogenic Isotope Geology*/ Cambridge Univ. Press, Cambridge
- Faure G (1977)/ *Isotope Geology*/ J.Wiley & Sons, New York
- Frisch W (1993)/ *Plattentektonik*/Wissensch. Buchgesellschaft; Darmstadt
- Gill R (1993)/ *Chemische Grundlagen der Geowissenschaften*/ Enke Verlag; Stuttgart
- Hall A (1989)/ *Igneous Petrology*/ J Wiley & Sons; New York
- Kerr A (1995)/ *Crustal Assimilation during turbulent Magma Ascent*/ Contr. Min. Petr. 119, p 142
- Mason B, Moore C (1985)/ *Principles of Geochemistry*/ Enke Verlag; Stuttgart
- Mittlefehldt (1978)/ *Rb- Sr studies of CI and CM chondrites*/ GCA, 43, pp201
- Niclas A (1995)/ *Die Ozeanischen Ruecken*/ Springer Verlag; Berlin
- O' Nions R (1983)/ *Die chemische Entwicklung des Erdmantels*/Spektrum; Heidelberg
- Richardson A (1989)/ *Geochemistry*/ Prentice and Hall; London
- Rollinson H (1995)/ *Using geochemical data*/ Longman; Singapore
- Veizer J (1989)/ *Strontium Isotopes in Seawater*/ An. Rev. EPSL 17, pp141
- Wilson M (1993)/ *Magmatic Differentiation*/ Jour. Geol. Soc. London, Vol150, p611
- Wilson M (1989)/ *Igneous Petrogenesis*/ Oxford Univ. Press; London

Stable Isotopes

Oxygen

Oxygen has three stable isotopes. Its composition in a sample is generally reported in terms of a parameter $\delta^{18}\text{O}$, which is the difference between $^{18}\text{O}/^{16}\text{O}$ ratio of the sample and that of a standard called SMOW (Standard Mean Ocean Water)

$$\delta^{18}\text{O} = [(^{18}\text{O}/^{16}\text{O})_{\text{sample}} - (^{18}\text{O}/^{16}\text{O})_{\text{SMOW}} / (^{18}\text{O}/^{16}\text{O})_{\text{SMOW}}] \times 1000$$

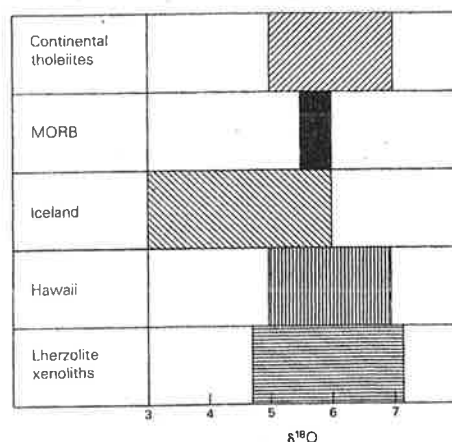
Contrasting radiogenic isotopes that do not change by physical influence ($\Delta P, T$) or fractional crystallisation, oxygen isotopes fractionate during partial melting and during crystal-liquid fractionation. This is because the mass difference between oxygen isotopes is much bigger due to their smaller weight, relative to the mass difference of e.g. Nd isotopes. However, at magmatic temperatures this fractionation is small (ca. 0.2‰ per 5wt% SiO_2).

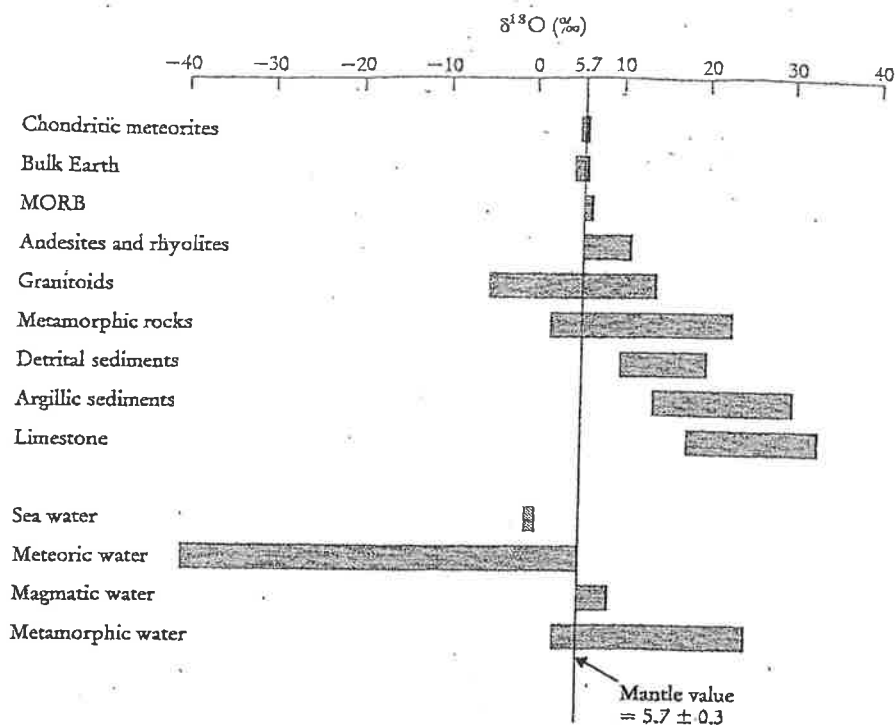
Therefore primitive basaltic magmas should have an isotope composition reflecting their mantle source (5.5-6‰). Evolved rocks such as granites and rhyolites should hence be enriched in $\delta^{18}\text{O}$ by ca. 1‰ assuming closed system differentiation and a SiO_2 increase of ca. 25 wt%.

Many granites and rhyolites show, however, higher or lower values which is attributed to either crustal contamination or hydrothermal overprint, respectively.

In a magma that undergoes fractionation there should consequently be a defined difference in $\delta^{18}\text{O}$ of between the various minerals and the melt under closed system conditions. This can be assessed using, for example, mineral separates. Partitioning of ^{18}O is different for different minerals but should occur at the same rate during magmatic differentiation. Therefore a 1:1 correlation of the $\delta^{18}\text{O}$ in two different mineral phases would result from closed system fractionation. If any deviation from such a 1:1 correlation is observed, disequilibrium has to be assumed.

Another interesting observation is the $\delta^{18}\text{O}$ zonation of oceanic crust. There, the basalts reflect the interaction of rocks with cold seawater. Generally speaking the heavy isotope always seeks the stronger bond and hence seawater-rock interaction would deplete the seawater and enrich the rock in ^{18}O . The depleted seawater then migrates to deeper crustal levels (say into the hotter gabbros) where it reacts with the hot minerals to form hydrous phases. The resulting rocks will be lower in $\delta^{18}\text{O}$. The typical ocean crust zoning is therefore from high $\delta^{18}\text{O}$ near the surface to low $\delta^{18}\text{O}$ towards the base of the oceanic crust.





Natural oxygen isotope reservoirs. Data from: Taylor (1974), Onuma *et al.* (1972), Sheppard (1977), Graham and Harmon (1983) and Hoefs (1987).

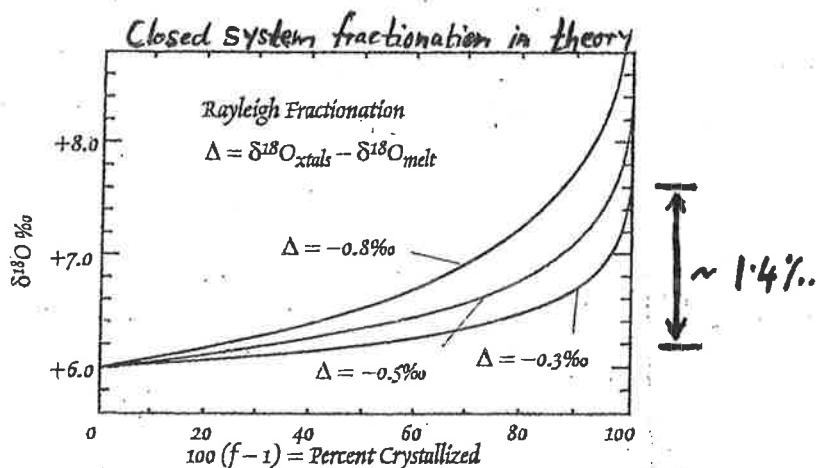
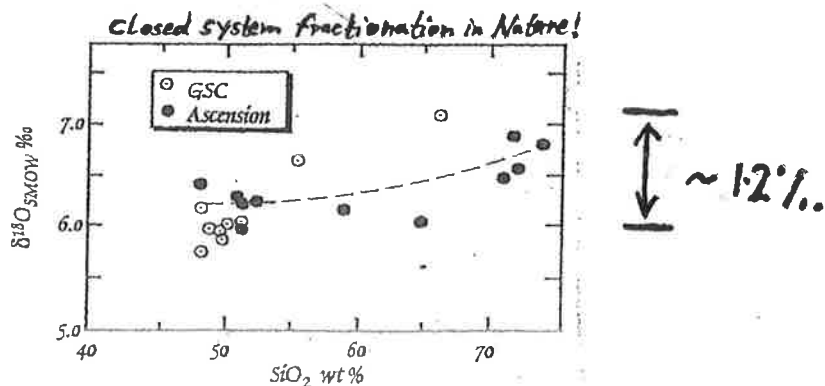
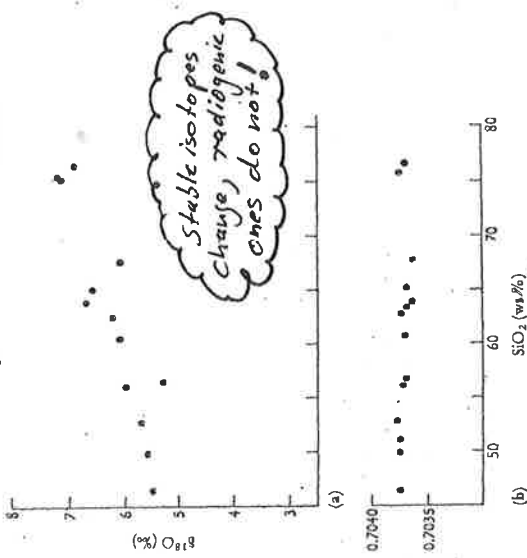


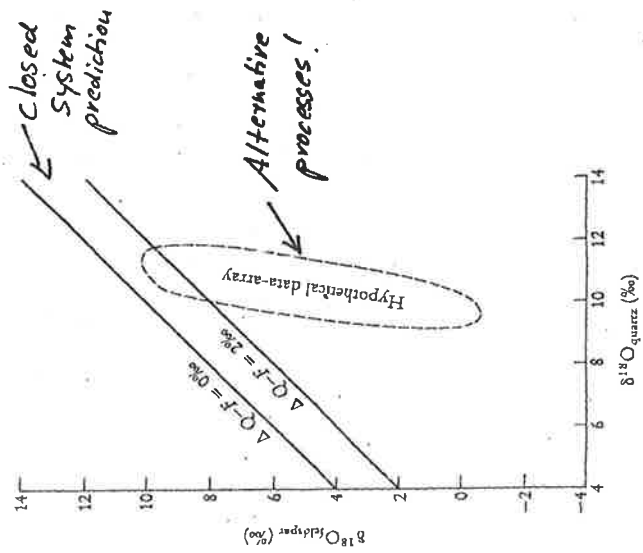
Figure 9.40. Plot of $\delta^{18}\text{O}$ versus fraction of magma solidified during Rayleigh fractionation, assuming the original $\delta^{18}\text{O}$ of the magma was +6. After Taylor and Sheppard (1986).



Closed system fractionation:

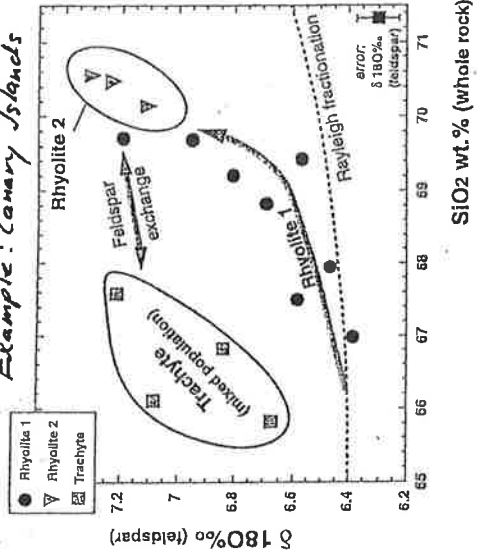


(a) Plot showing a positive correlation between $\delta^{18}O$ and SiO_2 for a fractional crystallization-related calc-alkaline gabbro-diorite-tonalite-trondhjemite suite from an oceanic-arc plutonic complex in the Solomon Islands. (b) The same suite of rocks shows no correlation between $^{87}Sr/^{86}Sr$ and SiO_2 . (Data from Chivas *et al.*, 1982.)

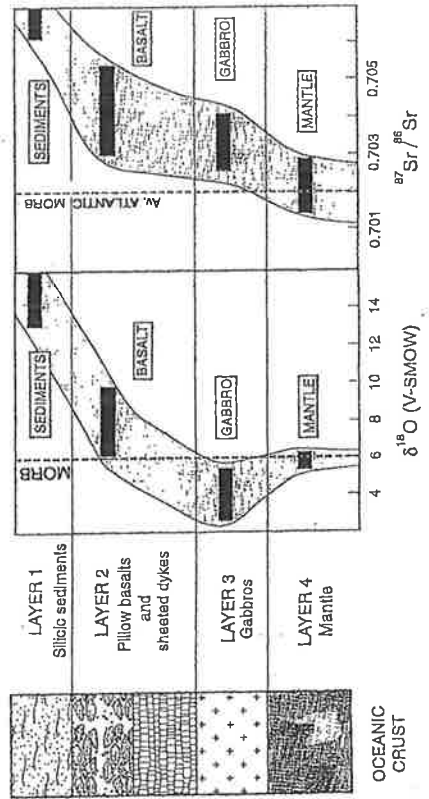


$\delta^{18}O_{quartz}$ vs $\delta^{18}O_{feldspar}$ diagram. Two 45° equilibrium lines are shown for quartz-feldspar Δ values of 0 ‰ and 2 ‰. A hypothetical disequilibrium array is shown with a steep positive slope. (Ehlers, 1997)

Deviation from closed system indicates mixing or contamination.
Example: Canary Islands



Chemical profile of oceanic crust (Hanssen & Toll, 03)



Hydrogen isotopes

There are two hydrogen isotopes ^1H and ^2D (deuterium). Hydrogen show the largest relative mass difference between two stable isotopes and hence a vast compositional range. They are therefore a very powerful tool in assessing the geochemistry of natural waters. Notation is the same as for oxygen with SMOW as standard.

In particular the combination of δD and $\delta^{18}\text{O}$ is used to evaluate geological processes involving water.

Sulphur isotopes

Sulphur has four stable isotopes and in geochemistry we are concerned with ^{34}S and ^{32}S . The notation of sulphur isotopes follows the same logic as oxygen isotopes where the standard (CDT) is derived from a troilite sample of the Canyon Diablo meteorite in the US.

Sulphur occurs in nature as native sulphur, sulphate and sulphide minerals, and as gaseous species (H_2S , SO_2). Generally there are three isotopically distinct reservoirs of $\delta^{34}\text{S}$:

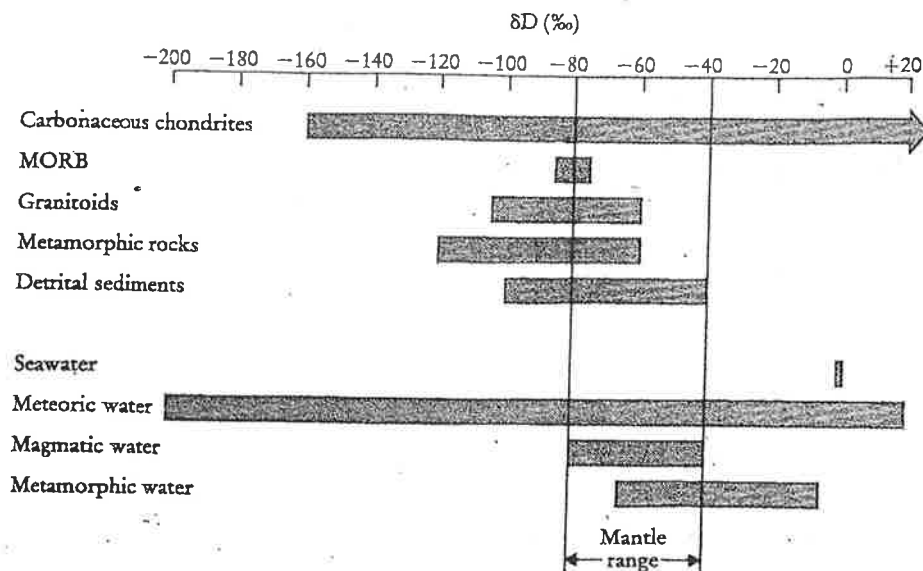
1. mantle derived sulphur $\delta^{34}\text{S} = 0 \pm 3\text{‰}$
2. seawater sulphur ca. $\delta^{34}\text{S} = +20\text{‰}$
3. strongly reduced sedimentary sulphur with large negative values

In high T magmatic processes sulphur isotopes behave similar to oxygen isotopes – that is they fractionate between minerals and liquid. Again, the range is small, generally on the order of 1 ‰. Another means of sulphur fractionation in magma is degassing, i.e. ex-solution of SO_2 , which is associated with a slightly higher degree of fractionation.

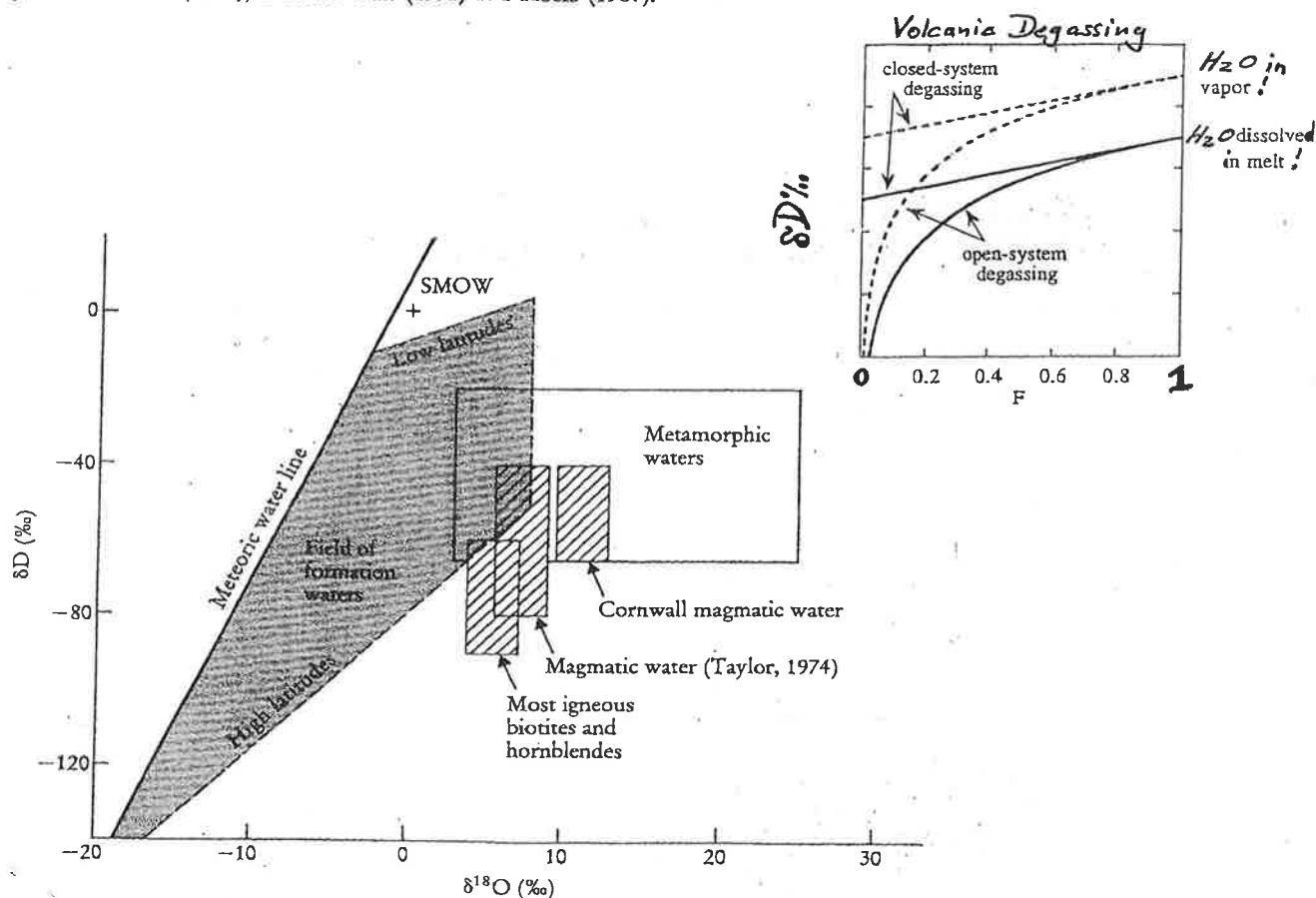
Whereas meteorites and mantle rocks have values roundabout 0, the continental crust has an average of +7‰. Arc magmas are often enriched in heavy sulphur 0-20 and granites show a broad range of -10‰ to +15‰. Modern seawater has a $\delta^{34}\text{S}$ of 18-21‰.

Sulphur isotopes therefore tell us that MORB rocks are derived from a source that is comparatively primitive, whereas arc magmas are likely to have gained a seawater component either during melting in the mantle (source contamination) or by assimilation of waterlogged sediments during ascent (crustal contamination). Similarly, granites appear to have had intimate contact to sediments prior to solidification.

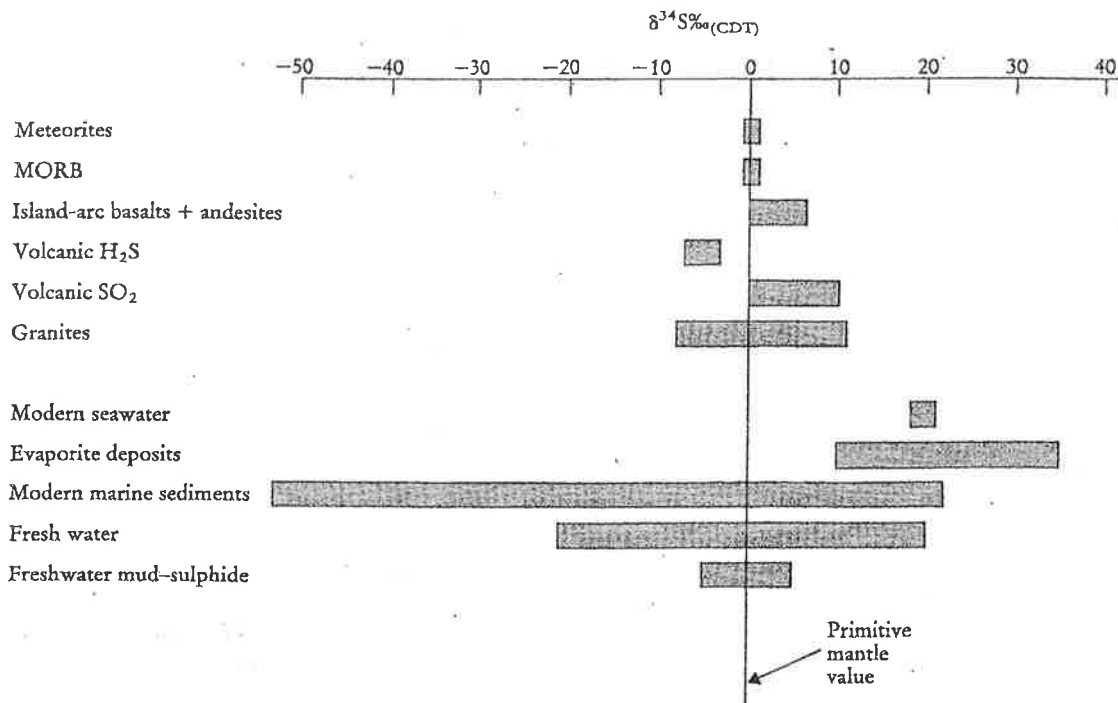
A major application of sulphur isotopes is for example the understanding of hydrothermal ore deposits, in particular those massive sulphide deposits that form at the seafloor in a black smoker environment. Since seawater has ca. $\delta^{34}\text{S}$ of 20‰ and basalt 0-2‰, the deposited sulphide minerals that show a range of 1.5-2‰ are clearly leached out of the underlying basalt. The water vented has in turn values up to 5.5‰, suggesting that seawater enters the crust where it is heated and reacts with the rock. This process leaches out sulphur and changes the S ratio of the host basalt. The heated water then rises up and precipitates sulphides on contact with the cooler seawater. The vented fluid is isotopically a mixture of seawater and basalt derived sulphur.



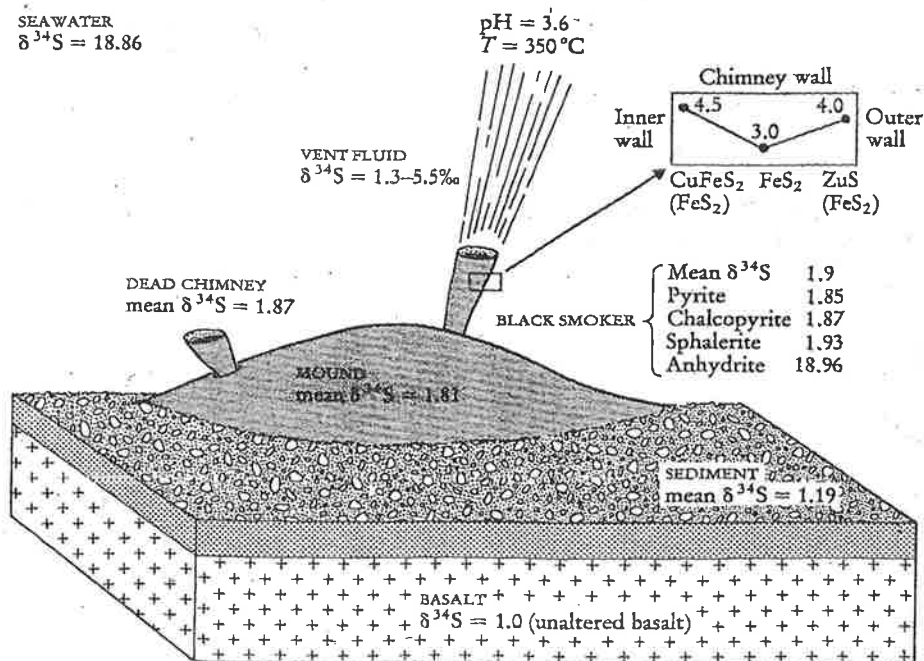
Natural hydrogen isotope reservoirs. Data from Taylor (1974), Graham and Harmon (1981), Kyser and O'Neil (1984), Deloule *et al.* (1991) and Hoefs (1987).



Plot of δD vs $\delta^{18}O$ diagram for different water types. The fields of magmatic water and formation waters are taken from Taylor (1974). The field for igneous hornblendes and biotites from Taylor (1974) and that of magmatic water from the granites of Cornwall from Sheppard (1977). The meteoric water line is from Epstein *et al.* (1965) and Epstein (1970). The metamorphic water field combines the values of Taylor (1974) and Sheppard (1981).



SULPHUR ISOTOPES IN BLACK SMOKER ENVIRONMENTS



Schematic representation of $\delta^{34}\text{S}$ values in a modern mid-ocean ridge hydrothermal vent system. Most values are taken from Kerridge *et al.* (1983) but with additions from Bluth and Ohmoto (1988) and Woodruff and Shanks (1988). The enlargement of the chimney wall shows changing $\delta^{34}\text{S}$ values and sulphide composition from inner to outer wall.

Ore-deposits and Mineral Resources

MINERAL DEPOSIT: Locally enriched concentration of minerals.

ORE: Resources of metals that can now be economically and legally extracted.

ORE DEPOSIT: The same as reserves when referring to concentrations of metallic minerals.

MINERAL RESERVES: Known deposits of earth materials from which useful amounts of ore are economically and legally recoverable with existing technology.

Distribution of Mineral Resources

DESCRIPTION: Mineral deposits are highly localized; they are neither uniformly nor randomly distributed.

CAUSE: Concentrations of valuable mineral deposits are due to special, sometimes unique, geochemical processes.

Origins of Mineral Deposits

IGNEOUS DEPOSITS:

1. **Pegmatites;** exceptionally coarse-grained igneous rock with interlocking crystals, usually found as irregular dykes, lenses, or veins, especially at the margins of batholiths (exploited for e.g. mica, tourmaline, beryllium, lithium and gemstones)
2. **Layered ultrabasic intrusions;** Crystal settling, i.e. the sinking of crystals in a magma due to their greater density, aided by magmatic convection and magma mixing may produce economically viable mineral concentrations (e.g. chromite deposits, type-localities Bushveld, ZA, Sudbury, N-America but also on the Isle of Rum, Scotland).
3. **Kimberlite diatremes;** Volcanic vents that originate from the mantle. Gas rich ultrabasic magma drilled through the crust and erupted explosively at the surface. Often these magmas carry diamonds that formed at great depth
4. **Disseminated Mineral deposits,** especially of metal, in which the minerals occur as scattered particles in the rock but in sufficient quantity to make the deposit a worthwhile ore (e.g. porphyry copper deposits).
5. **Hydrothermal ore deposits;** a mineral deposit that precipitated from a hot aqueous solution with or without demonstrable association with igneous processes (e.g. Cu, Sn, Pb, Sb, Ag, Au). Occurs also in veins (e.g. Pb-Zn mineralisation).
6. **Volcanogenic**—of volcanic origin, e.g., volcanogenic sediments. Massive sulfide deposits. Black smoker environment.

SEDIMENTARY DEPOSITS:

Mineral deposits resulting from the accumulation or precipitation of sediment.

These include

1. **Banded Iron Formations (BIF)** deposited in Precambrian time when the earth's atmosphere lacked free oxygen. Without oxygen, the iron that dissolved in surface water could be carried in solution by rivers from the continents to the oceans where it precipitated with silica to form beds of red chert and iron ore.
2. **Placer deposits** are concentrations of erosion resistant minerals such as gold, platinum, diamonds, and tin that were transported by moving water, i.e. rivers.
3. **Deep-ocean precipitation** → Manganese nodules are formed by precipitation on the deep ocean floor. The nodules are a mixture of manganese oxides, iron oxides, and hydro-oxides with small amounts of Cu, Co, Ni, Zn that grow in onion-like concentric layers by direct precipitation from ocean waters. However, currently no way to recover them.

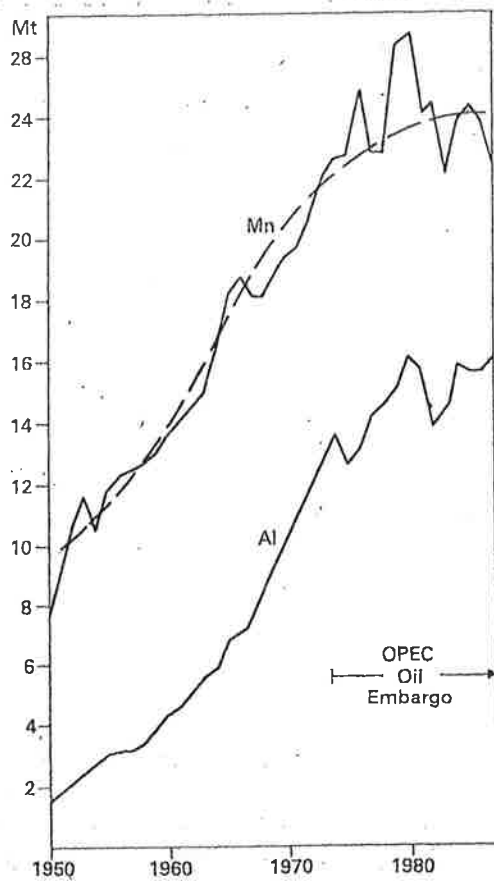


Fig. 1.6 World production of manganese and aluminium from 1950 to 1987 with general trend for manganese superimposed. (After Loftly *et al.* 1989.)

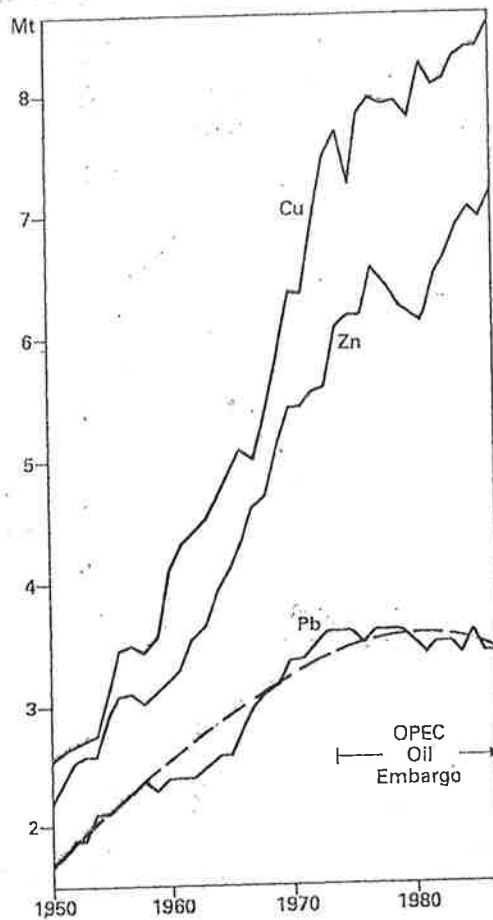


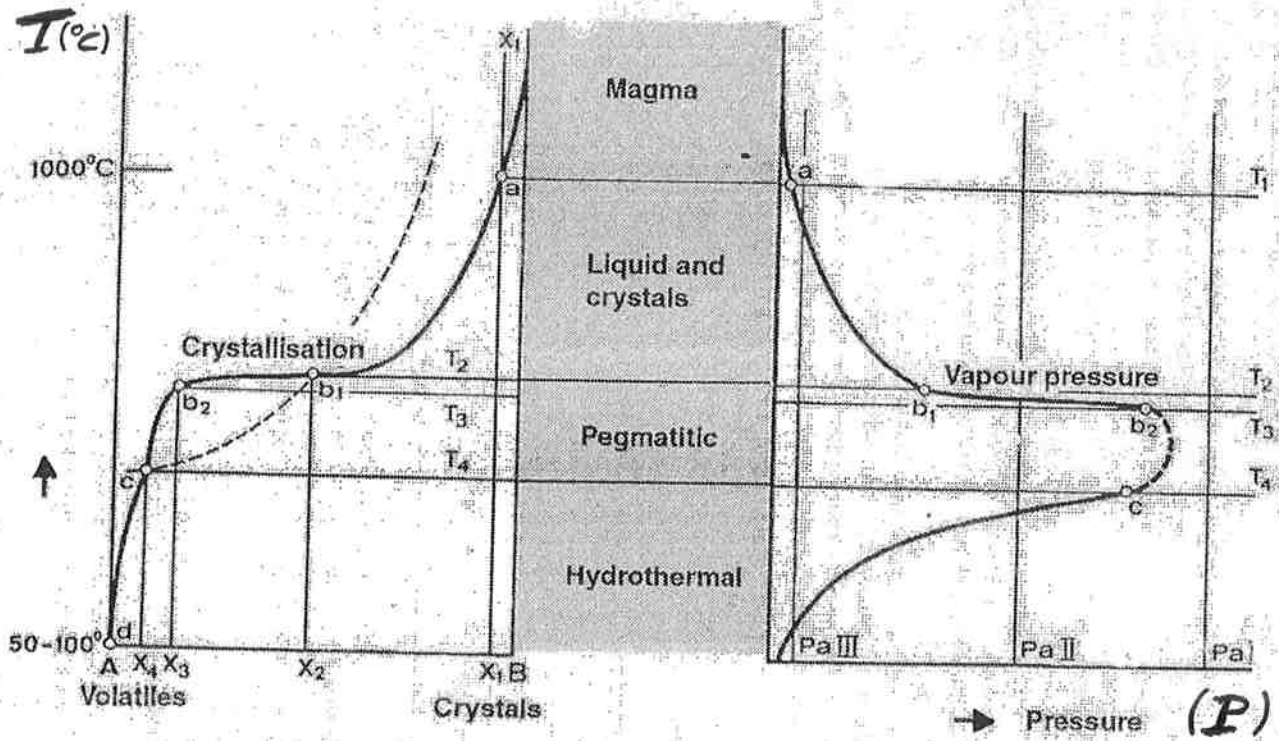
Fig. 1.7 World production of copper, zinc and lead from 1950 to 1987. General trend for lead superimposed. (After Loftly *et al.* 1989.)

Concentration Factors for Profitable Mining of Selected Metals

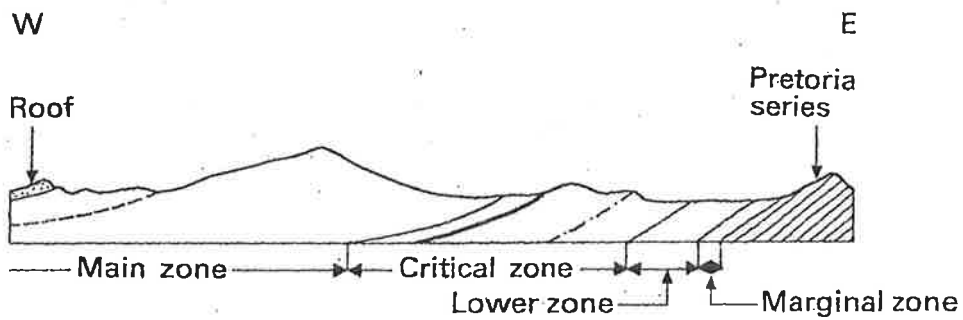
METAL	PERCENTAGE ABUNDANCE		CONCENTRATION FACTOR
	<i>Average in Earth's Crust</i>	<i>In Ore Deposit</i>	
Aluminium	8	35	4
Copper	0.0063	0.4-0.8	80-160
Gold	0.0000004	0.001	2,500
Iron	5	20-69	4-14
Lead	0.0015	4	2,500
Mercury	0.00001	0.1	10,000
Silicon	28.2	46.7	2
Titanium	0.57	32-60	56-105

SOURCE: U.S. Geological Survey Professional Paper 820, 1973.

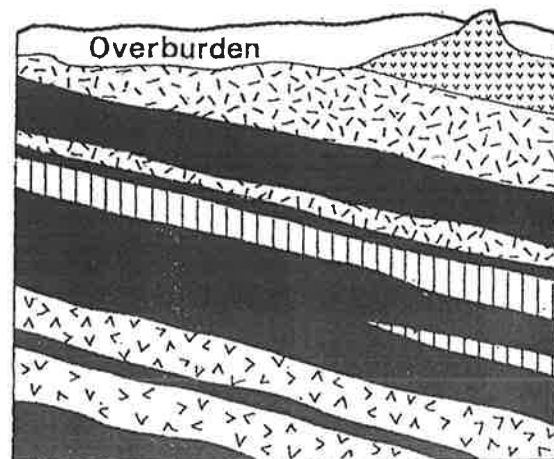
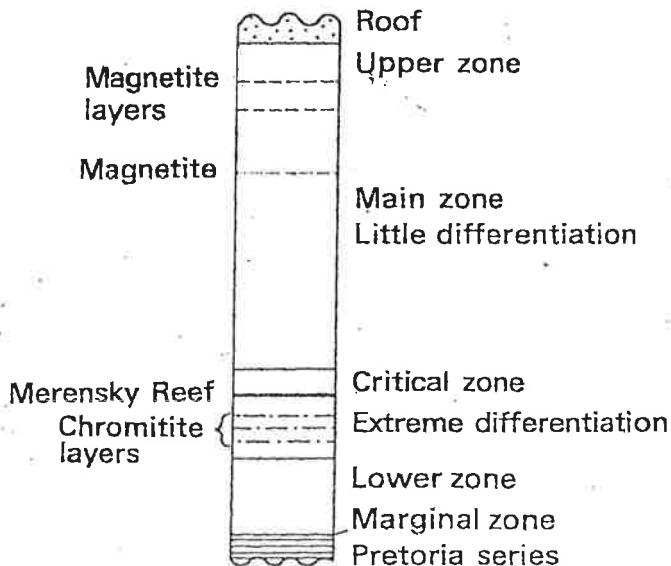
The pegmatite environment



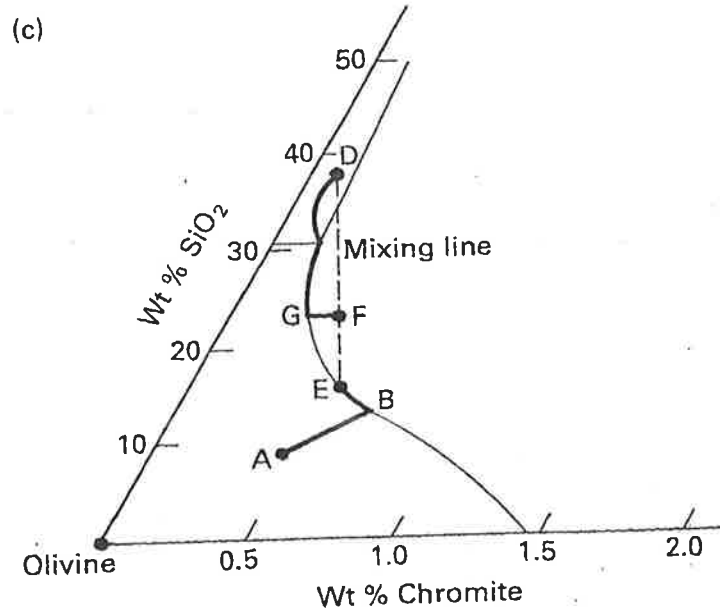
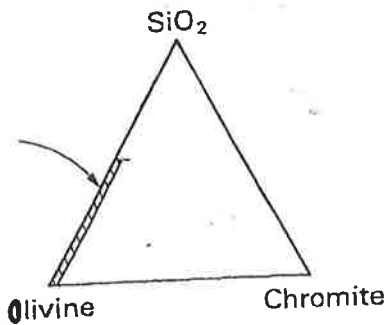
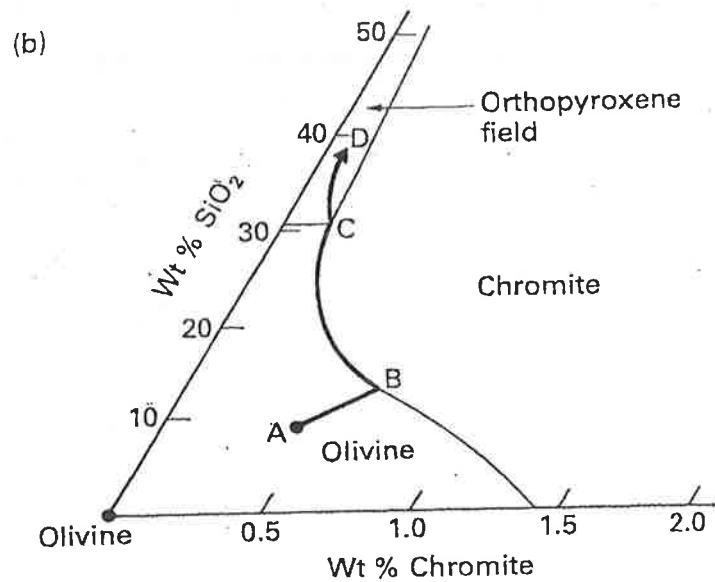
LAYERED
ULTRABASIC
INTRUSIONS:



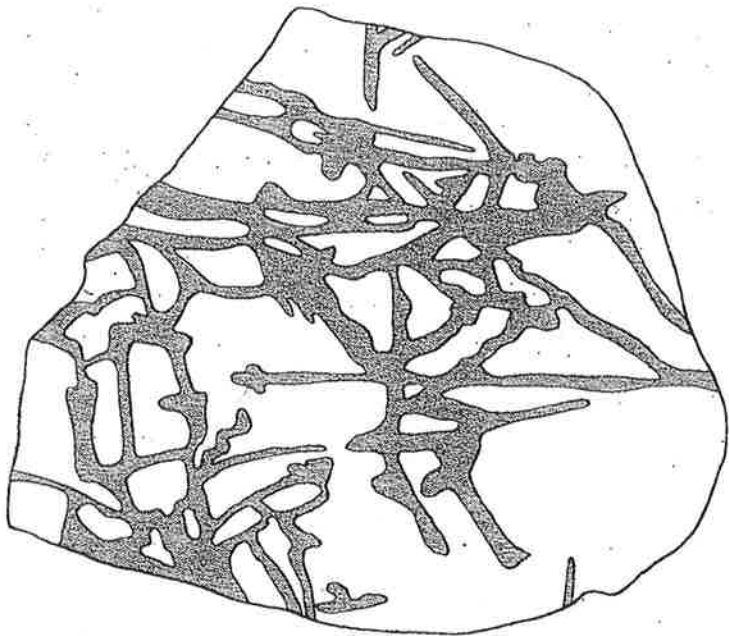
Section showing major zones in the Bushveld Complex, north of Steelpoort. Length of section, 30.5 km. (After Hall, 1932)



Chromitite layers in a section of the Bushveld Complex near Rustenburg.

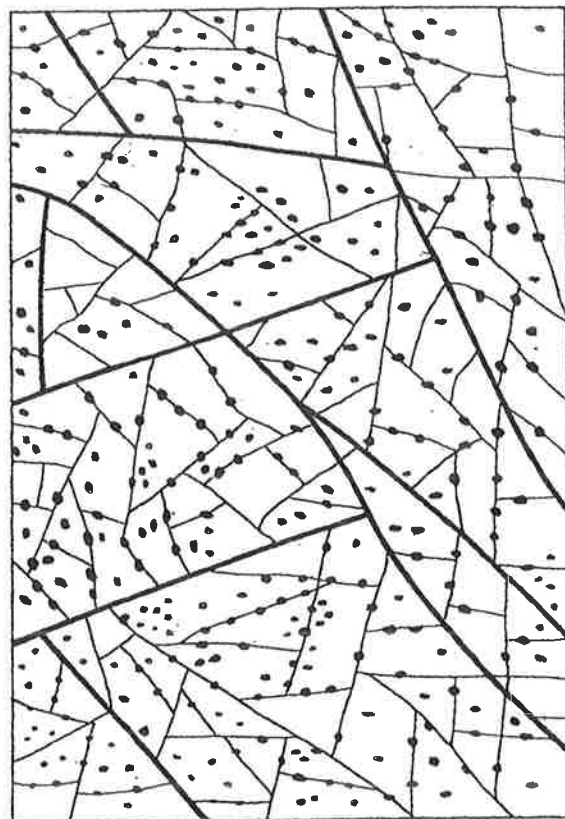


The phase diagram for the system olivine-chromite-silica. (a) Plot of mineral compositions. (b, c) A small portion adjoining the olivine corner. The horizontal scale is greatly expanded. (Modified from Irvine 1977.)

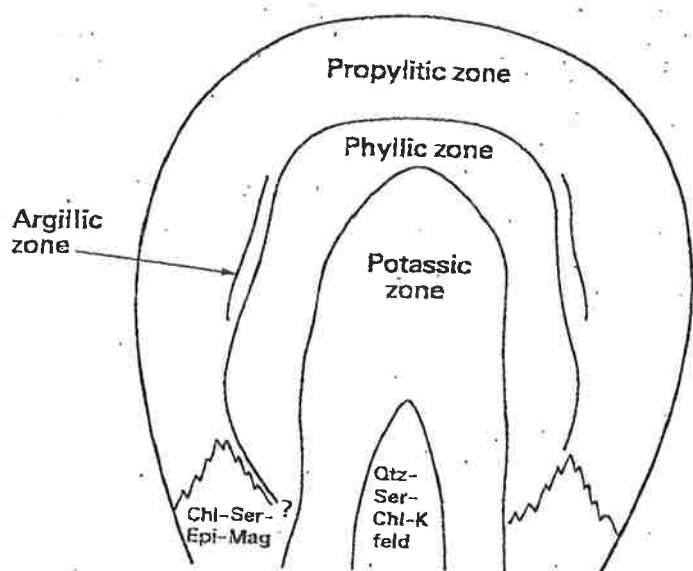


0 3 cm

Stockwork of molybdenite-bearing quartz veinlets in granite that has undergone phyllic alteration. Run of the mill ore, Climax, Colorado.



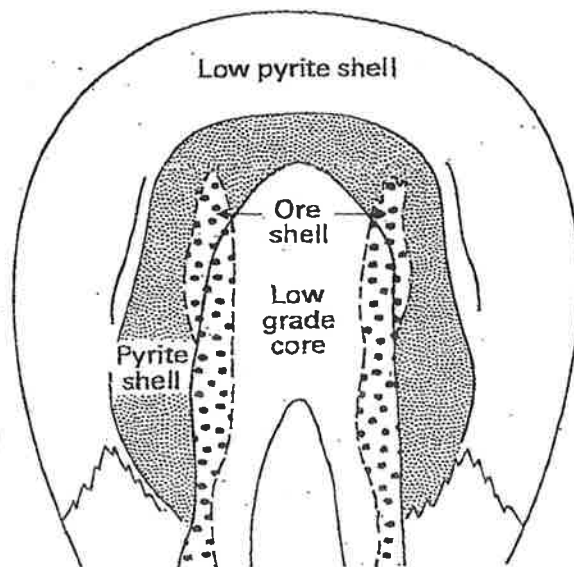
→ Disseminated ore-host relationship



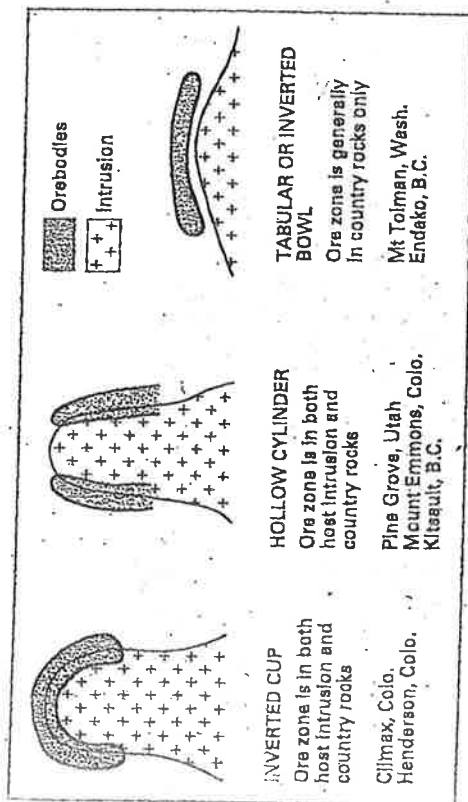
Hydrothermal alteration zoning pattern in the Lowell-Guilbert model of porphyry copper deposits. (After Lowell & Guilbert 1970.)

← Alteration zones associated with porphyry copper deposits.

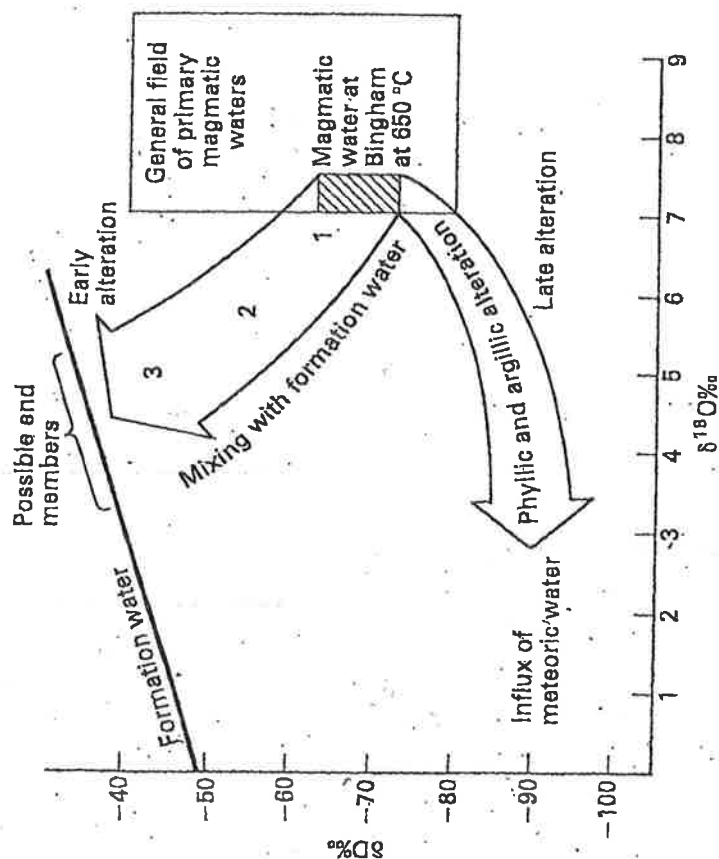
General architecture of a porphyry copper deposit



Schematic diagram of the principal areas of sulphide mineralization in the Lowell-Guilbert model of porphyry copper deposits. Solid lines represent the boundaries of the alteration zones shown in Fig. 14.4. (After Lowell & Guilbert 1970.)



Porphyry molybdenum orebody morphologies.



Changes in the calculated values of δD and $\delta^{18}O$ of water during the development of early and late hydrothermal alteration in the Bingham Canyon porphyry system.
 (1) potassic zone,
 (2) potassic-propylitic border,
 (3) propylitic zone. (After Bowman *et al.* 1987.)

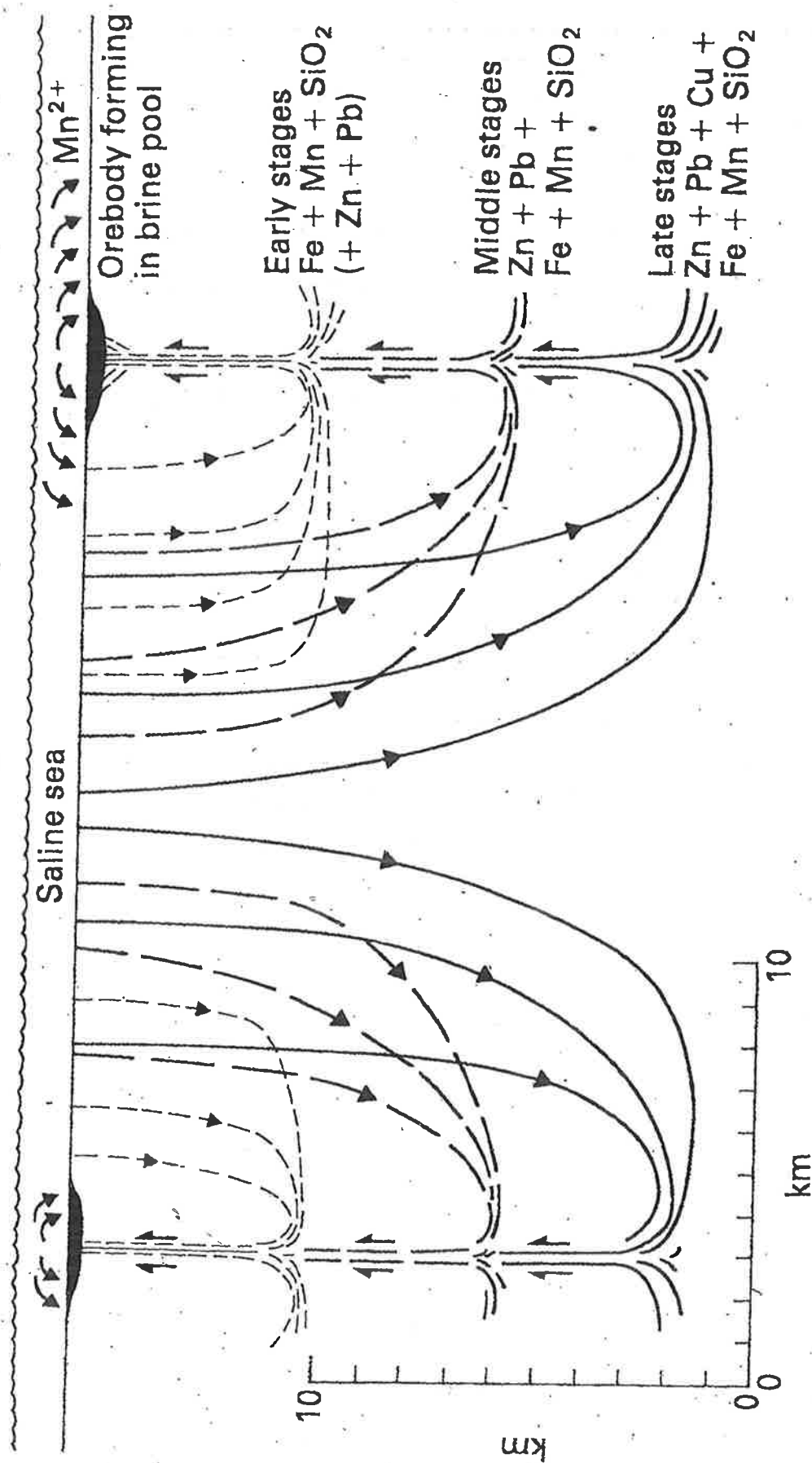


Diagram showing how sea water circulation through the crust might give rise to the formation of an exhalative, sediment-hosted, stratiform ore deposit. (After Russell *et al.* 1981.)

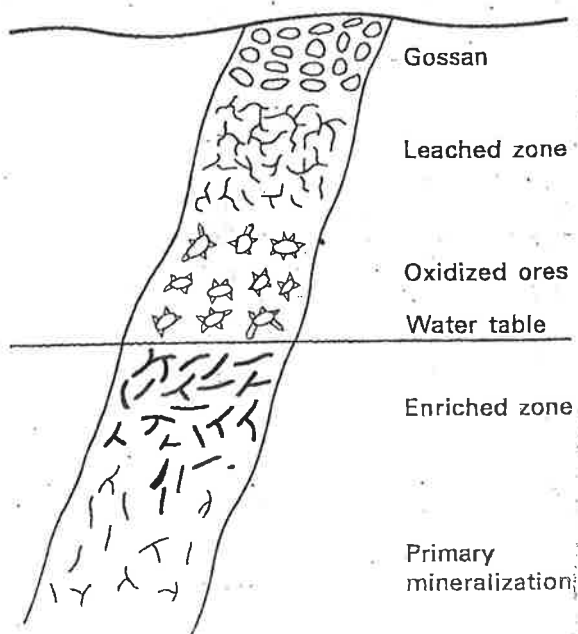
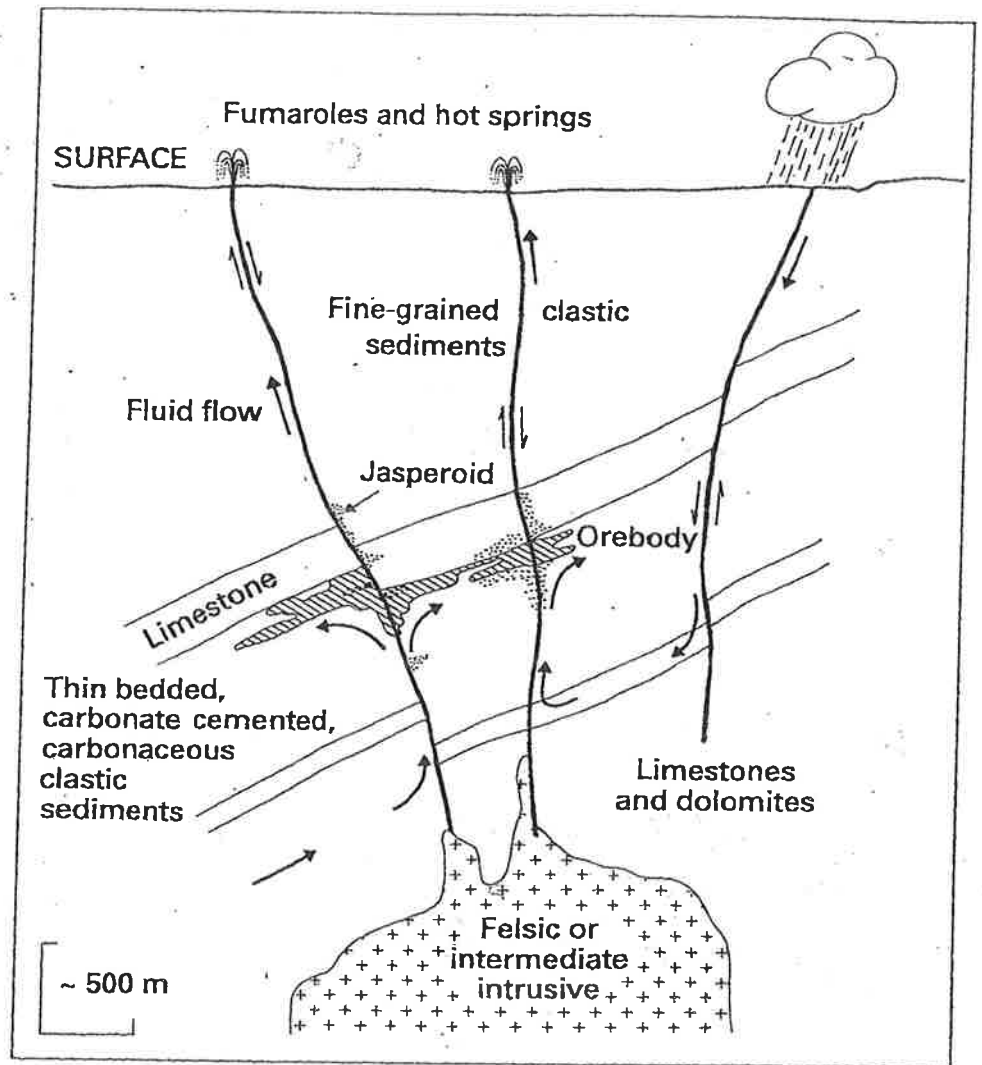
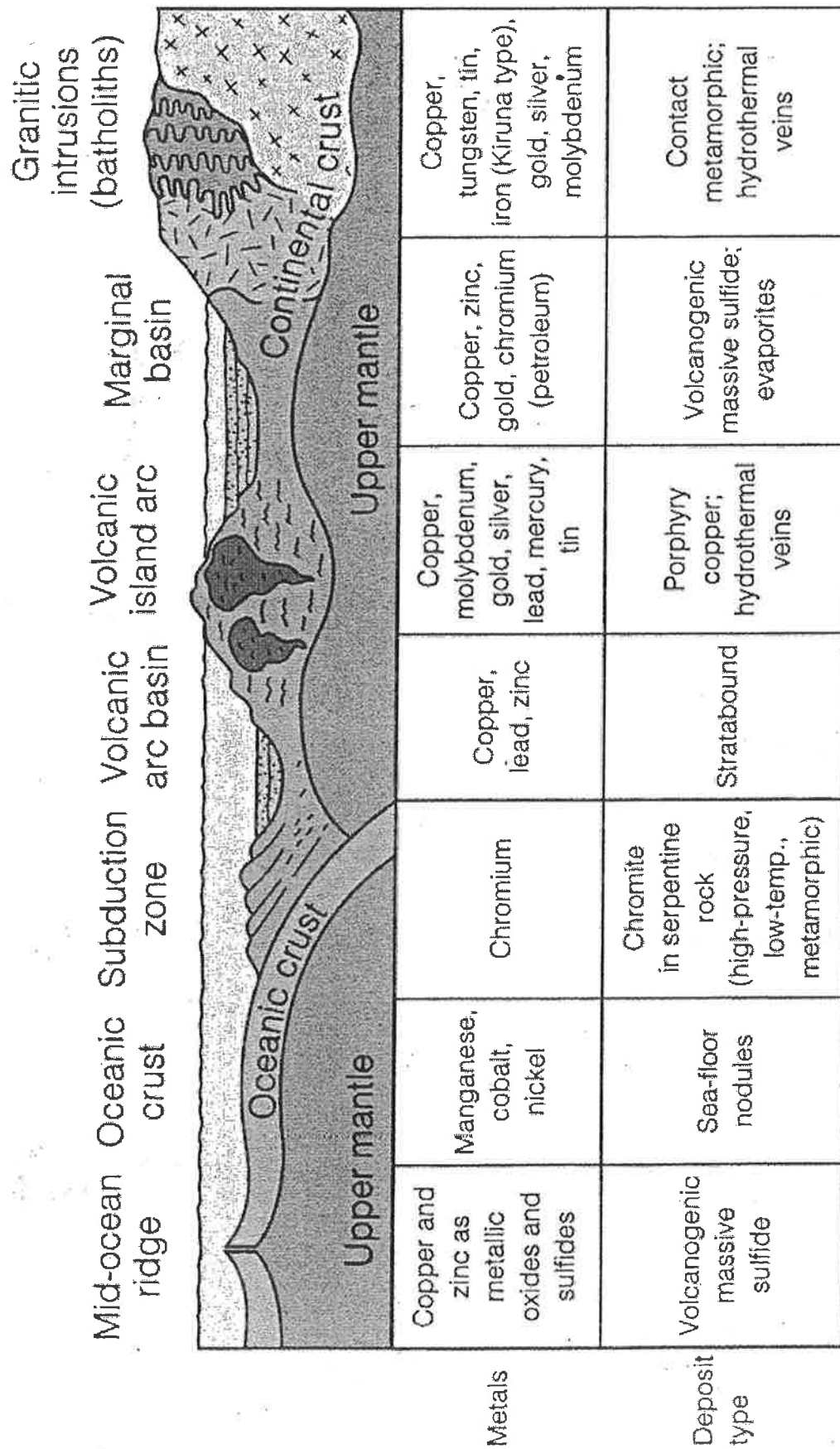


Fig. 19.5 Generalized section through a sulphide-bearing vein showing supergene enrichment. (Modified from McKean 1950.)



> **FIGURE** Relationships between metallic ore deposits and tectonic processes.

WEATHERING DEPOSITS

1. **Lateritic weathering**—concentrations of minerals due to the gradual chemical and physical breakdown of rocks in response to exposure at or near the earth's surface. For example bauxite, the principal aluminium ore. Fe and Al is left behind by the weathering process.
2. **Secondary enrichment**- process of mineral development that has occurred later than the enclosing rock. Ground water moving downward through disseminated sulfide deposit may dissolve the dispersed metals from above the water table to produce an enrichment below the water table (also known as supergene enrichment).

Environmental Impacts of Mining

UNDERGROUND MINING IMPACTS

1. Waste rock may result in visual pollution and be the source of toxic compounds in downstream hydrologic systems. Mitigated by state regulations requiring that waste-rock dumps be shaped to resemble natural landforms and planted with native vegetation.
2. Tailings also may leak toxic compounds; if they are dry, fine dust may contribute to air pollution. Mitigated by state regulations that generally require tailings ponds to be lined with plastic or impermeable clay to contain the toxins. Following abandonment, the tailings piles are dried out, sealed with impermeable clay to keep them dry, covered with soil, and seeded with plants. Impoundment dams are built to hold the leached water in a pond. Groundwater-monitoring wells may be required for periodic analyses of water quality.
3. Ground subsidence or ground-surface collapse from hardrock (underground) mining is rare, and little can be done about it when it occurs.
4. Acid mine drainage may be contained in ponds behind containment structures to protect downstream hydrologic systems from pollution. Monitoring wells are installed downstream as for tailings.

SURFACE MINING AND PROCESSING IMPACTS

1. Scarified ground, despoiled landscape, and disrupted drainage commonly remain from dredging and hydraulic mining and can be reclaimed by reshaping, adding topsoil, and landscaping.
2. Large open pits with oversteepened side walls that despoil the landscape and may pollute hydrologic systems that remain after open-pit mining are difficult or impossible to reclaim. Public is protected by enclosing the pit within a chain-link fence and posting warning signs. Pit floor may be partially back-filled and sealed with impermeable clay to protect ground water from pollution. Smaller open pits near urban areas may be utilised as sanitary landfill sites, sealed, and landscaped.
3. Cyanide heap-leach gold extraction methods cause minimal environmental problems due to strict regulation by state and federal agencies. Hazards to wildlife have been mitigated by placing nets over the lethal ponds. There is no demonstrated hazard from lethal fumes. Ground and surface waters are monitored by surface-water sampling and ground-water monitoring wells.